Multivariable Control of Air Temperature and Humidity in a Space Served by a Direct Expansion (DX) Air Conditioning (A/C) System

Qi Qi

A thesis submitted in partial fulfillment of the requirements

for the Degree of Doctor of Philosophy

Department of Building Services Engineering

The Hong Kong Polytechnic University

September 2009

Certificate of Originality

I hereby declare that this thesis is my own work and that, to the best of my knowledge and belief, it reproduces no material previously published or written, nor material that has been accepted for the award of any other degree or diploma, except where due acknowledgement has been made in the text.

Qi Qi

Department of Building Services Engineering

The Hong Kong Polytechnic University

Hong Kong SAR, China

September 2009

Abstract

Direct expansion (DX) air conditioning (A/C) systems are widely used in small- to medium-scaled buildings, offering many advantages over conventional chilled-water based air conditioning systems. These include a higher energy efficiency and a lower cost to own and maintain a DX A/C system. However, it is difficult to satisfy both indoor air temperature control and humidity control using a DX A/C system with a constant speed compressor and supply fan, which may hinder the wider use of DX A/C systems. Traditionally, on-off cycling a constant speed compressor and supply fan has been the principal method for capacity control for a DX A/C system to maintain indoor dry-bulb temperature only, leaving indoor humidity uncontrolled. Such a control method has led to a poor indoor thermal environment and a low energy efficiency as space overcooling is often seen in order to achieve better dehumidification.

The recent advancement of low-cost variable speed drive (VSD) technology offers tremendous opportunities for improving indoor thermal control and energy efficiency for DX A/C systems. Compressor speed can be continuously varied to modulate the output cooling capacity to match the actual thermal load. The supply fan speed can be also continuously altered to affect both sensible heat and latent heat transfer rates across a DX cooling coil. It is therefore possible to simultaneously control indoor air temperature and humidity by simultaneously varying the speeds of both compressor and supply fan in a DX A/C system. However, the related research work on developing a multivariable control strategy for simultaneously controlling both indoor air temperature

and humidity in spaces served by DX A/C systems cannot be indentified in published literature. Therefore a study on developing a multivariable control strategy that can simultaneously control indoor air temperature and humidity by varying speeds of both compressor and supply fan in a DX A/C system, through both modeling and experimental approaches, has been carried out and is reported in this Thesis.

The Thesis starts with reporting the development of a multivariable control-oriented dynamic model of an experimental DX A/C system. The dynamical model, which consisted of a set of differential equations, was derived based on the principles of energy and mass conservation. The dynamic model was nonlinear in nature, and was therefore linearized and written in a state-space representation which was highly suitable for multivariable control design. The linearized dynamic mathematical model for the experimental DX A/C system was experimentally validated. Experimental tests to obtain the open-loop responses of the experimental DX A/C system after being subjected to step changes in compressor speed and supply fan speed were carried out. The experimental open-loop responses for all major operational parameters obtained were found in good agreement with the simulated open-loop responses from the linearized dynamic model, suggesting that the linearized dynamic model was experimentally validated.

Secondly, the Thesis presents the development of a multi-input multi-output (MIMO) controller for simultaneously controlling indoor air temperature and humidity in a space served by the experimental DX A/C system. Based on the linearized dynamic model for

the experimental DX A/C system, a multivariable feedback control strategy has been formulated and the MIMO controller developed using the Linear Quadratic Gaussian technique. Controllability tests for both disturbance rejection capability and command following capability were carried out to evaluate the performance of the MIMO controller in the experimental DX A/C system. The experimental results demonstrated that the MIMO controller developed can effectively control the indoor air temperature and humidity simultaneously by varying compressor speed and supply fan speed in the experimental DX A/C system.

Finally, the development of a new controller for improving the control performance of degree of refrigerant superheat (DS) in a DX A/C system when the fluctuation of operating DS is resulted mainly from varying the speeds of its compressor and supply fan is reported. The new DS controller was developed from a conventional proportional-integral-derivative (PID) DS controller by adding two feed-forward channels so that information of speed changes of compressor and supply fan can be timely passed to the new DS controller to take appropriate control action. Controllability test results showed that an improved DS control performance can be achieved by using the new DS controller instead of a conventional PID DS controller, and resulting in a better operating performance of the DX A/C system in terms of operating efficiency and stability when its compressor speed and fan speed were varied as required by a capacity control algorithm.

Acknowledgements

I must express my sincere grateful thanks to my Chief Supervisor, Dr. Deng Shiming, Associate Professor from the Department of Building Services Engineering (BSE), The Hong Kong Polytechnic University, for his readily available supervision, invaluable suggestions, patient guidance and continuous help throughout the course of the project.

I would like to also thank my Co-supervisor, Dr. Chan Ming-yin, Assistant Professor from the BSE Department for his supervision and suggestions. Special thanks go to The Hong Kong Polytechnic University for financially supporting this project, and to Prof. Chen Wu of Jimei University and Dr. Li Zheng for their previous work in building the experimental DX A/C system. I would like also to thank my fellow students and the technicians in the Heating, Ventilation and Air Conditioning (HVAC) Laboratory of the BSE Department for their assistances in the experimental work.

Finally, I would like to express my deepest appreciation to my parents, my elder sister and all other family members, as well as Miss Cheng Wei. I could not have completed my research work without their understandings, encouragements and supports.

Table of Contents

List of Figures

Chapter 6

Chapter 7

Appendix B

List of Tables

Nomenclature

Variable	Description	Unit
A, B, C	coefficient matrices (in Equation (5.31))	DL
A_1	air side heat transfer area of the DX evaporator in dry-cooling region	m^2
A_2	air side heat transfer area of the DX evaporator in wet-cooling region	m^2
A_{s1}	air side cross section area of the DX evaporator in dry-cooling region	m^2
A_{s2}	air side cross section area of the DX evaporator in wet-cooling region	m^2
C_p	specific heat of air	kJ/(kg·K)
K_1, K_2	gain matrix	DL
K_P, K_I, K_D	proportional-integral-derivative coefficient	DL
K_s, K_c	coefficient	DL
L	Kalman filter gain matrix	DL
L_1	the length of the dry-cooling region on the air side of the evaporator	m
L_2	the length of the wet-cooling region on the air side of the evaporator	m
M	moisture load in the conditioned space	kg/s
M_{ref}	mass flow rate of refrigerant	kg/s
P_c	condensing pressure	Pa
P_e	evaporating pressure	Pa
P_r	Prandtl number	DL
Q, R, Q_0, R_0	weighting matrix	DL
Q_{load}	sensible heat load in the conditioned space	kW

Q_{spl}	heat gain of the supply fan	kW
R	the radius of cylinder	m
T_1	temperature of air leaving the DX evaporator	ºC
T_2	temperature of air in the conditioned space	ºC
T_3	temperature of air leaving the dry-cooling region of the DX evaporator	ºC
T_I	integral time	s
T_D	differential time	s
T_w	temperature of the DX evaporator wall	ºC
V	volume of the conditioned space	m^3
V_{h1}	air side volume of the DX evaporator in dry-cooling region	m^3
V_{h2}	air side volume of the DX evaporator in wet-cooling region	m^3
V_{com}	swept volume of the rotor compressor	m^3
W_1	moisture content of air leaving the DX evaporator	kg/(kg dry air)
W_2	moisture content of air in the conditioned space	kg/(kg dry air)
e	rotor eccentricity	m
f	air volumetric flow rate	m^3/s
h_1	enthalpy of air leaving the DX evaporator	kJ/kg
h_2	enthalpy of air in the conditioned space	kJ/kg
h_3	enthalpy of air leaving wet-cooling region of the evaporator	kJ/kg
h_{fg}	latent heat of vaporization of water	kJ/kg
h_{r1}	enthalpy of refrigerant at evaporator inlet	kJ/kg
h_{r2}	enthalpy of refrigerant at evaporator outlet	kJ/kg
h_{rc}	enthalpy of superheated refrigerant at compressor suction	kJ/kg

h_{re}	enthalpy of refrigerant leaving the receiver	kJ/kg
j_{e1} , j_{e2}	Colburn factors	DL
k_{spl}	coefficient of supply fan heat gain	kJ/m^3
l	stroke of cylinder	m
r	input reference	DL
r_a	radius of rotor	m
r_s	reference setpoint of DS	^{o}C
s	compressor speed	rpm
u	input variable vector	DL
u_{c0}	compressor speed at operating point	rpm
u_e	input of EEV	DL
u_s	supply fan speed	rpm
u_{s0}	supply fan speed at operating point	rpm
Δu_c	change of compressor speed	rpm
Δu_s	change of supply fan speed	rpm
v_s	specific volume of superheated refrigerant	m^3/kg
x	state variable vector	DL
y	output variable vector	DL
λ	compressor displacement coefficient	DL
λ_{sys}	eigenvalue (in Equation (5.34))	DL
α_1	heat transfer coefficient between air and the DX evaporator wall in dry-cooling region	kW/(m^2·K)
α_2	heat transfer coefficient between air and the DX evaporator wall in wet-cooling region	kW/(m^2·K)
β	compression index	DL
ρ	density of moist air	kg/m^3
ε	rotor relative eccentricity	DL

subscript

w	evaporator wall

Note: DL = Dimensionless

List of Abbreviations

A/C	air conditioning
COP	coefficient of performance
DAS	data acquisition system
DDC	direct digital control
DS	degree of refrigerant superheat
DX	direct expansion
EEV	electronic expansion valve
EER	energy-efficiency rating
GLC	globally linearizing control
GRNN	general regression neural network
HVAC	heating, ventilation and air conditioning
HPHE	heat pipe heat exchanger
LGU	load generating unit
LQG	linear quadratic gaussian
MBPC	model-based predictive control
MIMO	multiple-input multiple-output
PI	proportional-integral
PID	proportional-integral-derivative
RH	relative humidity
RTD	resistance temperature device
SCR	silicon control resistance
SHR	sensible heat ratio
SISO	single-input single-output
TEV	thermostatic expansion valve
VRV	variable refrigerant volume
VSD	variable speed drive

Chapter 1

Introduction

A direct expansion (DX) air conditioning (A/C) system has been widely used in small- to medium-scaled buildings. It consists of a DX refrigeration plant and an air-distribution sub-system. The DX refrigeration plant is mainly composed of a DX evaporator, a condenser, an expansion valve, a compressor, an oil separator and a receiver, etc. The evaporator in the DX refrigeration plant is used as a DX air cooling coil in the air-distribution sub-system to simultaneously cool and dehumidify the air passing through it. The conditioned air is then supplied to a conditioned space through an air duct work by a supply fan.

The use of DX A/C systems offers many advantages over conventional chilled-water based A/C systems. These advantages include a higher energy efficiency and a lower cost to own and maintain the systems. A DX A/C system can offer different levels of space air temperature control for indoor thermal comfort. However, it is difficult to satisfy both the indoor temperature control and humidity control simultaneously using a DX A/C system with a single speed compressor and a single speed supply fan, which may deter the wider use of DX A/C systems.

Traditionally, reheating has been the principal method for indoor humidity control for central A/C systems. This method is costly and energy inefficient since it uses a great deal of energy to overcool the air, and then more energy to reheat the air to a suitable

supply temperature. The use of reheating is however uncommon for DX A/C systems, nonetheless controlling indoor humidity at an appropriate level while also maintaining suitable indoor air temperature using a DX A/C system is difficult, since the cooling coil in a DX A/C system must perform both air cooling and dehumidification simultaneously. Most DX A/C systems are currently however equipped with a single-speed compressor and supply fan, relying on on-off cycling compressor as a low-cost approach to maintain only indoor air dry-bulb temperature. This results in either space overcooling or an uncontrolled equilibrium indoor relative humidity (RH) level.

The recent advancement of low-cost variable speed drive (VSD) technology offers tremendous opportunities for improving indoor thermal control and energy efficiency for DX A/C systems. Compressor speed can be continuously varied to modulate the output cooling capacity to match the space actual thermal load. The supply fan speed can be also altered to affect both sensible heat and latent heat transfer rates across a heat exchanger. Therefore it is possible to simultaneously control indoor air temperature and humidity by varying speeds of both compressor and supply fan in a DX A/C system.

Although there are limited related studies reported on indoor air temperature control and humidity control in open literatures, most of them treated indoor air temperature control and humidity control separately, using single-input single-output (SISO) control approach which resulted in poor control performance. No previously related research work on controlling indoor air temperature and humidity using multiple-input multiple-output (MIMO) control approach can be indentified in open literatures. Therefore it is

necessary to fill the gap and embark on a study on developing an MIMO control strategy that can simultaneously control indoor air temperature and humidity by varying the speeds of both compressor and supply fan in a DX A/C system, through both mathematical modeling and experimental approaches.

This Thesis begins with in Chapter 2 a critical literature review of various issues on both the effects of humidity on human thermal comfort and indoor thermal environmental control, and the modeling and control for DX A/C systems. Firstly an extensive literature review on a number of issues related to the suitable range of indoor relative humidity (RH) for thermal comfort, the effects of RH level on human thermal comfort, the sources of indoor moisture and the methodologies of removing moisture from air such as the mechanical dehumidification and chemical dehumidification, etc., is presented. Secondly a review of previous modeling studies of DX A/C systems and their components such as evaporator, condenser, expansion valve and compressor, is reported. This is followed by reviewing various issues related to capacity control, indoor humidity control and advanced control strategies developed for or adopted in DX A/C systems. A number of important issues where further in-depth research work is required to achieve appropriate control over both indoor air temperature and humidity using a DX A/C system have been identified.

Chapter 3 presents the research proposal which covers the aims and objectives, the project title, and research methodologies adopted for the research work reported in this thesis.

Chapter 4 describes an experimental DX A/C system available to facilitate the research work reported in this thesis. Detailed descriptions of the experimental DX A/C system and its major components are firstly given. This is followed by describing the computerized measuring devices and a data acquisition system (DAS). A computer supervisory program used to operate and control the experimental DX A/C system is also detailed. The availability of the experimental system has been expected to be helpful in successfully carrying out the research work proposed in Chapter 3.

Chapter 5 reports on the development of a multivariable control-oriented dynamic model for the experimental DX A/C system, based on the principles of energy and mass conservation. The dynamic model consisted of a set of differential equations, and was linearized and written in a state-space representation which was highly suitable for multivariable control design. The dynamic model developed was experimentally validated. Experimental tests to obtain the open-loop responses of the DX A/C system after being subjected to step changes in compressor speed and supply fan speed have been carried out. The measured experimental open-loop responses for all major operational parameters were compared with the simulated open-loop responses from the dynamic model, and a good agreement between the measured and simulated open-loop responses was found and the model was thus experimentally validated.

In Chapter 6, both the development of an MIMO feedback controller for simultaneously controlling indoor temperature and humidity in a space served by a DX A/C system and its controllability tests using the experimental DX A/C system are presented. The

MIMO controller was designed based on the linearized dynamic model reported in Chapter 5 using Linear Quadratic Gaussian (LQG) technique. The controllability tests for both disturbance rejection capability and command following capability were carried out to evaluate the performance of the MIMO controller using the experimental DX A/C system. The controllability test results demonstrated that the MIMO controller developed can effectively control the indoor air temperature and humidity simultaneously to their respective setpoints by varying both compressor speed and supply fan speed in the experimental DX A/C system.

Chapter 7 reports on the development of a new controller for degree of refrigerant superheat (DS), for improving the control performance of DS in a DX A/C system when the fluctuation of operating DS was resulted mainly from varying speeds of its compressor and supply fan as required by a capacity controller such as the MIMO controller developed for the experimental DX A/C system. The new DS controller was developed from a conventional proportional-integral-derivative (PID) DS controller by adding two feed-forward channels so that information of speed changes of compressor and supply fan can be timely passed to the new DS controller. Controllability test results showed that an improved DS control performance can be achieved when using the new DS controller, and consequently a better operating performance of the experimental DX A/C system in terms of operating efficiency and stability has been achieved.

Finally, the conclusions of this thesis and the proposed future work are presented in Chapter 8.

Chapter 2

Literature review

2.1 Introduction

Heating, Ventilation and Air Conditioning (HVAC) systems, which are widely used in commercial and residential buildings, play an important role in controlling suitable indoor built environment in buildings. With pursuing high quality living and working environments, the HVAC industry is struggling to improve thermal environmental control in spaces while at the same time to achieve high energy efficiency in operating HVAC systems. It has been reported that energy used for building cooling and heating accounted for more than half of the total energy use in commercial and public buildings in Hong Kong [Lam 2000].

The use of DX A/C systems has become widespread, in particular in small- to medium-scaled buildings. Compared to chilled-water based central air conditioning systems, the use of DX A/C systems is more advantageous because they are simpler, more energy efficient and generally cost less to own and maintain. In a DX A/C system, its DX evaporator is used directly as a cooling coil to simultaneously cool and dehumidify the air passing through it. This distinguishes itself from a conventional central chilled-water based A/C system where chilled water is used for cooling and dehumidifying air. Given their simplicity in structure and flexibility in installation, DX A/C systems are widely used in residences. For example, in Hong Kong the annual total sale of DX residential

air conditioners was around 400,000 units in 2000 [Zhang 2002]. Air-conditioning is the largest single electricity-consuming end-use accounting for on average 36.8% of the total residential electricity use in HK [Lam 1996]. According to Department of Energy in USA, packaged rooftop DX A/C units consumed approximately 60% of the total energy used for cooling [Bordick and Gilbride 2002].

In buildings, controlling indoor humidity at an appropriate level is important since this directly affects indoor thermal comfort and indoor air quality (IAQ) [Fanger 2001, Mazzei et al. 2005]. As pointed out in ASHRAE Standard 62.1-2005, indoor relative humidity (RH) level should be controlled within a relatively narrow range at between 30% and 60%. However, for most applications where DX air conditioners such as window units or split-type units are used, indoor air temperature is often controlled by on-off cycling the compressor in a DX air conditioner. Hence while indoor sensible load is satisfied through altering the length of on-off period, dehumidification is only a by-product of the cooling process. Therefore indoor humidity is not directly controlled and it fluctuates as a result of changing the match between the output sensible and latent capacities of a DX A/C unit and the space sensible and latent loads. When the output latent capacity is inadequate to meet the space latent load, indoor humidity would increase. In order to improve the indoor thermal environmental control in buildings, in particular the buildings located in hot and humid climates, it is therefore essential to develop new control strategies that enable the simultaneous control over indoor air temperature and humidity in spaces served by DX A/C systems.

This Chapter presents a critical literature review on various issues related to both the effects of humidity on human thermal comfort and indoor environmental control, and the modeling and control for DX A/C systems. An extensive literature review on a number of issues related to the suitable range of indoor relative humidity for thermal comfort, the effects of RH level on human thermal comfort, the sources of indoor moisture and the methodologies of removing moisture from air such as the mechanical dehumidification and chemical dehumidification, etc., is firstly presented. Secondly a review of previous studies of modeling DX A/C systems and their components such as evaporator, condenser, compressor and expansion valve, is reported. This is followed by reviewing various issues related to capacity control, indoor humidity control and advanced control strategies developed for or adopted in DX A/C systems. A number of important issues where further in-depth research work is required to achieve appropriate control over both indoor air temperature and humidity using a DX A/C system have been identified.

2.2 Effects of humidity on human thermal comfort and indoor thermal environmental control

2.2.1 Effects of humidity on thermal comfort and sources of indoor moisture

The problem of having an inappropriate level of indoor humidity can be found in different types of buildings, such as office buildings, supermarkets, libraries, hotels, as

well as residential buildings, etc. Very often a building A/C system is unable to properly deal with the thermal load imposed when its latent part is high, due to either a large internal moisture generation or the ingress of humid outdoor air through either ventilation or infiltration. The mismatch between space latent load and equipment output latent capacity can result in an inappropriate level of indoor humidity, degrading occupants' comfort and productivity. In buildings, it has been recommended that the suitable range for indoor relative humidity be between 30% and 60%, and the upper limit be set at 60% RH [ASHRAE 2000]. A large number of investigations have been carried out on the levels of relative humidity affecting IAQ and human thermal comfort [de Dear et al. 1989, Tanabe and Kimura 1994, Armstrong and Liaw 2002, Miro 2005]. The studies showed that indoor air relative humidity levels have both direct and indirect impacts on occupants' thermal comfort in different ways. A high level of indoor air relative humidity may cause health problems for occupants due to the growth of contaminated aerosols produced by spray humidification systems [Arens and Baughman 1996]. A low relative humidity level also has comfort and health impacts since it can lead to the drying of skin and mucous surfaces, promoting the accumulation of electrostatic charges in fabric and others materials in buildings [Green 1982, Berglund 1998].

For an appropriate indoor humidity control, it is indispensable that the amount of moisture removal must be equal to the amount of moisture introduced into a space. The sources of indoor moisture can be classified as being external and internal. One external source for indoor moisture is the infiltration of outdoor air. The amount of moisture in a

conditioned space due to air infiltration is a function of infiltrated air mass flow rate, moisture content difference between outdoor air and indoor air. Although the infiltration through a building enclosure is intermittent and unintentional, it has been emphasized that its effects on indoor RH level cannot be overlooked [Fairey and Keresteciogl u 1985, Straube 2002]. Henderson et al. [1992] showed that infiltration would have a great impact on space latent cooling load through simulation in typical buildings in both Miami and Atlanta. The other important source of indoor moisture is the outdoor air ventilated through A/C systems. In ASHRAE Standard 62.2P, Ventilation and Acceptable IAQ in Low-rise Residential Buildings, there is a special consideration that the moisture from outdoor ventilation air is of particular concern, especially in hot and humid climates [Sherman 1999] where the latent cooling load from ventilation air can be greater than the sum of all other latent cooling loads.

The internal sources for indoor moisture load mainly include the moisture gains from occupants and other indoor activities, such as washing, cooking etc. However, one source for indoor moisture is related to the operation of a DX A/C system when its compressor is on-off controlled. In a space served with a DX A/C unit, a supply fan in the DX A/C unit is normally run continuously regardless of its compressor's operating status. When the compressor is on, moisture is condensed over cooling coil surface and collects in a drain pan. However, if the supply fan is still on when the compressor cycles off, moisture on the wet cooling coil and drain pan may be reintroduced into air stream due to constant air circulation, resulting in a rise in RH level in the conditioned space [Kosar et al. 1998, Amrane et al. 2003, Shirey and Henderson 2004]. The moisture load

contributed by human occupancy, as pointed out by the ASHRAE Handbook of HVAC Systems and Equipment 2000, depends on the number of occupants and the level of their physical activity [ASHRAE 2000]. A number of investigations on improving the prediction accuracy of internal humidity level have been undertaken [Thomas and Burch 1990, Keresteciogl u and Gu 1990, Budaiwi et al. 1999, Galbraith and Lean 1993, Galbraith et al. 1997]. The study undertaken by Lucas and Miranville [2004] took into account the moisture transfers between walls and air inside a space, and improved the forecast accuracy of the amount of water condensed on an internal wall surface.

Therefore in buildings the sources of indoor moisture load would mainly include building occupants and ventilation air. In order to maintain an adequate level of thermal comfort, these moisture loads must be removed and indoor relative humidity kept within the recommended range.

2.2.2 Dehumidification using in A/C systems

The use of HVAC systems for indoor thermal environmental control gains increasing attention, especially in the light of developing a recent standard on ventilation [ASHRAE 2005], so that an optimal level of indoor humidity may be reached and maintained to ensure a comfortable and healthy indoor environment. For buildings located in hot and humid subtropical region, indoor humidity level is often higher than the recommended level, thus dehumidification using A/C systems becomes necessary.

There are mainly two types of dehumidification used in HVAC systems: mechanical dehumidification and chemical dehumidification.

2.2.2.1 Mechanical dehumidification

Mechanical dehumidification, which is widely known to be based on cooling by vapor compression refrigeration systems or using chilled water, utilizes mechanical means to cool air and so to dehumidify it. If the air comes into contact with a cooling coil whose mean surface temperature is lower than air dew point temperature, condensation of a part of the water vapor in the air and thus dehumidification is obtained. The moisture content of air leaving a cooling coil depends on the apparatus dew point of the coil, which is principally a function of either the refrigerant temperature inside the coil when a DX cooling coil is used, or the chilled water temperature when a chilled water coil is used. To increase the dehumidification capacity of a cooling coil, it would be better to use a large number of fins, with a moderate air velocity, and with a low fin density [Mazzei et al. 2005]. The dehumidification behavior of a standard cross-flow type plate heat exchanger, used as a dehumidifier and cooler, was investigated by Saman and Alizadeh [2002] both experimentally and numerically. In many HVAC systems, mechanical dehumidification is widely used. This is also true for DX A/C systems, since it would be costly and complicated to use other types of dehumidification techniques in DX A/C systems. Mechanical dehumidification has strong advantages at a higher dehumidifying demand where cooling is needed in addition to dehumidification because the cooling coils cool and dehumidify the air simultaneously. It is energy-efficient

compared to other methods of removing moisture from air. However, the disadvantage of mechanical dehumidification is that because the sensible cooling capacity and latent cooling capacity of a cooling coil are coupled, it is not easy to simultaneously control temperature and humidity of the air leaving the cooling coil. Therefore energy is often wasted in traditional HVAC systems by over cooling and reheating the air to maintain an appropriate level of humidity in spaces.

2.2.2.2 Chemical dehumidification

Chemical dehumidification removes the moisture from the air by transferring it to a water absorbing material such as desiccants through adsorption or absorption. Desiccants are materials with a high affinity for water vapor and may be in the form of either solid or liquid. If the physical or chemical nature of the desiccant, generally being solid such as silica gel, remains unchanged in a dehumidification process, then adsorption takes place. Conversely absorption takes place when a change occurs, generally with liquid desiccants. Liquid desiccants are used as a dehumidification agent in many industrial applications and have been investigated for use in space conditioning applications [Peng and Howell, 1981]. Dehumidification equipment using solid desiccant may be classified into two types, active type and passive type. The equipment using heated reactivation air is called an active dehumidifier. The heat used for reactivation often comes from distributed power generation or natural gas, all of which are inexpensive during humid seasons. A passive dehumidifier however uses a

building's dry exhaust air instead of heated air for reactivation [Harriman III et al. 1999, Harriman III et al. 2001]. A solid-desiccant based dehumidifier is more compact but, presents a higher pressure drop for both the air to be dehumidified and the air for regeneration, therefore a higher fan power is required. The final temperature of the processed air is always high, leading to a decrease of the adsorption capacity of desiccant. In addition, heat generated by a solid desiccant dehumidifier affects occupants' thermal comfort [Andersson and Lindholm 2001, Capehart 2003, Subramanyam et al. 2004, Alpuche et al. 2005].

Comparing to a solid desiccant-based system, a liquid desiccant-based system needs a lower fan power. The use of a liquid desiccant-based system can easily control the air temperature during absorption, resulting in a lower temperature of the processed air. Another advantage of using liquid desiccant is better air cleaning. It is believed that the liquid desiccant's washing action in hospital environment would both reduce airborne bacteria and remove particulate matter [Dai et al. 2001, Dieckmann et al. 2004, Rowland et al. 2005, Elsarrag et al. 2005]. Latent heat and sensible heat of water vapor extracted from the air are dumped into cooling water of the absorber, in order to keep a low dew point of the processed air. This operation is cooled by a chiller, thus requiring further additional operating costs. Therefore the operating costs using desiccants for dehumidification are higher when compared to other indoor humidity control strategies [Lstiburek 2002].

2.3 Modeling of DX A/C systems

The research work based on mathematical modeling has gained more and more recognition because mathematical modeling could not only save the cost of research, but also help understand the operating characteristics of a physical system under study over its entire operating range. In the field of HVAC and Refrigeration, simulation-based research has become more and more popular [Xu et al. 1996]. Simulation can be applied to system design, optimization and developing new control strategies. It can also help investigate the operational performance of a system, to verify the feasibility of a new control strategy and to detect and diagnose the faults of a system, etc.

A large number of literature have been found on modeling both the steady state and the dynamic behaviors of HVAC and Refrigeration systems. These models can be classified into two broad groups: empirical and physical models. In empirical models one tries to estimate the functional form of the relations amongst variables and the numerical parameters without requiring detailed information of system components. Examples of empirical models include regression analysis, polynomial curve fits and artificial neural networks. Given the difficulty to characterize accurately all the components in an HVAC or refrigeration system and the noticed general good behavior in time response and accuracy of empirical models, empirical approaches are widely used for modeling HVAC and refrigeration systems [Navarro-Esbri et al. 2007].

The physical models are based on detailed information of the elements in a physical system and derived from physics laws. Simulation-based research based on physical models can be classified into the following two types, lumped- and distributed-parameter modeling. Distributed-parameter mathematical modeling can reflect well the distributive characteristics of a system's parameters, which is particularly useful in, for example, studying the air flow field inside an evaporator. However carrying out distributed-parameter simulation research is time-consuming, with perhaps poor calculation stability. On the other hand, although lumped-parameter simulation research is relatively simple and is hard to reflect the detailed distribution of parameters along the dimension of a system component, it is more useful in studying its overall performance, and consequently usually more effective in carrying out research work related to system control. Furthermore, modeling may also be classified into dynamic and steady-state modeling. Steady-state modeling should be sufficiently accurate for most long-term system simulations or for design optimization. However, it is not suitable for control application where it is necessary to investigate system's transient responses to sudden disturbances. Dynamic modeling is required when carrying out research work related to the control for a physical system.

Generally, a DX A/C system may be considered as consisting of four basic components and a conditioned space. Therefore the models of various components in a DX A/C system are separately reviewed as follows.

2.3.1 Heat exchangers (evaporator and condenser) modeling

Modeling heat exchangers has always been in the spotlight of simulation-based research work for HVAC and Refrigeration systems. Diversified approaches have been employed to establish the models for evaporators and condensers. The models of heat exchangers can generally be divided into three types: (1) single node model or lumped parameter model, (2) multi-node model or distributed parameter model, and (3) zone model or partially lumped parameter model.

A single-node model, such as the logarithmic mean temperature difference method, is simple. But its accuracy is limited and it is ineffective for use with a heat exchanger where the phase change takes place. A multi-node model divides a heat exchanger into several control volumes and the parameters in each control volume are lumped. It has a higher accuracy than a single node model or lumped parameter model, but the time needed for simulation becomes longer. A zone model divides a heat exchanger into several zones and the parameters in each zone are also lumped. Usually three zones, i.e., a superheated zone, a two-phase zone and a sub-cooling zone, are included for a condenser; and two zones, i.e., a two-phase zone and a superheated zone are included for an evaporator. Both the accuracy and the calculation speed for a zone model are between those of a lumped parameter model and those of a distributed parameter model. There is little difference between the prediction accuracy between a zone model and a distributed parameter model, while the calculation speed of a zone model is obviously

faster than that of a distributed model, so a zone model is suitable for system simulation when the accuracy requirement is not too high.

Many investigations on modeling heat exchangers using lumped-parameter models [Chi and Didion 1982, Vargas and Parise 1995, and Nyers and Stoyan 1994], and using the distributed-parameter models [MacArthur 1984 and Bensafi et al. 1997] have been carried out. Wang and Touber [1991] suggested that distributed parameter models provided the most complete information and best insight into the dynamic behavior of an evaporator. Jia et al. [1995] presented a distributed parameter model for predicting the transient performance of a DX air cooling evaporator. The model was capable of predicting the distributions of the refrigerant velocity, void fraction, temperature, tube wall temperature, air temperature and humidity, in both location and time domains. The dynamic behavior of the evaporator was investigated with a response to a step change in the inlet refrigerant flow rate. Simulation results were compared with the experimental measurements in a commercial evaporator using refrigerant R134a as the working fluid. The comparison results indicated that the model provided a reasonable accurate estimation of the dynamic response. Another general distributed parameter model for evaporators by Jia et al. [1999] took into account the non-homogeneous flows of the liquid and vapor refrigerant in the two-phase region and was applicable to both cocurrent-flow and counter-flow configurations. Porkhial et al. [2004] developed a distributed parameter model for predicting the transient performance of an evaporator. The model was capable of predicting the refrigerant temperature distribution, tube wall temperature, inventory mass of refrigerant as a function of location and time.

Partially lumped parameter models by Deng [2000] and Domanski [1991] used a different approach where for example a condenser was divided into three zones, i.e., two-phase, superheated and sub-cooling zone. Three zones were modeled separately based on the different heat transfer and fluid flow characteristics. This approach can adequately represent the overall thermal characteristics in a heat exchanger in operation to carry out research work related to control, and its simulation stability and computational speed may be well ensured. He et al. [1997] developed a partially lumped parameter model for a two-phase flow heat exchanger, which was described mathematically by a set of complex, coupled and nonlinear partial differential equations based on the principles of mass and energy conservation, with the assumptions that the heat exchanger was a long, thin horizontal tube, and that the refrigerant flowing through the heat exchanger tube was one-dimensional.

Zhang and Zhang [2006] developed a model based on the moving boundary approach to describe the transient behavior of the DX evaporator in a vapor compression refrigeration system, which allowed the superheated region in the evaporator to be included or excluded. A time-variant, rather than a constant, mean void fraction was employed to improve the robustness of a traditional moving boundary model under larger disturbances. Numerical integration was applied to getting the mean refrigerant properties in both the two-phase region and the superheated region. The temperature at the interface between the two phase and the superheated regions was also evaluated. Qualitative case studies showed that the model can well predict the transient behaviors

of the evaporator under larger disturbances and maintain the robustness of the model regardless whether the superheated region exists or not.

When modeling a heat exchanger, its heat transfer and fluid flow characteristics are embodied in mathematical correlations of heat transfer coefficients and the total pressure drop. For a refrigerant-to-air heat exchanger using different internal micro-fin tube for heat transfer enhancement, its air-side heat transfer resistance may account for over 80% of the total heat transfer resistance. Hence, the correlations of air-side heat transfer coefficients would significantly affect the modeling accuracy for the overall heat transfer. A set of relatively simple correlations for the average heat transfer coefficient for a plate-finned tube was developed by Turaga et al [1988]. The experimental comparison by Corberan and Melon [1998] showed that the correlations for a multiple-row heat exchanger having flat fins provided by Gray and Webb [1986] agreed well with the experimental data. It was recommended that an air-side heat transfer coefficient for wavy and louvered fins, which were widely used in air conditioning and refrigeration installations, could be evaluated using the coefficient for a flat fin and multiplying it by an enhancement factor appropriate to a given fin design. Webb [1990] developed an enhancement factor correlation for wavy fins that can take into account the flow conditions and geometric variables of a heat exchanger. Currently, the most commonly enhanced surface used in DX A/C systems is of louvered fin type that can provide a higher average heat transfer coefficient. Wang et al. [1999 and 2000] proposed general heat transfer correlations for louvered fin geometry having round tube configuration under dry and wet conditions, respectively. A total of 49 samples of

louvered fin-and-tube heat exchangers with different geometric parameters, including louver pitch, louver height, longitudinal tube pitch, transverse tube pitch, tube diameter, and fin pitch were included in the correlations developed.

In lumped-parameter models of a heat exchanger, the refrigerant pressure drop through a heat exchanger was often neglected or a fixed value was assumed. In fact, the refrigerant pressure drop in a heat exchanger, particularly in an evaporator, impacted on the performance of a refrigeration system, as this would directly affect the evaporating or condensing pressure. More importantly, this would also affect the compressor suction pressure and the degree of refrigerant superheat, and hence the refrigerant state at compressor suction. The refrigerant state at suction was very important to calculate the refrigerant mass flow rate passing through a compressor, and then the cooling capacity of a refrigeration system. The uncertainty of refrigerant flow rate would reduce the accuracy of simulation for a DX refrigeration system. According to the correlations by Pierre [1964], the refrigerant pressure drop through a heat exchanger was proportional to the square of refrigerant flow rate. Although there have been many reported studies on the pressure drop for various refrigerants including R134a inside a heat exchanger [Cavallini et al. 2001], a general average pressure drop correlation has been in fact hard to establish because an average pressure drop would be closely related to the configuration of internal tube surface and actual heat exchanger's geometry such as circuitry arrangements, etc.

It is well known that the key operating parameters of a DX cooling coil, such as evaporating temperature, refrigerant mass flow rate, coil face velocity and inlet air temperature, would have significant influence on its performance. Liang et al. [1999] developed a distributed simulation model for a DX cooling coil in which there were three heat transfer zones on its refrigerant side, and two zones on its air side, e.g., dry-cooling zone and wet-cooling zone. The model used a numerical method to calculate the partially wet and totally wet fin efficiency. On the basis of this model, a number of parameters which reflected the characteristics of air cooling coils used in diverse humid environments were analyzed. It was found that the performance of the coil was significantly affected by levels of indoor air relative humidity, which was a very significant parameter in determining the energy requirement and the quality of air conditioning in a humid environment. A high humid environment would imply a higher cooling load and hence a higher energy requirement compared to a low humid environment.

2.3.2 Compressor modeling

A compressor is the most complex component in a vapor compression refrigeration machine. The compressor turns the low pressure vapor refrigerant into high pressure vapor refrigerant such that it can condense in a condenser to reject heat to a second fluid, and a refrigeration cycle can go on. There are several types of compressors for air

conditioning applications, such as reciprocating compressor, rotary screw compressor, scroll compressor and centrifugal compressor.

For both reciprocating compressors and scroll compressors, many different models with different degrees of complexity were found in the literature. There were models of reciprocating compressors in which a compressor was divided into several control volumes based on elements such as compression chamber and valves, etc. These models required input data very difficult to obtain or known only to the manufacturer of the compressor. The space volumes of the different elements and the effective surface areas of valves were also required. The transient fluid conservation equations (mass, momentum and energy) were integrated over the entire compressor domain and the energy balance for the refrigerant inside the cylinder was computed for each time step of an operating cycle [Perez-Segarra et al. 2003, Rigola et al. 2003, Todescat and Fagotti 1992]. In the model developed by Popovic and Shapiro [1995], eight sets of input data were sufficient to determine the mass flow rate of refrigerant and the required input compressor power. Winandy et al. [2002a] pointed out that the refrigerant mass flow rate was affected by the clearance volume re-expansion, the pressure drop in the suction valve and the heat transfer from the fictitious isothermal compressor wall. Jahnig et al. [2000] developed a simple thermodynamic model for reciprocating compressors used in domestic appliances.

The models for scroll compressors [Chen et al. 2002a and 2002b] required the knowledge of pocket volumes and perimeters for every six degrees of rotation, the

height, thickness and pitch of the scrolls that were quite difficult to obtain. In those models, the whole compressor was divided into several chambers and a compression process was simulated for every gas pocket. It required the evaluation of areas, volume, pressure, temperature and specific volume for every crank angle. Mass and energy conservation equations were developed for each chamber. These models [Winandy et al. 2002b] were thermodynamics based and had the same philosophy as those used in reciprocating compressors. The refrigerant mass flow rate was affected by the increase of suction temperature of refrigerant and a compression process was considered isentropic.

Duprez et al. [2007] developed simple but thermodynamically realistic models for reciprocating and scroll compressors used in residential air conditioners or heat pumps. These models can calculate the mass flow rate of refrigerant and the power consumption from the knowledge of operating conditions (e.g., evaporating temperature and the refrigerant temperature at the compressor inlet). Parameters appearing in these models were found in the technical datasheets of the compressors or fitted in such a way that the calculated mass flow rate and electrical power matched those given in these datasheets.

There have been also many investigations concerning models to simulate the behaviors of open or hermetic refrigeration compressors. Some of these models were complex and took into account the refrigerant mass flow conditions through the inlet and outlet valves and the heat exchange in various internal components of a compressor [Yasuda et al. 1983]. Other models did not take into account the variation of mass flow in a

compressor, thus assuming the same mass flow at the inlet and the outlet of the compressor. The enthalpy at the compressor outlet was calculated considering a compression process as being isentropic [Koury et al. 2001].

Compared to an evaporator or a condenser, the dynamics of a compressor may be negligible, quasi-steady modeling was therefore usually applied. This was achieved by assuming that a compressor reached its specified operating speed instantly. Generally, a polytropic compression process was assumed and a mathematical model for compressors can be established by using the traditional thermodynamic approach [Domanski and Mclinden 1992, Matthew and Banasal 1998]. A model developed by using this approach was suitable for system simulation, and particularly for energy performance analysis and the investigations related to system control. When modeling, the volumetric and electric efficiencies were usually represented by an empirical correlation or determined using the actual performance data with the aid of curve fitting or regression analysis. The latter that can achieve a better approximation than the former, required a set of detailed tested performance data of compressor from manufacturers or in-situ tests. Therefore for research work related to the control of a DX refrigeration system, the model for its compressor should be simple in structure and fast in response for easy incorporation into the complete model of a DX A/C system. In fact, the accuracy of a compressor model when simulating refrigerant mass flow rate and discharge temperature was mostly important for simulation-based research work related to system control.

2.3.3 Expansion valve modeling

The expansion device in a refrigeration system controls the refrigerant mass flow and balances the system pressure. Various expansion devices such as a capillary tube, a short tube orifice and a thermostatic expansion valve (TEV) are used in small refrigeration systems, air-conditioners and heat pumps. Even though capillary tubes and short tube orifices have the advantages of simplicity, low cost and low starting torque for a compressor, they are not appropriate for use in a system that requires precise flow control over a wide range of operating conditions. A TEV adopts a mechanical control method to maintain a constant degree of superheat at evaporator outlet. Therefore, the response time of a TEV is relatively slow, and this slowness may cause an unstable operating condition. However, an electronic expansion valve (EEV) has the advantages of rapid response owing to electronic signal transmission, zero activating degree of superheat, nearly linear valve characteristic, a wide range of flow rates and easy realization of programmed control, etc. It is expected that an EEV would gain a wider future application in DX A/C systems. Therefore, an EEV is indispensable if the advantages of a DX A/C system having a variable-speed compressor are to be maximized. As an essential component in a DX A/C system, an EEV acts as a throttling device where the expansion of refrigerant takes place, and usually regulates the refrigerant flow rate such that a desired degree of superheat at the exit of an evaporator can be maintained.

Commonly, an expansion valve can be represented by a steady-state model due to its very small thermal inertia. Refrigerant expansion is generally treated as an isenthalpic process when modeling an expansion valve. Refrigerant mass flow passing through an expansion valve is usually calculated by using an empirical correlation. Deng [2000] presented a relatively simple model for an expansion valve. The model simply considered the refrigerant mass flow rate proportional to the degree of refrigerant superheat, however, the actual fluid-flow characteristic in an expansion valve was hard to be represented by the model. MacArthur [1984] represented an expansion valve by an orifice equation. Park et al. [2007] developed an empirical correlation for predicting the mass flow rate passing through an EEV by modifying a single-phase orifice equation with consideration of EEV's geometries and operating conditions. Geometric parameters that were included in the empirical correlation were orifice diameter, orifice length and the EEV's opening. One representative model for expansion valve was developed by Damasceno and Rooke [1990], based on the specifications given by manufacturer and the empirical fitting for one set of distributor nozzle and tube size.

2.3.4 Air conditioned space modeling

Two types of mathematical methods have been used in modeling air-conditioned spaces or buildings. One was the frequency domain method, such as Flourier Transformation; the other the time domain method, such as Transfer Function [Stephenson and Mitalas 1971], Thermal Response Factors [Stephenson and Mitalas 1967], and State Space method [Hong and Jiang 1997]. Masato et al. [2000] derived a simplified dynamic

model for an air conditioned space for control analysis, which can provide an indicative temperature distribution inside the space. The whole space under study was divided into five zones and the dynamics of each zone described by a lumped-parameter model.

2.4 Control issues for DX A/C systems

One of main purposes of controlling an A/C system is to ensure that the desired air temperature and/or humidity in a conditioned space served by the A/C system are maintained. If A/C systems were always operated with constant loads, little or no capacity control would be needed. However, most A/C systems are designed to meet the demands under the worst conditions, i.e., the hottest or coldest climate conditions, thus for most of time the systems are operated at part-load condition. Therefore an important function of the controllers for A/C systems is to ensure that indoor thermal comfort and energy efficiency of A/C systems can be maintained. In recent years, the advancement of low-cost digital technology in the measurement and control field has brought the use of Direct Digital Control (DDC) to A/C systems. DDC-based control for A/C systems permits continuous monitoring of system parameters, fault detection, diagnosis and alarm, etc. [Capuano et al. 1999]. However, there are also a number of deficiencies associated with the control of A/C systems even DDC technology is applied to A/C systems' control. These include capacity control and humidity control, among others.

2.4.1 Capacity control

Building heating or cooling loads do not stay unchanged but vary with time, it is therefore important to implement certain capacity control schemes to continuously adjust the output capacity of DX A/C systems to match the varying building loads. Several methods of capacity control have been applied to DX A/C installations.

Firstly, the most commonly used method in small size residential DX A/C systems is intermittent running of compressor, e.g., on/off cycling. The disadvantage of this method is that it imposes wear and tear on the compressor and reduces the life of compressor. In addition, it is difficult to maintain a steady indoor air temperature within a suitable range.

Secondly, capacity control can be achieved by using suction-gas throttling, hot-gas by-pass or cylinder-unloading, etc. In the hot-gas by-pass control method, the refrigerant is by-passed from the compressor and injected back into the suction line to decrease the cooling capacity, whereas in the cylinder-unloading scheme, one or more cylinders are unloaded to decrease the refrigerant mass flow rate being circulated, hence the cooling capacity. However, with suction gas throttling, the suction gas throttled occupies a large volume at the inlet of a compressor and thus decreases the refrigerant mass flow rate, and hence the system's capacity. A numerical investigation on the above three capacity control methods for HFC-134a refrigeration systems was carried out by Yaqub and Zubair [2001]. The study results showed that the cylinder-unloading method was mostly

suitable because of a high coefficient of performance (COP) in comparison with the other two methods. However, the capacity reduction was restricted to about 25%, 50%, or 75% of the total in a 4-cylinder compressor. On the other hand, the hot-gas by-pass scheme will lead to the lowest COP. Moreover, it was not suitable from the thermodynamic point of view. In addition, a very high compressor discharge temperature will restrict the capacity reduction down to around 50%. For the suction-gas throttling method, precise indoor air temperature and humidity control may be achieved and the COP was in between those by the other two methods. Furthermore, the compressor discharge temperature was the lowest, and a wide range of capacity reduction was possible with this method, depending upon the degree of throttling at compressor inlet.

Thirdly, the method of capacity control is to vary the flow of refrigerant by using variable speed compressors in DX A/C systems. Variable speed compressor coupled with EEV in a variable refrigerant volume (VRV) A/C system can modulate precisely the refrigerant flow rate and hence system's cooling capacity, making the accurate matching between output cooling capacity and varying thermal load possible. It was reported that through the modulation of compressor speed, the output cooling capacity from a residential split-type DX A/C system could be varied between 50 and 100% of its full capacity in proportion to the change in room temperature [Lida et al. 1982]. Currently with the advancement of variable speed compressor and EEV technologies, inverter-aided DX A/C systems can vary their cooling outputs between 20% and 100% of the full load. The use of variable speed compressor for capacity control may offer the

potential for greater energy savings during part load operations. On the other hand, the energy performance of a conventional DX A/C system with a single speed compressor at part load condition was degraded dramatically [Silver et al. 1990]. During part load operation, the condensing and evaporating pressures/temperatures of a DX A/C system will respectively decrease and increase with a lower compressor speed, which would substantially increase its COP [Scalabrin and Bianco 1994]. Yang and Lee [1991] presented an analysis for an inverter-driven variable speed air conditioning system used in a hot and humid region. The results indicated that the use of variable-speed compressor could provide an annual energy saving of 20%. Furthermore, it can be expected that the pull-down time needed for a DX A/C system to reach a temperature setting during start-up can be reduced because a compressor can operate initially at its highest speed. Energy saving through using variable speed compressors in residential and commercial air conditioning systems was also analyzed by Cohen et al. [1974]. It was emphasized that energy could be saved on a seasonal basis because the system would operate more efficiently at lower capacity, due to the reduced frictional losses in the compressor and the reduced pressure ratio imposed on the compressor. It was concluded that variable capacity control could provide energy savings of 28%-35% on a seasonal basis, without significant changes in system sizes. Other advantages such as reduced torque requirements at initial start up, low noise operation under most load conditions and fewer on/off cycles can also be obtained.

In the past, variable speed compressors were generally regarded to be suitable only for use in small-scale A/C systems, but not in medium- or large-scaled A/C systems due to

the lack of sufficient development and component integration. Fortunately, in recent years medium- to large-scaled variable speed compressors have gained great improvement in various aspects and been widely used in medium-capacity multi-evaporator A/C systems [Youn et al. 2002]. In order to demonstrate the benefit and feasibility of variable speed technology used in large-scale centrifugal chiller systems, Lenarduzzi and Yap [1998] established a demonstration installation of variable speed compressor in retrofitting a chilled-water based A/C system. The system was monitored for one cooling season and the results showed that variable speed drive technology could also work successfully in large-scale A/C systems. It was estimated that approximately 41% of energy saving could be achieved for this particular site and the power quality and total harmonic distortion problem induced could be neglected. Therefore, the VRV technology featured with variable speed compressor and EEV has been proven to be an energy efficient and practical way to realize capacity control in medium- or large-scaled A/C systems. Qureshi and Tassou [1996] made theoretical and practical comparisons of various capacity control methods at full- and part-load conditions, and results showed that a variable speed operation was the most energy efficient technique for capacity control in A/C systems.

2.4.2 Humidity control

Inadequate humidity control may be found in many residential and commercial buildings. Such has been exacerbated by the following three facts in recent years. Firstly,

as required by ANSI/ASHRAE Standard 62-2001 [ASHRAE 2001], Ventilation for Acceptable Indoor Air Quality, ventilation requirements in all commercial buildings are enhanced. The additional ventilation imposes greater heating and cooling loads on HVAC equipment, resulting in a larger equipment size and higher energy use. The ventilation requirements have a particularly strong impact on indoor humidity control. In most regions, additional ventilation increases the latent load more than the sensible cooling, imposing a disproportionate demand on HVAC equipment [Huang and Franconi 1999]. Secondly, since the world energy crisis in the 1970s, building sensible cooling loads have decreased due to the improved envelope design and the increase in energy efficiency for lighting installations. The reduced space sensible cooling loads have also imposed a disproportionate dehumidification load on HVAC equipment. Thirdly, unitary air-conditioning equipment has shown dramatic improvements in efficiency over the past years. Much of this improvement is due to better compressor design and the increase of heat exchange surface areas. A larger coil allows a higher evaporating temperature, thus giving a higher system efficiency. However, a warmer cooling coil reduces the relative dehumidification capacity of building HVAC equipment [Brandemuehl and Katejanekarn 2004].

Traditionally, the principal method for indoor humidity control used in large central HVAC systems is to overcool air to extract more moisture and then to reheat it to a suitable supply temperature. This strategy is inherently costly and inefficient since it uses a great deal of energy to overcool air and then more energy to reheat it. However, reheating is uncommon in DX A/C units, thus the problem of indoor humidity control is

often encountered in spaces served by DX A/C units. In a DX A/C unit, dehumidification is less straightforward since a DX A/C unit removes moisture only when cooling the air passing through it. Dehumidification is affected by the condensing action at a cooling coil. The cooling coil has also a role to play in temperature control, thus this duel role of cooling and dehumidification for the cooling coil makes the controlled variables of temperature and humidity to become coupled. The current trend in designing a DX A/C unit is to have a smaller moisture removal capacity, in an attempt to boost its energy-efficiency rating (EER) and COP [Kittler 1996]. One of the methods used to improve efficiency is to increase the heat exchanger surface area. Such a strategy allows a DX A/C unit to run at a higher refrigerant temperature in its evaporator and a lower refrigerant temperature in its condenser, resulting in a lower latent capacity of the unit. Furthermore, when a DX A/C unit is operated at part load conditions, indoor humidity control problem could worsen with on-off cycling its compressor. The compressor will remove the sensible load with very little run-time to easily satisfy the thermostat setpoint and cycle off long before moisture removal can be affected [Hourahan 2004]. Indoor RH would rise to above the design level [Shirey and Henderson 2004].

Investigations have been carried out on control methodologies for reducing high indoor humidity during part-load conditions [Howell et al. 1987]. Chua et al. [2007] compared the following three control strategies for indoor air humidity control using large central chilled water based A/C systems, chilled water flow control, bypass air control and variable air volume control. Simulation results indicated that the chilled water flow

control strategy resulted in the highest indoor humidity throughout the range of outdoor air conditions studied. The variable air volume control could however maintain the indoor humidity at a low and acceptable value as compared to the other two control strategies but there were two distinct disadvantages. Firstly as the supply air flow rate dropped during part-load operations, the problem of stuffiness and stillness of air in a space may arise. Secondly, the supply air flow rate may be reduced to a low value that it cannot provide the required minimum ventilation rate. Niu et al. [2002] studied a HVAC system combining chilled-ceiling with desiccant cooling for maintaining the indoor air humidity within a comfort zone and to reduce the risk of water condensation on chilled panels. The results revealed that the use of chilled-ceiling combined with desiccant cooling might conserve up to 44% of primary energy use, compared to the use of a conventional constant volume all-air system.

Several enhanced dehumidification technologies may be used in DX A/C systems. These include thermally activated desiccant systems [Nagaya et al. 2006], heat pipe technology [Xiao et al. 1997, Yau 2007], and dual-path systems that pre-treat ventilation air, etc. The function of a heat pipe heat exchanger (HPHE) is to recover heat from warm outdoor air to reheat the dew-point of air stream and therefore to save reheat power. Kosar [2006] compared three enhanced dehumidification components in a conventional DX A/C system, e.g., a wraparound heat pipe heat exchanger, a desiccant dehumidifier in a wraparound configuration and a post coil desiccant dehumidifier regenerated by using condenser waste heat. These integrated systems provided the ability to reduce typical sensible heat ratio (SHR) levels for DX A/C systems at ARI-

rating conditions of 0.75 to below 0.50 in certain enhanced dehumidification systems while limiting losses in their COP and capacity.

As a general guideline, the dehumidifying or moisture-removal capacity of a DX A/C system increases when lowering both its evaporating temperature and the air face velocity across its DX coil. The previous field studies [Shirey 1993] have demonstrated the impacts of supply air flow rate and evaporating temperature on dehumidification. Hence, a DX A/C system incorporating VRV technology and a variable speed supply fan should be able to achieve accurate temperature and humidity control. Kalman et al. [1995] presented a control strategy in which the speed of a variable speed compressor was regulated in accordance with the change of space temperature, while that of supply fan in accordance with the space relative humidity. A PID control algorithm, where the controller parameters could be derived analytically based on a simulation model developed for the system, was used in this study. The feasibility to control the space temperature and relative humidity simultaneously by the coincident variation of compressor speed and supply fan speed, respectively, was verified experimentally. Similarly, Andrade and Bullard [2002] investigated, by means of simulation, the roles of supply air and refrigerant flow rate and their interactions on the performance of an air conditioner equipped with a variable-speed supply fan and compressor. Andrade and Bullard pointed out that varying the indoor blower speed could provide the necessary humidity control by adjusting the evaporator surface temperature to meet latent loads at any compressor speed. In addition, how the overall system efficiency of the air conditioner was affected by changes in compressor and air blower speeds was also

discussed. A DDC-based control algorithm developed by Li and Deng [2007a, 2007b] used space SHR as a controlled variable to simultaneously control space air temperature and relative humidity using a DX A/C system, however, it had to wait for a long time to obtain the numerical values of variables required in the control algorithm.

For the selection of a humidity control method, it may depend on the application of HVAC systems, which defines the load characteristics, operating conditions and system constraints. For example, a lightly populated small office will have thermal loads dominated by envelope heat gains. With a light occupancy, it will have a small ventilation requirement, and thus cooling and dehumidification loads could be met in most climates by a conventional DX A/C system. By contrast, a large lecture hall may have few windows and a very high ventilation demand, resulting in a large dehumidification load relative to sensible cooling load. In such an application, it may make sense to directly condition the ventilation air or use desiccant dehumidification technology.

2.4.3 MIMO control strategies in A/C systems

A/C systems are usually nonlinear, strong-coupled multivariable systems with multiply inputs and multiply outputs. However, A/C systems have been often controlled using single-input single-output (SISO) control strategies, such as PI and PID control. Research studies have demonstrated that the use of SISO control strategies may result in

an operating performance inferior to the use of multi-input multi-output (MIMO) control strategies [Tiwari et al. 2004]. The main difference between MIMO feedback control and SISO feedback control is that MIMO control uses multiple feedback signals to generate multiple control inputs, considering the coupling effects among variables in a system. However, SISO control only uses one feedback signal to generate a single control input. Because of the coupled nature of system parameters, MIMO control strategies are therefore more effective in simultaneously achieving effective control over multiple objectives such as temperature, humidity, capacity and efficiency in A/C systems.

A number of investigations have been carried out on applying MIMO control strategies to A/C and refrigeration systems. He et al. [1997] considered that there were strong cross-coupling effects among various operating parameters in a vapor compression refrigeration cycle, such as evaporating temperature, condensing temperature and degree of superheat, etc. A proper coordination between the opening of an EEV and compressor speed would improve control behavior of degree of superheat, and the ability to withstand external disturbances while effectively modulating the system cooling capacity. Therefore, in order to improve the transient behavior of the refrigeration cycle in terms of maintaining a desired degree of superheat and evaporating temperature, an MIMO feedback controller was designed based on a low-order lumped-parameter dynamic model [He et al. 1998]. Controllability test results showed that the MIMO controller could effectively improve the operating performance and energy efficiency of the vapor compression refrigeration cycle. Shah et al. [2004] developed an MIMO

adaptive control strategy for a general automotive air conditioning system. This MIMO adaptive control strategy was to control the degree of superheat and evaporating pressure in vapor compression systems by using varying both the expansion valve opening and airflow rate over an evaporator. Simulated results demonstrated that the MIMO adaptive approach was successful in controlling two objectives of both the degree of refrigerant superheat and the evaporating pressure. Furthermore, a numerical investigation for the MIMO globally linearizing control (GLC) for an industrial evaporator in an alumina refinery was carried out by Kam and Tade [2000]. Simulated results indicated that the MIMO GLC structure provided superior servo and regulatory control to multi-loop SISO PI controllers that were used to regulate the evaporator on-site.

Anderson et al. [2002] investigated a robust MIMO controller for an HVAC system for the potential improvements of system performance. The controller differed dramatically from prevalent control method for HVAC systems using multiple SISO control loops. Experimental results demonstrated that the application of the robust MIMO controller to an HVAC system offered a dramatic improvement in performance over PI-based HVAC system controllers. Furthermore, the improved operating performance may be realized without increasing operating cost. Another MIMO controller to control the temperature in, and the ventilation to multiple zones in a building was developed by Yuan and Perez [2006]. Simulated results under four types of typical weather conditions demonstrated that the controller was capable of maintaining ventilation air requirements to, and temperature in the multiple zones.

Thermal loads for buildings often vary or thermal load disturbances occur to building A/C systems. An MIMO disturbance rejection controller was developed by Arguello-Serrano and Velez-Reyes [1999]. The controller was capable of reducing the effect of thermal load disturbances on a space and hence, more effective in maintaining indoor thermal comfort conditions. The MIMO controller can obtain online estimations of the thermal loads affecting the space by an estimator developed, and these estimations were then used by the MIMO controller to reduce the effects of the disturbances on the space to maintain indoor thermal comfort.

2.4.4 Advanced control strategies employed in A/C systems

With the rapid development of the powerful and flexible DDC technologies, advanced control strategies based on artificial intelligence, such as fuzzy control [Angelov 2003], predictive control [Jin et al. 2005], system identification [Desta et al. 2005], neural network [Mahmoud and Ben-Nakhi 2003], find increasingly wide applications in HVAC systems.

In recent years fuzzy control has been viewed as an alternative to the standard PID control in various applications due to its robustness, fast time response and easy implementation. The core part of fuzzy control is its control rules that are derived from experience of experts and the previous knowledge about a control object. So et al. [1997]

designed a new self-learning fuzzy controller in which the control policy was adaptable to changes in both a control process and the environment. Therefore the controller can always operate at its optimal settings. A fuzzy self-tuning PID control method was developed for improving the control of refrigerant flow by using an EEV in an automobile air conditioning system [Li et al. 2004]. Experimental results showed that the control method can feed adequate refrigerant flow into the evaporator under various operational conditions. The temperature of the air leaving the evaporator dropped by approximately 3 ºC as compared to that under a conventional PID control. Aprea et al. [2004] developed a control algorithm based on fuzzy logic to continuously regulate compressor speed in a vapor compression refrigeration plant. The experimental results showed a meaningful energy saving equal to about 13% when the fuzzy control was used to control the cooling capacity to replace a classical thermostatic controller which imposed on/off cycles on the compressor.

Model-based predictive control (MBPC) has become a major research topic over the last few decades and it has also been successfully applied in industry due to its ability to control multivariable systems in an optimal way. MBPC refers to a class of computer control algorithms that utilize an explicit process model to predict the future response of a plant. Thompson and Dexter [2005] developed a fuzzy model-based predictive control scheme for controlling the supply air temperature in an A/C system. In this control scheme, a fuzzy decision-maker was used to find the membership function of the optimum fuzzy control signal. Fuzzy predictions of future behavior of the system were generated using a generic neurofuzzy model. The performance of the fuzzy model-based

controller was compared to that of a conventional controller for a laboratory test rig. Test results showed that satisfactory control of the supply air temperature was possible, at both high and low air flow rates. Leducq et al. [2006] developed a strategy of dynamic optimization of vapor compression refrigeration cycles using a MBPC algorithm. From the experiments results, energy savings when using MBPC were between 8% and 20%, depending on the number of actuators available for optimization.

Alcala et al. [2005] proposed the use of weighted linguistic fuzzy rules in combination with a rule selection process to develop accurate fuzzy logic controllers dedicated to the intelligent control of HVAC systems concerning energy performance and indoor thermal comfort requirements. A genetic optimization process considering an efficient approach to perform rule weight derivation and rule selection was developed.

The neural network technology is based on the operating mechanism of a human brain and has a strong ability to approximate a nonlinear function. It is usually used to model complicated, nonlinear control objects, and then performs identification and optimization. A general regression neural network (GRNN) for identification and control was employed in a feedback controller for an air conditioning system [Ahemd et al. 1998a, 1998b and 1998c]. A memory-based neural network was selected to capture the input-output regression characteristics of the air conditioning system. It was testified that GRNN possessed simplicity, robustness and excellent capability in system identification. Lin and Yeh [2007a, b] used system identification method to produce a low-order, linear model for an A/C system with multi-evaporators. The experimental

results indicated that the controller developed based on the model can successfully regulate the indoor temperatures and maintain the steady-state degree of superheat at acceptable levels.

2.5 Summary

With the pursuing of high quality living and comfortable working environment, more and more attentions have been paid to improving thermal environmental control in spaces using A/C systems. DX A/C systems have been widely used in small- to medium- scaled buildings in recent decades. Compared to large central chilled water-based A/C installations, DX A/C systems have a number of advantages. Most DX A/C systems are currently equipped with single-speed compressors and supply fans relying on on-off cycling compressors to maintain only indoor dry-bulb temperature, resulting in either space overcooling or an uncontrolled equilibrium indoor RH level.

Much research work on the impact of humidity on human thermal comfort and indoor environmental control indicated that indoor relative humidity should be maintained within a suitable range for thermal comfort. Indoor moisture which can cause high indoor relative humidity problem may come from both external and internal sources. In order to improve the thermal comfort for occupants, moisture loads may be removed by using mechanical dehumidification or chemical dehumidification in A/C systems.

Mechanical dehumidification utilizes mechanical means to cool air and so to dehumidify it. In most conventional HVAC systems, much energy is wasted by over cooling and reheating the air to maintain a suitable indoor humidity level. On the other hand, indoor moisture load may be dealt with by using chemical dehumidification, such as using solid or liquid desiccant. However, using desiccant based dehumidification would make A/C systems more complex and the operating costs would be higher compared to using other indoor humidity control method.

Simulation-based research has been regarded as an efficient and effective means to investigate the operating characteristics and control performance of various A/C systems. Dynamic modeling was necessary in carrying out research work related to the control of DX A/C systems. A considerable number of previous investigations have focused on the dynamic modeling of a DX refrigeration plant, hence these would not take the interaction between the refrigeration plant and an air-distribution sub-system into account. When modeling a DX A/C system, the dynamics of both its DX refrigeration plant and its air-distribution sub-system should be considered. The duel role of cooling and dehumidification for the cooling coil in a DX A/C system makes the controlled variables of temperature and humidity to become coupled. Therefore it is necessary to develop a dynamic model for a DX A/C system, which must take the coupling effect between temperature and humidity into account.

The major hurdle to the wider use of DX A/C systems has been the mismatch between their output sensible and latent cooling capacities and the varying sensible and latent

cooling loads in the conditioned spaces they serve, leading to poor indoor humidity control. Previous studies indicated that capacity control for DX A/C systems can be realized by the intermittent running of compressor, i.e., on/off cycling compressor. The cooling capacity of DX A/C systems may also be controlled by using suction-gas throttling, hot-gas by-pass or cylinder-unloading. However, the previous studies suggested that varying the flow of refrigerant using variable speed compressors was the most energy efficient way for capacity control in DX A/C systems.

Various control strategies have been used for controlling A/C systems, such as conventional PI and PID control strategies, which are of SISO nature. However, A/C systems are nonlinear, strong-coupled multivariable systems. There are strong cross-coupling effects among various operating parameters in a DX A/C system, such as evaporating temperature, condensing temperature, degree of refrigerant superheat, indoor air temperature and humidity, etc. Previous related studies have demonstrated that the use of MIMO control strategies can result in better control performances than the use of SISO control strategies. However, these studies focused mainly on refrigeration systems, but not on the air handling process in a DX A/C system. Other advanced control strategies such as fuzzy control, predictive control and neural network based control were also widely used in HVAC systems.

For buildings located in hot and humid subtropics, indoor humidity control using a DX A/C system has always been a challenge. However, it looks promising that the advancement of variable speed technology would help alleviate the humidity control

problem encountered when using DX A/C systems. Previous studies indicated that indoor air temperature may be controlled by varying compressor speed and indoor air humidity by varying supply fan speed, respectively. The performance of these decoupled SISO feedback loops is inherently poor in terms of transient behavior and energy efficiency, due to the strong-coupling among feedback loops. However, the research work using multivariable feedback control, considering the coupling effect of air temperature and humidity, for simultaneously controlling indoor air temperature and humidity using a DX A/C system has been scarcely reported in open literature. Therefore, it is necessary to develop an MIMO based control strategy to simultaneously control the air temperature and humidity in a conditioned space, and to investigate the control characteristics and energy performance of a DX A/C system under such an MIMO based control strategy.

Chapter 3

Proposition

3.1 Background

From the literature review presented in Chapter 2, it is evident that DX A/C systems are widely used in small- to medium-scaled buildings due to their advantages of simple configuration, a higher energy efficiency and a low cost to own and maintain. When a DX A/C system is equipped with a single-speed compressor and single-speed supply fan, only indoor air dry-bulb temperature is normally controlled by on-off cycling compressor, resulting in either space overcooling or an uncontrolled equilibrium indoor RH level, thus reducing indoor thermal comfort. This is particular true for residential buildings located in hot and humid subtropics. Therefore, developing an appropriate indoor thermal environmental control strategy for DX A/C systems has always been a challenge.

With the fast development of low-cost variable speed drive (VSD) technology in recent years, many DX A/C systems are currently equipped with a variable speed compressor and variable speed supply fan. Previous related investigations showed that indoor air temperature and humidity may be simultaneously controlled by varying compressor speed and supply fan speed. Therefore it is possible to develop an MIMO based control strategy to simultaneously control the indoor air temperature and humidity using a DX A/C system having variable speed compressor and variable speed supply fan.

Simulation-based research has been increasingly recognized as an efficient and powerful tool to study the operating performance, and to develop advanced control strategies for HVAC systems. The literature review presented in Chapter 2 also reveals that although there have been a large number of reported studies on modeling DX A/C systems, a dynamic mathematical model for a DX A/C system which is suitable for designing a multivariable controller for simultaneously controlling indoor air temperature and humidity, cannot be indentified in open literature. Many of the previously reported models of DX A/C systems are either steady-state models or not suitable for multivariable control design. Therefore it is necessary to develop a dynamic mathematical model for a DX A/C system, which is suitable for multivariable control to simultaneously control indoor air temperature and humidity, thus improving thermal comfort of occupants.

3.2 Project title

The thesis focuses on the following major issues related to developing multivariable control strategy for simultaneous indoor air temperature and humidity control in a space served by a DX A/C system: (1) establishing a multivariable dynamical model for a DX A/C system, and experimentally validating the dynamical mathematical model developed; (2) designing an MIMO controller for the DX A/C system based on the developed dynamic model; (3) carrying out controllability tests for the MIMO controller for simultaneously controlling indoor air temperature and humidity using an

experimental DX A/C system. The proposed research project is therefore entitled "Multivariable control of air temperature and humidity in a space served by a direct expansion (DX) air conditioning (A/C) system".

3.3 Aims and objectives

The objectives of the research work reported in this thesis are as follows:

(1) To develop a multivariable control-oriented dynamic mathematical model which is highly suitable for designing a multivariable controller for the experimental DX A/C system having a variable-speed compressor and a variable-speed supply fan, and to validate the dynamic model developed by comparing the simulated and measured results of open-loop responses of major operating parameters;

(2) To design an MIMO controller for the experimental DX A/C system based on the dynamic model developed using Linear Quadratic Gaussian (LQG) technique;

(3) To carry out controllability tests for the MIMO controller and to evaluate the performance of the MIMO controller for simultaneously controlling indoor air temperature and humidity in a space served by the DX A/C system;

(4) To develop a new DS controller, as the replacement to a conventional PID DS controller, for improving the operating performance and stability of the DX A/C

system when the fluctuation of operating DS is mainly caused by the changes of compressor speed and supply fan speed, and to carry out the controllability tests for the new DS controller.

3.4 Research methodologies

The research methodologies for this study are based on dynamic modeling and experimental tests. Firstly, a multivariable control-oriented dynamic model of the experimental DX A/C system will be developed based on the principles of mass and energy conservation. The lumped-parameter method will be followed when modeling the DX evaporator of the experimental DX A/C system, where a dry-cooling region and a wet-cooling region on its air side, and a two-phase region and a superheated region on its refrigerant side will be assumed.

The multivariable control-oriented dynamic model developed for the experimental DX A/C system which consists of a set of differential equations will be nonlinear in nature. Therefore the dynamic model developed needs to be linearized and written in a state-space representation which is highly suitable for a multivariable controller design. The dynamic model after linearization will be experimentally validated using the experimental DX A/C system. The measured open-loop responses of the major operating parameters in the experimental DX A/C system after being subjected to step

changes of compressor speed and supply fan speed will be compared to the simulated results using the model.

Secondly, the MIMO controller will be designed based on the linearized dynamic model using LQG technique. Controllability tests for the MIMO controller will be carried out with respect to disturbance rejection and following command, respectively, after being subjected to heat load disturbance in a conditioned space and changes of indoor air temperature and humidity settings. This is to ascertain whether the MIMO controller developed could behave as expected in simultaneously controlling indoor air temperature and humidity in the space served by the experimental DX A/C system.

Finally, a new DS controller, as the replacement to a conventional PID DS controller in a DX A/C system, for improving the operating performance and stability of the system when the fluctuation of the operating DS is mainly caused by the speed changes of both compressor and supply fan, will be further developed for the DX A/C system. The new DS controller will be developed from a conventional PID DS controller by adding two feed-forward channels so that information of speed changes of compressor and supply fan can be timely passed to the new DS controller. The new DS controller will be digitally implemented in the experimental DX A/C system, and controllability tests for the new DS controller carried out to see whether the expected control results may be achieved.

Chapter 4

Description of the Experimental DX A/C System

4.1 Introduction

An experimental DX A/C system is available in the HVAC Laboratory of Department of Building Services Engineering in The Hong Kong Polytechnic University. Advanced technologies such as variable-speed compressor and supply fan, and electronic expansion valve (EEV), as well as a computerized data measuring, logging and control system, have been incorporated into the experimental DX A/C system.

This Chapter presents firstly detailed descriptions of the experimental DX A/C system and its major components. This is followed by describing the computerized instrumentation and a data acquisition system (DAS). Finally, a computer supervisory program used to operate and control the experimental DX A/C system is detailed.

4.2 Detailed descriptions of the experimental system and its major components

The experimental DX A/C system is mainly composed of two parts, i.e., a DX refrigeration plant (refrigerant side) and an air-distribution sub-system (air side). The schematic diagrams of both the DX refrigeration plant and the complete experimental DX A/C system are shown in Fig. 4.1 and Fig. 4.2, respectively.

4.2.1 The DX refrigeration plant

As shown in Fig. 4.1, the major components in the DX refrigeration plant include a variable-speed rotor compressor, an EEV, a high-efficiency tube-louver-finned DX evaporator and an air-cooled tube-plate-finned condenser. The evaporator is placed inside the supply air duct to work as a DX air cooling coil. The design air face velocity for the DX cooling coil is 2.5 m/s. The nominal output cooling capacity from the DX refrigeration plant is 9.9 kW. The actual output cooling capacity from the DX refrigeration plant can however be modulated from 15% to 110% of the nominal capacity. Other details of the compressor can be found in Table 4.1. The compressor is driven by a variable-speed drive (VSD). The EEV includes a throttling needle valve, a step motor and a pulse generator. It is used to maintain the degree of refrigerant superheat at the evaporator exit. The working fluid of the plant is refrigerant R22, with a total charge of 5.3 kg.

In addition, two three-way connectors and two flexible joints, whose locations are indicated in Fig. 4.1, are reserved in the refrigerant pipeline for the purpose of possibly modifying the system for other related studies. A condenser air duct, which is not normally required in real applications, is used to duct the condenser cooling air carrying the rejected heat from the condenser away to outside the Laboratory. The condenser fan, housed inside the condenser air duct, can also be variable-speed operated. An electrical heater controlled by Solid State Relay (SSR) is used to adjust the temperature of the cooling air entering the condenser for various experimental purposes. A refrigerant mass

flow meter is installed upstream of the EEV. Other necessary accessories and control devices, such as an oil separator, a refrigerant receiver, a sight glass and safety devices, are provided in the refrigeration plant to ensure its normal and safe operation.

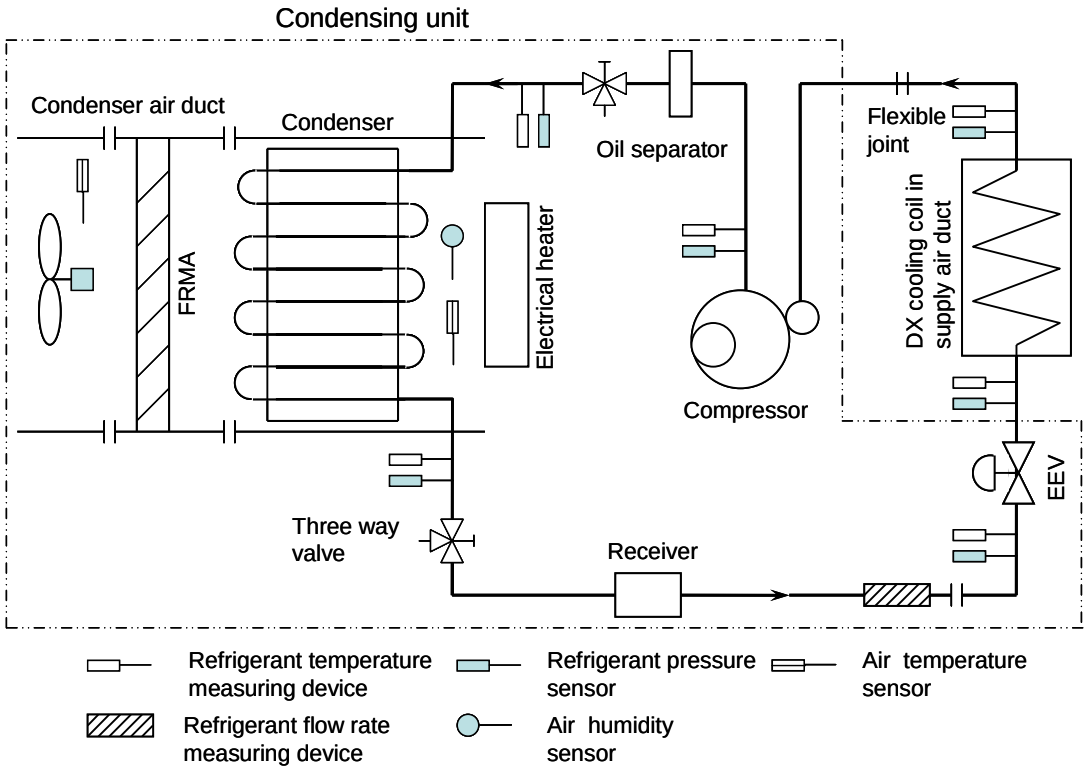

Fig. 4.1 The schematic diagram of the DX refrigeration plant

Table 4.1 Details of the variable speed rotor compressor

Model	HITACHI THS20MC6-Y
Allowable Frequency range	15~110 Hz
Rated Capacity	9900 W at 90 Hz
Displacement	3.04 ml/rev

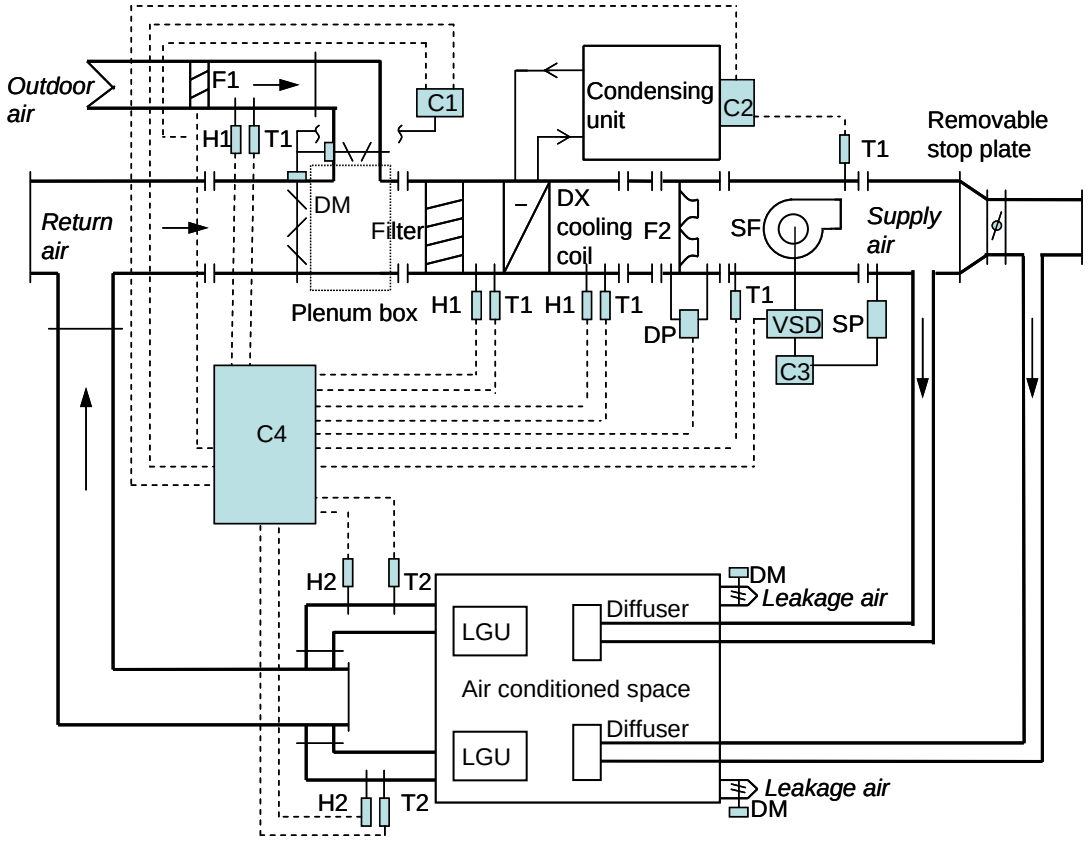

C1-controller of outdoor/return air damper	C2-controller of condensing unit	C3-controller of supply fan
C4-data acquisition and control unit	DM-damper	DP-differential pressure transducer
F1-hot film anemometer	F2-supply airflow rate measuring apparatus	H1-air wet-bulb temperature sensor
H2-air humidity meter	LGU-load generating unit	SF-supply fan with motor outside duct
SP-static pressure measuring device	T1,T2-air dry-bulb temperature sensor	VSD-variable speed drives

Fig. 4.2 The schematic diagram of the complete experimental DX A/C system

4.2.2 The air-distribution sub-system

The air-distribution sub-system in the experimental DX A/C system is schematically shown in Fig. 4.2. It includes an air-distribution ductwork with return and outdoor air dampers, a variable-speed centrifugal supply fan with its motor placed outside the duct,

and a conditioned space. The supply fan is driven by a VSD. The details of the supply fan are given in Table 4.2.

The air conditioned space measures 6.8 m (L)×3.9 m (W)×2.9 m (H). Inside the space, there are sensible heat and moisture load generating units (LGUs). The units are intended to simulate the cooling load in the conditioned space. Its heat and moisture generation rate as regulated by SSR may be varied manually or automatically with a pre-set pattern through operator's programming. In addition, leakage outlets with residual-pressure relief dampers are installed in the space so that a positive internal pressure of not more than 20 Pa can be maintained at all time. In the air-distribution sub-system of the experimental DX A/C system, return air from the space mixes with outdoor air in a plenum box upstream of an air filter. The mixed air is filtrated and then cooled and dehumidified by the DX cooling coil. Afterwards, the cooled and dehumidified air passes through the supply fan, to be supplied to the space to deal with the cooling load from LGUs.

Table 4.2 Details of the variable speed supply fan

Model	KRUGER BSB 31
Nominal flow rate	1700 m^3/h (0.47 m^3/s)
Total pressure head	1100 Pa

4.3 Computerized instrumentation and data acquisition system (DAS)

The computerized instrumentation for the experimental DX A/C system is also shown in both Fig. 4.1 and Fig. 4.2. The system is fully instrumented for measuring all of its

operating parameters, which may be classified into three types, i.e., temperature, pressure and flow rate. Since all measurements are computerized, all sensors and measuring devices are able to output direct current (DC) signal of 4-20 *mA* or 1-5 *V*, which are transferred to a DAS for logging and recording.

4.3.1 Sensors/measuring devices for temperatures, pressures and flow rates

Eleven sets of air temperature and humidity measuring sensors are located in the air-distribution sub-system of the experimental DX system. Air RH is indirectly measured via measuring air dry-bulb and wet-bulb temperatures. As shown in Fig. 4.1, there are five temperature sensors for measuring refrigerant temperatures in the DX refrigeration plant. To ensure fast response of the sensors for facilitating the study of transient behaviors of the DX refrigeration plant, these temperature sensors are inserted into the refrigerant circuit, and are thus in direct contact with the refrigerant. The temperature sensors for air and refrigerant are of platinum Resistance Temperature Device (RTDs) type, using three-wire Wheatstone bridge connection and with a pre-calibrated accuracy of ±0.1℃. The specifications of the RTDs are: CHINO Pt100/0℃-3W, Class A, SUSΦ 3.2-150L.

Refrigerant pressures in various locations in the DX refrigeration plant are measured using pressure transmitters with an accuracy of ±0.13% of full scale reading (Model: SETRA C206). The atmospheric pressure is measured with a barometer having an accuracy of ±0.05kPa (Model: VAISALA PTB-101B).

There are two sets of air flow rate measuring apparatus (FRMA) in the air-distribution system. One set of FRMA is used to measure the total supply airflow rate, i.e., the airflow rate passing through the DX cooling coil. The other is for measuring the airflow rate passing through the condenser. The two sets of FRMA are constructed in accordance with ANSI/ASHRAE Standard 41.2, consisting of nozzles of different sizes, diffusion baffles and a manometer with a measuring accuracy of ±0.1% of full scale reading (Model: ROSEMOUNT 3051). The number of nozzles in operation can be altered automatically.

Outdoor airflow rate is measured using a hot-film anemometer with a reported accuracy of ±0.1 m/s (Model: EE70-VT62B5). The anemometer is installed 500 mm, which is longer than the recommended length of entrance of 200 mm by its manufacturer, downstream of the outdoor air inlet, to ensure the measuring accuracy of outdoor airflow rate. The power consumption of the variable-speed compressor is measured using a pulse-width-modulation (PWM) digital power meter with a reported uncertainty of ±2% of reading (Model: EVERFINE PF9833). The refrigerant mass flow rate passing through the EEV is measured by a Coriolis mass flow meter with a reported accuracy of ±0.25% of full scale reading (Model: KROHNE MFM1081K+F). The supply air static pressure is measured using a manometer with a reported accuracy of ± 0.1% of full scale reading (Model: ROSEMOUNT 3051).

In order to ensure the measuring accuracy for the temperatures of the air flowing inside air duct, standardized air sampling devices recommended by the ISO Standard 5151 are

used in the experimental DX A/C system.

4.3.2 The data acquisition system

A data acquisition unit (Model: AGLIENT 34970A/34902A) is used in this experimental DX A/C system. It provides up to 48 channels for monitoring various types of system parameters. The DC signal from various measuring devices/sensors can be scaled into their real physical values of the measured parameters using a logging & control (L&C) supervisory program which is developed using LabVIEW programming platform. The minimum data sampling interval is one second. It should be noted that the flow rates of both supply air and condenser cooling air are calculated using the air static pressure drops across their respective nozzles. The outdoor airflow rate is evaluated by multiplying the measured air velocity with the sectional area of the outdoor air duct. The output cooling capacity from the DX refrigerant plant is calculated based on the enthalpy-difference of air across the DX cooling coil.

4.4 LabVIEW logging & control (L&C) supervisory program

A computer supervisory program which is capable of performing simultaneously data-logging and parameter-controlling is necessary. It needs to communicate with not only the data acquisition unit, but also conventional standalone digital programmable PI controllers which are to be detailed in Section 4.5. A commercially available

programming package, LabVIEW, provides a powerful programming and graphical platform for data acquisition and analysis, as well as for control application.

A data L&C supervisory program has been developed using LabVIEW, with all measured parameters real-time monitored, curve-data displayed, recorded and processed. The program can also perform the retrieval, query and trend-log graphing of historical data for measured parameters. The program runs on a personal computer (PC).

The LabVIEW-based L&C supervisory program enables the PC to act as a central supervisory control unit for different low-level control loops, which will be also discussed in Section 4.5, in the experimental DX A/C system. The PC can therefore not only modify the control settings of those standalone microprocessor-based PI controllers, but also deactivate any of these controllers. The LabVIEW-based L&C supervisory program also provides an independent self-programming module (SPM) by which new control algorithms may be easily implemented through programming. A SPM performs in a similar manner to a central processing unit of a physical digital controller. The variables available from all measured parameters can be input to, and processed according to a specified control algorithm in a SPM to produce required control outputs. Once a SPM is initiated to replace a given standalone controller, the controller must be deactivated, but works as a digital-analog converter to receive the control output from the SPM. An analogue control signal is then produced by the controller to initiate the related actuator for necessary control action.

4.5 Conventional control loops in the experimental system

Totally, there are ten conventional control loops in this experimental DX A/C system. These loops either are activated using the LabVIEW-based supervisory program or use PI controllers which are of digital programmable type with RS-485 communication port (Model: YOKOGAWA UT350-1). Resetting controller's proportional band, integral times and setpoints is allowed.

Among the ten control loops, four are for varying heat and moisture generation rate of the LGUs located inside the space. Electrical power input to the LGU is regulated using SSR according to the instructions from their respective control loops to simulate the space cooling load. In addition, there is one control loop for maintaining the condenser inlet air temperature at its setting through regulating electrical power input by SSR.

The remaining five conventional PI control loops are as follows: supply air temperature by regulating the compressor speed; supply air static pressure by regulating the supply fan speed; condensing pressure by regulating the condenser fan speed; degree of refrigerant superheat by regulating EEV opening; outdoor airflow rate by jointly regulating both outdoor and return air dampers' openings. These five control loops can be activated by using either the conventional physical digital PI controller available in the experimental DX A/C system or a SPM specifically for any new control algorithm to be developed.

The control of supply air temperature is used as an example for illustration. When the conventional PI controller is enabled, the controller measures the supply air temperature using the temperature sensor and then compares the measured with its setpoint. A deviation is processed in the controller according to a pre-set PI control algorithm and an analogue control signal of 4~20 *mA* is produced and sent by the PI controller to the VSD for compressor motor to regulate its speed. On the other hand, such a conventional PI controller may be replaced by a SPM to be specifically developed based on a new control algorithm for compressor speed control. The SPM may take the advantages of using simultaneously multiple input variables, e.g., supply air temperature and its setpoint, evaporating and condensing pressures, degree of refrigerant superheat, etc. Control outputs can then be created by using the SPM according to the new control strategy and algorithm, and communicated to the physical digital PI controller which works only as a digital-analog converter. An analog control signal is then generated and sent to the VSD of compressor for its speed control.

4.6 Summary

An experimental DX A/C system is available for carrying out the proposed project. The system consists of two parts: a DX refrigeration plant and an air-distribution sub-system.

The experimental DX A/C system has been fully instrumented using high quality sensors/measuring devices. Totally forty-three operating parameters in the system can be measured and monitored simultaneously and ten conventional PI feedback control

loops are provided. Two sets of airflow rate measuring apparatus are constructed in accordance with ANSI/ASHRAE Standard 41.2. Sensors for measuring refrigerant properties are in direct contact with refrigerant, and a Corioli mass flow meter is used for measuring the refrigerant flow rate being circulated in the DX refrigerant plant.

A L&C supervisory program has been developed specifically for this experimental DX A/C system using LabVIEW programming platform. All parameters can be real-time measured, monitored, curve-data displayed, recorded and processed by the L&C program. The LabVIEW-based L&C program provides an independent SPM by which any new control algorithms to be developed may be implemented.

The availability of such an experimental DX A/C system is expected to be extremely useful in developing a multivariable control strategy for simultaneously controlling indoor air temperature and humidity in a space served by a DX A/C system having a variable-speed compressor and supply fan. A multivariable control-oriented dynamic mathematical model for the DX A/C system can be developed and experimentally validated. An MIMO controller for simultaneous control of indoor air temperature and humidity can be developed, and the controllability tests for the MIMO controller carried out using the experimental DX A/C system.

Chapter 5

Multivariable Control-oriented Modeling of the Experimental DX A/C System and its Experimental Validation

5.1 Introduction

Simulation study has become increasingly popular for research work in the past few decades. Its applicability to design optimization and developing control strategies for refrigeration and air conditioning systems has been widely accepted by HVAC industry. The operation of a DX A/C system is dynamic in nature and the coupling among the system's various control loops is intense. Therefore, there has been a strong need for a dynamic model that could effectively reflect the dynamic characteristics of a DX A/C system. A good dynamic model can be significantly useful in developing multivariable control strategies for a DX A/C system. As presented in Chapter 2, there have been many reported studies which mainly focused on either modeling of refrigeration systems or using conventional control strategies for DX A/C systems. For example, indoor air temperature and humidity can be individually controlled by using a conventional control strategy such as PID control without much consideration on the coupling effect of air temperature and humidity. Thus indoor air temperature and humidity may not be simultaneously controlled to their respective settings and consequently the level of indoor thermal comfort is reduced. Therefore in order to facilitate developing a multivariable control strategy to simultaneously control indoor air temperature and humidity using a DX A/C system, a dynamic model for a DX A/C system which both

considers the coupling effect of air temperature and humidity and is suitable for developing multivariable control algorithms, becomes highly necessary.

This Chapter reports on the development of a multivariable control-oriented dynamic model for the experimental DX A/C system. It takes into consideration the coupling effect of indoor air temperature and humidity. The multivariable control-oriented dynamic model developed has been experimentally validated by comparing the measured open-loop responses of the major operating parameters of the experimental DX A/C system after being subjected to step changes of compressor speed and supply fan speed with the same simulated using the model. The multivariable control-oriented model developed is expected to be greatly helpful for developing an MIMO control strategy for a DX A/C system to simultaneously control indoor air temperature and humidity.

5.2 The development of the multivariable control-oriented dynamic model for the experimental DX A/C system

A detailed description of the experimental DX A/C system consisting of a DX refrigeration plant and an air air-distribution sub-system is reported in Chapter 4. For the purpose of model development, a conceptual model of the experimental DX A/C system is shown in Fig.5.1. The DX refrigeration plant is mainly composed of a DX evaporator, a condenser, an EEV, a variable speed compressor. The evaporator in the DX

refrigeration plant is used as a DX cooling coil in the air-distribution sub-system to simultaneously cool and dehumidify the air passing through it. The conditioned air is then supplied to a conditioned space through an air duct work using a variable speed supply fan. The EEV is used for controlling the degree of refrigerant superheat at a suitable level. In developing the model, a lumped-parameter modeling approach was adopted.

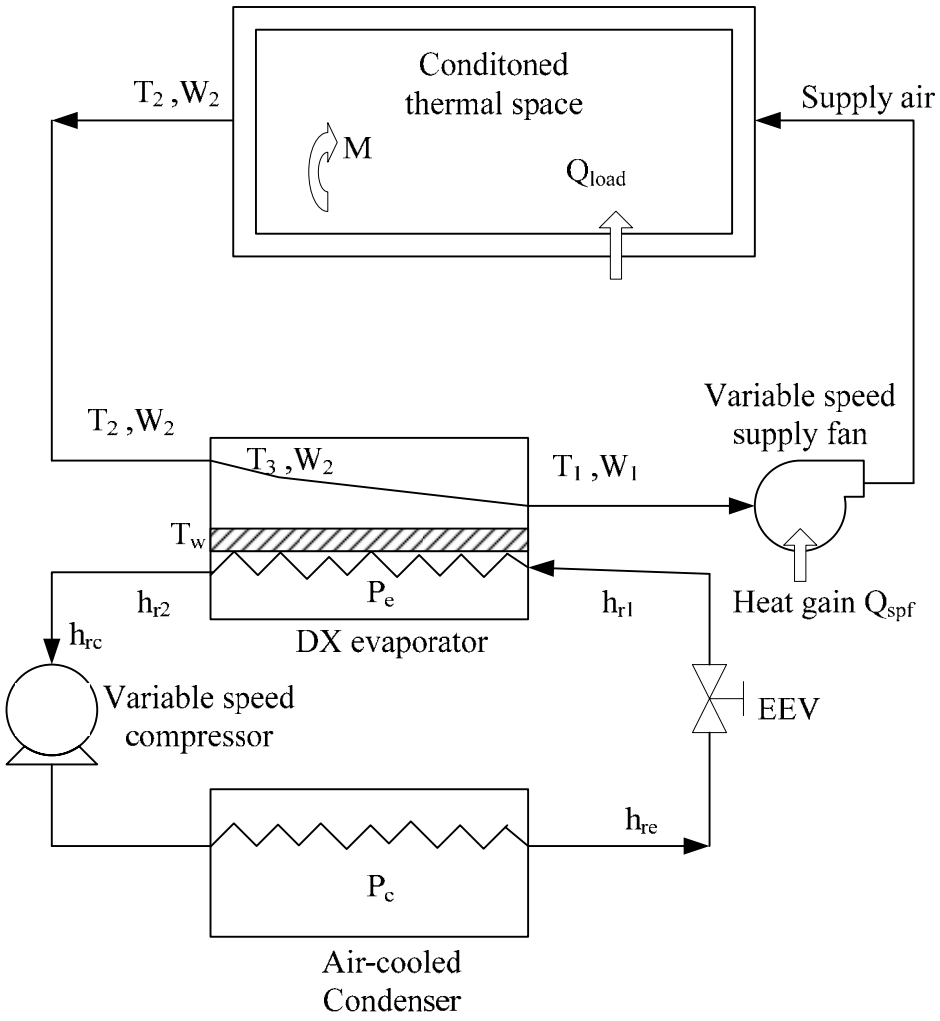

Fig. 5.1 The conceptual model of the experimental DX A/C system

The multivariable control-oriented dynamic model for the experimental DX A/C system was mainly derived from the principles of energy and mass conservation. The following assumptions were made in developing the dynamic model for the DX A/C system: (1) perfect air mixing inside all heat exchangers and the thermal space, and no fresh air intake to the system; (2) negligible thermal losses in air ducts; (3) there were two regions on the air side of the DX evaporator, i.e., dry-cooling region and wet-cooling region.

The indoor air temperature and humidity in the conditioned thermal space would change slowly due to the thermal inertia of indoor air. In the DX A/C system to be modeled, with the assumption of perfect air mixing, air temperature, T_2, and air moisture content, W_2, leaving the conditioned space can be regarded as being equal to indoor air temperature and moisture content in the conditioned thermal space, respectively. The temperature and moisture content of the air leaving the DX cooling coil, were T_1 and W_1, respectively, as shown in Fig. 5.1. Based on the principle of energy conservation, the sensible energy balance equation for the conditioned space can be written as follows:

$$C_{\mathrm{p}}\rho V\frac{dT_2}{dt} = C_{\mathrm{p}}\rho f(T_1 - T_2) + Q_{load} + Q_{spl} \tag{5.1}$$

where V was the volume of the conditioned space, Q_{load} the space sensible load, Q_{spl} heat gain of the supply fan, f the air volumetric flow rate.

The heat gain of supply fan increased with the air flow rate, and can be written as follows:

$$Q_{spl} = k_{spl} f \tag{5.2}$$

where k_{spl} was a coefficient.

On the other hand, the moisture mass balance inside the conditioned space can be written as follows:

$$\rho V \frac{dW_2}{dt} = \rho f (W_1 - W_2) + M \tag{5.3}$$

where M was the moisture load in the conditioned space.

For the DX evaporator in the experimental DX A/C system, it was assumed that there were two cooling regions on its air side, e.g., dry-cooling region and wet-cooling region. Wet cooling of air occurred when the tube-fin surface temperature was below the dew-point temperature of air entering the evaporator; otherwise, dry-cooling of air occurred. Corresponding to the assumed two regions on the air side, the refrigerant side of DX evaporator was assumed to have a two-phase region and a superheated region, as shown in Fig. 5.2.

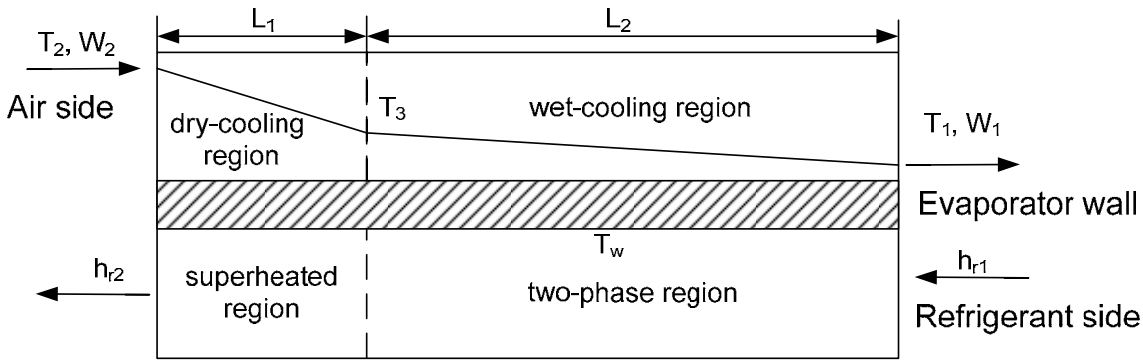

Fig.5.2 The schematic diagram of the DX evaporator

At the air side of the evaporator, with the assumption of no fresh air, the temperature and moisture content of the air entering evaporator were T_2 and W_2, respectively. The air temperature decreased along the evaporator wall and was equal to T_3 at the end of dry-cooling region. Since the dry-cooling region was usually small, the temperature of the entire evaporator wall was assumed at the same T_w. Applying the energy balance principle in the dry-cooling region on the air side yielded:

$$C_p \rho V_{h1} \frac{dT_3}{dt} = C_p \rho f (T_2 - T_3) + \alpha_1 A_1 (T_w - \frac{T_2 + T_3}{2}) \tag{5.4}$$

where f was air flow volume rate, T_w the temperature of evaporator tube wall, A_1 the air side heat transfer area of evaporator in dry-cooling region, V_{h1} the air side volume of evaporator in dry-cooling region.

The air side volume of evaporator in dry-cooling region can be calculated as follows:

$$V_{h1} = A_{s1} L_1 \tag{5.5}$$

where L_1 was the length of the dry-cooling region on the air side of the evaporator, A_{s1} the air side cross section area of the evaporator in dry-cooling region.

On the other hand, in the wet-cooling region, there was not only sensible heat transfer between the air and evaporator wall, but also latent heat transfer. The coupled air cooling and dehumidification mainly took place in the wet-cooling region. Therefore the energy balance in the wet-cooling region can be written in enthalpy form:

$$\rho V_{h2} \frac{dh_1}{dt} = \rho f (h_3 - h_1) + \alpha_2 A_2 (T_w - \frac{T_3 + T_1}{2}) \tag{5.6}$$

where h_3 was enthalpy of air leaving wet-cooling region of evaporator, T_1 the temperature of air leaving evaporator, A_2 the air side heat transfer area of evaporator in wet-cooling region, V_{h2} the air side volume of evaporator in wet-cooling region.

The air side volume of evaporator in wet-cooling region can be calculated as follows:

$$V_{h2} = A_{s2} L_2 \tag{5.7}$$

where L_2 was the air side length of the wet-cooling region, A_{s2} the air side cross section area of the evaporator in wet-cooling region.

The air side convective heat transfer coefficients for the louver-finned evaporator in both dry-cooling and wet-cooling regions were evaluated as follows [Chen 2005]:

$$\alpha_1 = j_{e1}\rho\upsilon\frac{C_p}{\Pr^{\frac{2}{3}}} \tag{5.8}$$

$$\alpha_2 = j_{e2}\rho\upsilon\frac{C_p}{\Pr^{\frac{2}{3}}} \tag{5.9}$$

where j_{e1}, j_{e2} were the Colburn factors, *Pr* the *Prandtl* number, υ the air velocity.

The relationship among air enthalpy, h_1, air temperature, T_1, and moisture content, W_1, was as follows:

$$h_1 = C_p T_1 + h_{fg} W_1 \tag{5.10}$$

where h_{fg} was the latent heat of vaporization of water.

Substitute Equation (5.10) into Equation (5.6), the energy balance equation for moist air in the wet-cooling region on the air side of evaporator can be rewritten as follows:

$$C_{\mathrm{p}}\rho V_{h2}\frac{dT_1}{dt} + \rho V_{h2}h_{fg}\frac{dW_1}{dt} = C_{\mathrm{p}}\rho f(T_3 - T_1) + \rho f h_{fg}(W_2 - W_1) + \alpha_2 A_2(T_w - \frac{T_3 + T_1}{2}) \tag{5.11}$$

Therefore the energy balances for moist air in dry-cooling region and wet-cooling region on air side of DX evaporator can be expressed by Equation (5.4) and Equation (5.11), respectively.

The degree of refrigerant sub-cooling in a condenser with a receiver is a normally rather small, and the refrigerant in the receiver can be assumed to be the saturated liquid refrigerant at condensing pressure in order to simplify the model of refrigerant side. Therefore, after knowing the real-time measured condensing pressure, the enthalpy of refrigerant leaving the receiver, h_{re}, can be obtained using the R22 State Equations [Cleland 1986]. Neglecting the energy loss in the refrigerant line and approximating the refrigerant throttling process in an EEV as being isenthalpic, the enthalpy of refrigerant entering the DX evaporator was given by.

$$h_{r1} = h_{re} \tag{5.12}$$

The enthalpy of superheated refrigerant at compressor suction, h_{rc}, can be evaluated based on the real-time measured pressure and the temperature of superheated refrigerant using the R22 State Equations. Neglecting the energy loss in the refrigerant line between DX evaporator and compressor suction owing to good thermal insulation, the enthalpy of the refrigerant leaving the DX evaporator was given by:

$$h_{r2} = h_{rc} \tag{5.13}$$

For the variable speed compressor, the transient characteristics of the compressor can be neglected when compared to those of both the DX evaporator and condenser. Therefore, a steady-state approach was adopted when modeling the variable speed compressor. The swept volume of the compressor, V_{com}, was calculated using the related compressor's geometric parameters as follows [Chen 2005]:

$$V_{com} = \pi r_a^2 l \varepsilon (2 - \varepsilon) \tag{5.14}$$

where l was the stroke of cylinder, r_a the radius of rotor and ε the rotor relative eccentricity.

The rotor relative eccentricity, ε, was evaluated by:

$$\varepsilon = \frac{e}{R} \tag{5.15}$$

where e was the rotor eccentricity and R the radius of cylinder.

The compressor displacement coefficient, λ, was given by [Chen 2005]:

$$\lambda = 1 - 0.015\left[\left(\frac{P_c}{P_e}\right)^{\frac{1}{\beta}} - 1\right] \tag{5.16}$$

where β was the compression index which was assumed to be a constant at 1.18. P_c and P_e were the condensing pressure and evaporating pressures, respectively.

The refrigerant mass flow rate leaving the compressor was assumed to be equal to that at the compressor inlet. Therefore, the refrigerant mass flow rate can be determined by:

$$M_{ref} = \frac{sV_{com}}{v_s}(1 - 0.015\left[\left(P_c / P_e\right)^{\frac{1}{\beta}} - 1\right]) \tag{5.17}$$

where s was the compressor speed, v_s specific volume of superheated refrigerant, which can be obtained from measured pressure and temperature of refrigerant at compressor suction using the R22 State Equations.

Due to the significant difference in thermal inertia for both refrigerant and air, dynamic responses to changes on the air side were much slower than that on the refrigerant side. When the air side waited for a long time to fully respond, the refrigerant side was already in its steady-state for a quite while. Thus the same refrigerant mass flow rate at both the inlet and outlet of the DX evaporator was assumed. Therefore the energy balance equation for the evaporator wall can be written as follows:

$$(C_{\mathrm{p}}\rho V)_w \frac{dT_w}{dt} = \alpha_1 A_1 (\frac{T_2 + T_3}{2} - T_w) + \alpha_2 A_2 (\frac{T_3 + T_1}{2} - T_w) - M_{ref}(h_{r2} - h_{r1}) \qquad (5.18)$$

The supply air leaving a DX evaporator is generally assumed to be at 95% saturated. The relationship between air moisture content and temperature can be derived by plotting and curving fitting:

$$W_1 = (0.0198T_1^2 + 0.085T_1 + 4.4984)/1000 \qquad (5.19)$$

Therefore

$$\frac{dW_1}{dt} - (2 \times 0.0198T_1 + 0.085)\frac{dT_1}{dt}/1000 = 0 \qquad (5.20)$$

Equations (5.1), (5. 3), (5.4), (5.11), (5.18) and (5.20), all of which were the first order differential equations, form the dynamic model of the experimental DX A/C system. Therefore the dynamic model of the experimental DX A/C system can be written as follows:

$$
\begin{cases}
C_{\mathrm{p}}\rho V\dfrac{dT_2}{dt} = C_{\mathrm{p}}\rho f(T_1 - T_2) + k_{spl} f + Q_{load} \\
\rho V\dfrac{dW_2}{dt} = \rho f(W_1 - W_2) + M \\
C_{\mathrm{p}}\rho V_{h1}\dfrac{dT_3}{dt} = C_{\mathrm{p}}\rho f(T_2 - T_3) + \alpha_1 A_1(T_w - \dfrac{T_2 + T_3}{2}) \\
C_{\mathrm{p}}\rho V_{h2}\dfrac{dT_1}{dt} + \rho V_{h2} h_{fg}\dfrac{dW_1}{dt} = C_{\mathrm{p}}\rho f(T_3 - T_1) + \rho f h_{fg}(W_2 - W_1) + \alpha_2 A_2(T_w - \dfrac{T_3 + T_1}{2}) \\
(C_{\mathrm{p}}\rho V)_w\dfrac{dT_w}{dt} = \alpha_1 A_1(\dfrac{T_2 + T_3}{2} - T_w) + \alpha_2 A_2(\dfrac{T_3 + T_1}{2} - T_w) - s\dfrac{V_{com}\lambda}{v_s}(h_{r2} - h_{r1}) \\
\dfrac{dW_1}{dt} - (2\times 0.0198 T_1 + 0.085)\dfrac{dT_1}{dt}/1000 = 0
\end{cases}
\tag{5.21}
$$

Since the purpose of developing the dynamic model for the experimental DX A/C system was to assist the design of a multivariable controller to simultaneously control indoor air temperature and humidity, it was suggested [Tewari 2002, Skogestad and Postlethwaite 1996] that the above differential equations, i.e., Equation (5.21), should be written in state-space representation, such that it did not formally distinguish between a multivariable system and a single variable system, allowing an efficient design and analysis for a multivariable system in the same manner as for a single variable system. Hence the multivariable control-oriented dynamic model in state-space representation may be expressed in the following compact format:

$$
\dot{X} = D^{-1}\bullet g_1(X, U) + D^{-1}\bullet g_2(Z) \tag{5.22}
$$

where the state variables $X = [T_1, T_2, T_3, T_w, W_1, W_2]^T$ and $\dot{X} = \frac{dX}{dt}$, the input variables $U = [f, s]^T$, and the disturbance variables $Z = [Q_{load}, M]^T$, g_1, g_2 were the functions, defined as follows:

$$g_1(X,U) = \begin{bmatrix} C_p \rho f (T_1 - T_2) + k_{spi} f \\ \rho f (W_1 - W_2) \\ C_p \rho f (T_2 - T_3) + \alpha_1 A_1 (T_w - \frac{T_2 + T_3}{2}) \\ C_p \rho f (T_3 - T_1) + \rho f h_{fg} (W_2 - W_1) + \alpha_2 A_2 (T_w - \frac{T_3 + T_1}{2}) \\ \alpha_1 A_1 (\frac{T_2 + T_3}{2} - T_w) + \alpha_2 A_2 (\frac{T_3 + T_1}{2} - T_w) - s \frac{V_{com} \lambda}{v_s} (h_{r2} - h_{r1}) \\ 0 \end{bmatrix} \tag{5.23}$$

$$g_2(Z) = \begin{bmatrix} Q_{load} \\ M \\ 0 \\ 0 \\ 0 \\ 0 \end{bmatrix} \tag{5.24}$$

$$D = \begin{bmatrix} 0 & C_p \rho V & 0 & 0 & 0 & 0 \\ 0 & 0 & 0 & 0 & 0 & \rho V \\ 0 & 0 & C_p \rho V_{h1} & 0 & 0 & 0 \\ C_p \rho V_{h2} & 0 & 0 & 0 & \rho V_{h2} h_{fg} & 0 \\ 0 & 0 & 0 & (C_p \rho V)_w & 0 & 0 \\ 1 & 0 & 0 & 0 & (2 \times 0.0198 T_1 + 0.085)/1000 & 0 \end{bmatrix} \tag{5.25}$$

5.3 Model linearization

The developed dynamic model expressed in state-space representation, i.e., Equation (5.22), was nonlinear since the relationship between state variables and input variables was nonlinear. It would be difficult to design an MIMO controller for nonlinear systems based on modern control theory, therefore it was necessary to linearize the dynamic model of the experimental DX A/C system.

In most cases, a DX A/C system was designed to operate in the vicinity of a predetermined setpoint given that thermal space cooling load did not significantly change. As long as the control system can properly regulate the dynamic deviation of the controlled objectives from their setpoints, the controlled system can be well represented by a linearized model around the setpoints. Hence, the state variables, X, and control inputs, U, can be expressed as follows, respectively:

$$X = x + x^0 \tag{5.26}$$

$$U = u + u^0 \tag{5.27}$$

where x^0 and u^0 were the state vector and input vector, both evaluated at a steady state operating point, and x and u represented the small dynamic deviation from x^0 and u^0, respectively. For the DX A/C system to be modeled, the sensible and moisture content load disturbance can be regarded as being constant at a steady state. Therefore the

linearized model describing the system's dynamic deviation at an operating point can be written as:

$$\dot{x} = \left.\frac{\partial g_1}{\partial X}\right|_{x^0,u^0} x + \left.\frac{\partial g_1}{\partial U}\right|_{x^0,u^0} u = A(x^0,u^0)x + B(x^0,u^0)u \tag{5.28}$$

Since the derivation of steady state variables was zero, the derivation of variables can be written as follows:

$$\frac{d(x+x^0)}{dt} = \frac{dx}{dt} + \frac{dx^0}{dt} = \frac{dx}{dt} \tag{5.29}$$

Therefore the dynamic model of the DX A/C system can be linearized as follows:

$$\begin{cases} C_p\rho V\dfrac{d\delta T_2}{dt} = C_p\rho(T_{1s}-T_{2s})\delta f + C_p\rho f_s(\delta T_1-\delta T_2) + k_{spl}\delta f \\ \dfrac{d\delta W_2}{dt} = \dfrac{(W_{1s}-W_{2s})}{V}\delta f + \dfrac{f_s}{V}(\delta W_1-\delta W_2) \\ C_p\rho V_{h1}\dfrac{d\delta T_3}{dt} = C_p\rho f_s(\delta T_2-\delta T_3) + C_p\rho(T_{2s}-T_{3s})\delta f + \alpha_1 A_1(\delta T_w - \dfrac{\delta T_2+\delta T_3}{2}) \\ \rho V_{h2}\dfrac{d(C_p\delta T_1 + h_{fg}\delta W_1)}{dt} = \rho f(C_p(\delta T_3-\delta T_1)+h_{fg}(\delta W_3-\delta W_1)) \\ +\rho(C_p(T_{3s}-T_{1s})+h_{fg}(W_{3s}-W_{1s}))\delta f + \alpha_2 A_2(\delta T_w - \dfrac{\delta T_3+\delta T_1}{2}) \\ (C_p\rho V)_w\dfrac{d\delta T_w}{dt} = \alpha_1 A_1(\dfrac{\delta T_2+\delta T_3}{2}-\delta T_w) + \alpha_2 A_2(\dfrac{\delta T_3+\delta T_1}{2}-\delta T_w) - \dfrac{\delta s V_{com}\lambda}{v_s}(h_{r2}-h_{r1}) \\ \dfrac{d\delta W_1}{dt} - (2\times 0.0198T_1+0.085)\dfrac{d\delta T_1}{dt}/1000 = 0 \end{cases} \tag{5.30}$$

where the variables T_{1s}, T_{2s}, T_{3s}, T_{ws}, W_{1s}, W_{2s} and f_s were the values of the variables at their steady state operating points, respectively. And δT_1, δT_2, δT_3, δT_w, δW_1, δW_2, δf and δs were the dynamic deviations of the variables from their steady state operating points, respectively.

Therefore the linearized multivariable control-oriented dynamic model of the DX A/C system in state-space representation, which was highly suitable for multivariable control design, can be written as:

$$\begin{cases} \dot{x} = Ax + Bu \\ y = Cx \end{cases} \tag{5.31}$$

where the state variables $x = [\delta T_1, \delta T_2, \delta T_3, \delta T_w, \delta W_1, \delta W_2]^T$, input variables $u = [\delta f, \delta s]^T$, and the output variables $y = [\delta T_2, \delta W_2]^T$, which were the dynamic deviations of air temperature and moisture content from their setpoints, respectively. A, B, and C were the coefficient matrices.

For the DX A/C system, when the system was operated at the point of T_2 = 24 ºC, W_2 = 0.01135 kg/(kg dry air), T_1=13.25 ºC, W_1 = 0.00903 kg/kg(dry air) and f = 0.347 m^3/s, the system matrices A, B and C were calculated as follows:

$$A = \begin{bmatrix} -5.731 & 0 & 0.0756 & 4.1883 & -5287 & 5287 \\ 0.0045 & -0.0045 & 0 & 0 & 0 & 0 \\ 0 & 4.6577 & -12.692 & 8.0346 & 0 & 0 \\ 0.0139 & 0.0067 & 0.0206 & -0.0412 & 0 & 0 \\ 0.0006 & 0 & 0 & 0 & 0 & 0 \\ 0 & 0 & 0 & 0 & 0.0045 & -0.0045 \end{bmatrix} \tag{5.32}$$

$$B = \begin{bmatrix} 55.035 & 0 \\ -0.098 & 0 \\ 172.5 & 0 \\ 0 & -5.931 \\ 0 & 0 \\ -0.00003 & 0 \end{bmatrix} \qquad C = \begin{bmatrix} 0 & 1 & 0 & 0 & 0 & 0 \\ 0 & 0 & 0 & 0 & 0 & 1 \end{bmatrix} \tag{5.33}$$

The eigenvalues of the linearized dynamic model for the DX A/C system were shown in Equation (5.34) for the operating point. All the eigenvalues had negative real parts, suggesting that the system was asymptotically stable [Stefani et al. 2002].

$$\lambda_{sys} = \begin{bmatrix} \text{-2.46e-017} \\ \text{-4.51e-003} \\ \text{-2.85e-002} \\ \text{-6.15e-001} \\ \text{-5.12e+000} \\ \text{-1.27e+001} \end{bmatrix} \tag{5.34}$$

5.4 Validation of the dynamic model

Simulation results using the linearized dynamic model, i.e., Equation (5.31), have been compared with the experimental data obtained from the experimental DX A/C system for the purpose of model validation. The simulation results and experiment results were the open-loop responses to step changes in compressor speed and supply fan speed, respectively. When the experimental DX A/C system was operating around a steady state condition, step changes were introduced to the controllable inputs such as compressor speed and supply fan speed. The same operating conditions and step changes were also input to the model to obtain simulation results to facilitate the comparison.

The following comparisons were based on the steady state operational condition of around 24 ºC indoor air temperature and 0.0113 kg/(kg dry air) moisture content, or 60% RH in the conditioned space. The numerical values of both the system parameters used in the simulation and the operating condition of the DX A/C system are given in Table 5.1 and Table 5.2, respectively. The linearization of the model was also based on this operating condition. Figures 5.3 to 5.8 present the comparisons between the simulation results and experimental data in response to a step change in compressor speed from 3960 rpm to 4488 rpm (from 66 Hz to 75 Hz), introduced at 420 s. When the compressor speed increased, the temperature and moisture content of the air in conditioned space decreased due to the increased output cooling capacity of the DX A/C system, as shown in Fig. 5.3 and Fig. 5.4. As seen in both figures, there existed a good

agreement between the simulated responses and experimental results. Similar observations can be obtained for other operating parameters such as the temperature and moisture content of air leaving the DX evaporator (Fig. 5.5 and Fig. 5.6), indoor air relative humidity (Fig. 5.7) and output cooling capacities (Fig. 5.8). In Fig. 5.8, it is seen that the increase in output latent cooling capacity was more than that in output sensible cooling capacity, when the total output cooling capacity was increased due to the increase in compressor speed, which resulted in a lower evaporating temperature or a lower evaporator wall temperature. Hence, as seen in Fig. 5.7, indoor air RH was reduced due to the increased output latent cooling capacity.

Table 5.1 Numerical values of the system parameters

C_p	= 1.005 kJ/kg	A_1	= 4.14 m^2
ρ	= 1.2 kg/m^3	A_2	= 17.65 m^2
h_{fg}	= 2450 kJ/kg	V_{h1}	= 0.04 m^3
V	= 77 m^3	V_{h2}	= 0.16 m^3

Table 5.2 Operating condition of the experimental DX A/C system

T_1	= 13.25 ºC	P_c	= 1.812×10^6 Pa
W_1	= 9.03/1000 kg/kg dry air	P_e	= 0.486×10^6 Pa
T_2	= 24 ºC	Q_{load}	= 4.49 kW
W_2	= 11.35/1000 kg/kg dry air	M	= 0.96/1000 kg/s
T_3	= 17 ºC	M_{ref}	= 0.042 kg/s
T_w	= 13 ºC	s	= 3960 rpm
SH	= 6 ºC	f	= 0.347 m^3/s

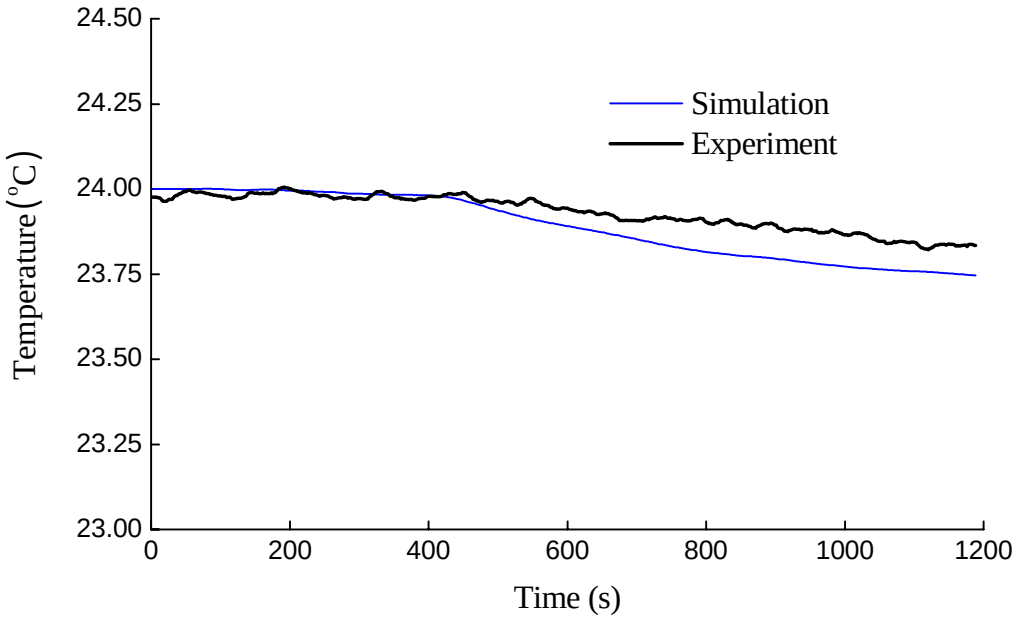

Fig. 5.3 Simulated and measured air temperature in the conditioned space in response to a step change in compressor speed

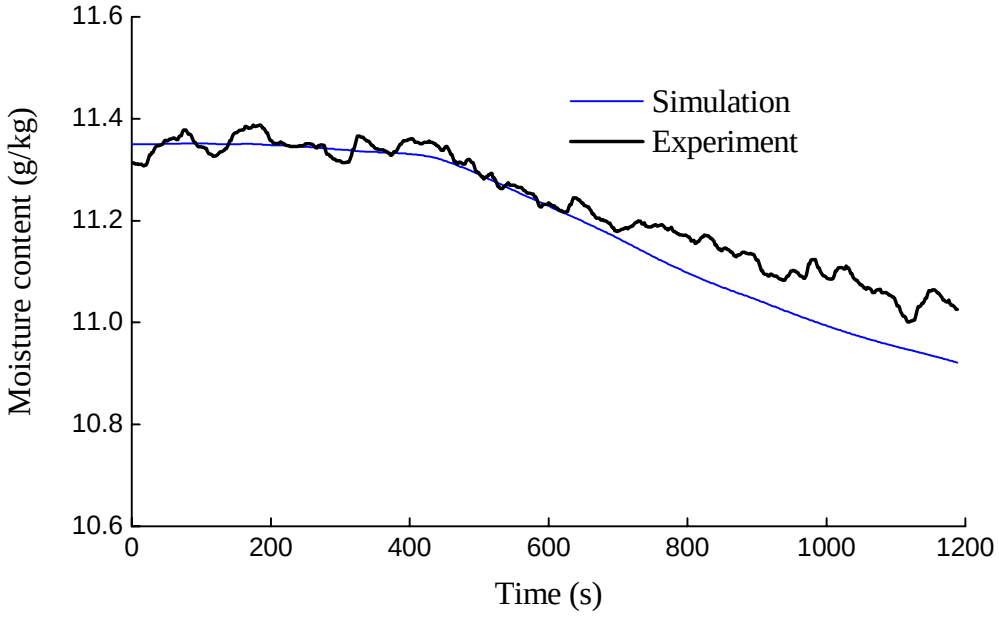

Fig. 5.4 Simulated and measured air moisture content in the conditioned space in response to a step change in compressor speed

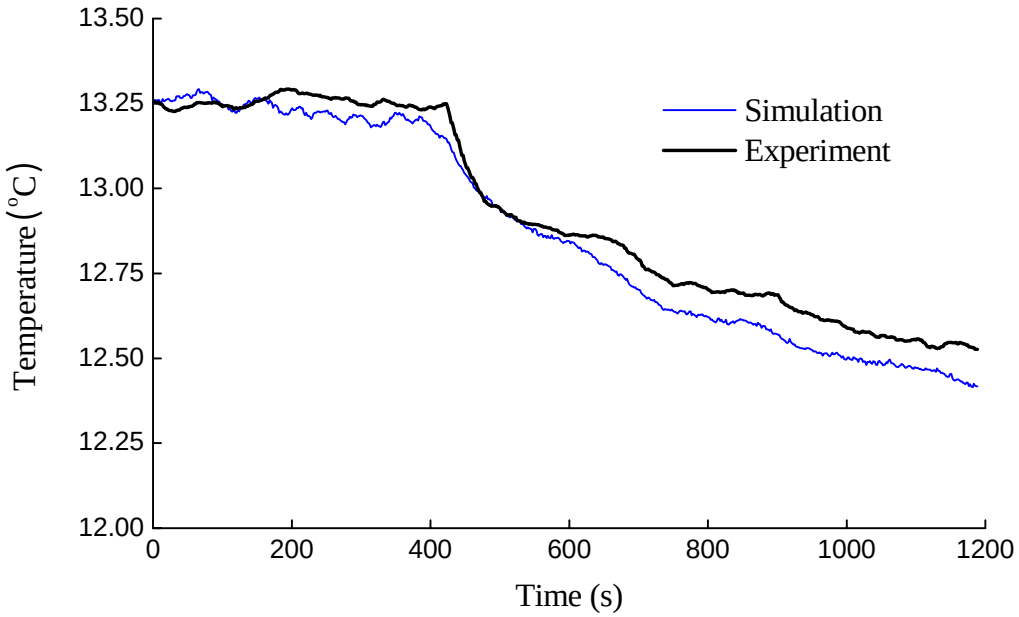

Fig. 5.5 Simulated and measured temperature of the air leaving evaporator in response to a step change in compressor speed

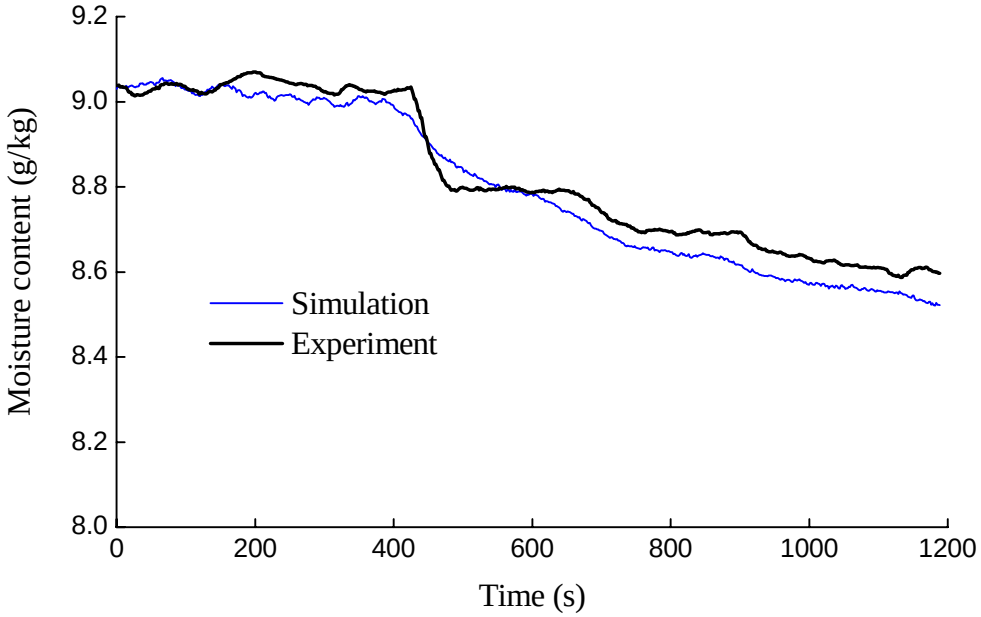

Fig. 5.6 Simulated and measured moisture content of the air leaving evaporator in response to a step change in compressor speed

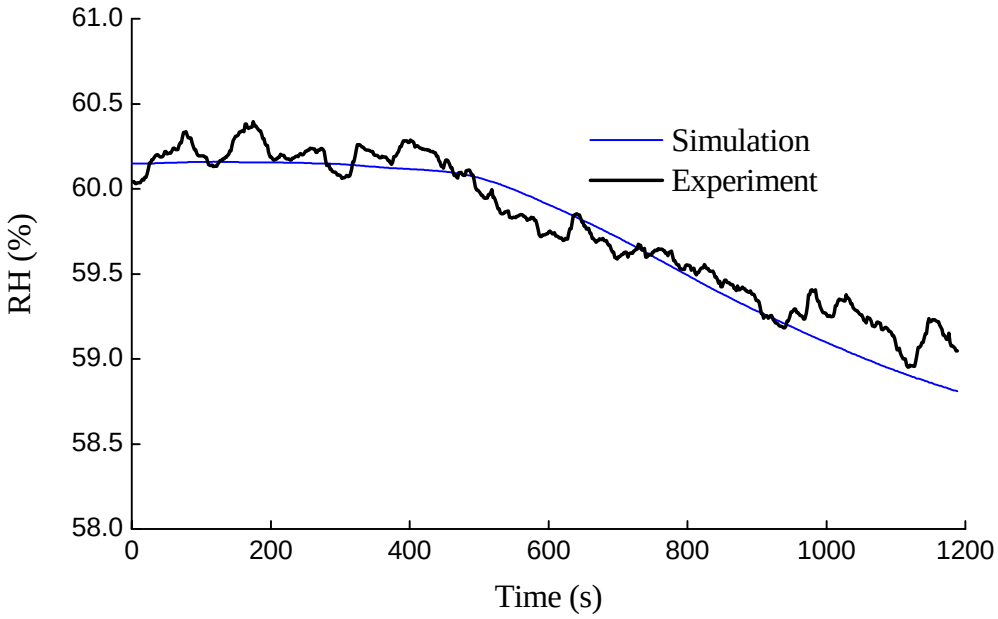

Fig. 5.7 Simulated and measured relative humidity in the conditioned space in response to a step change in compressor speed

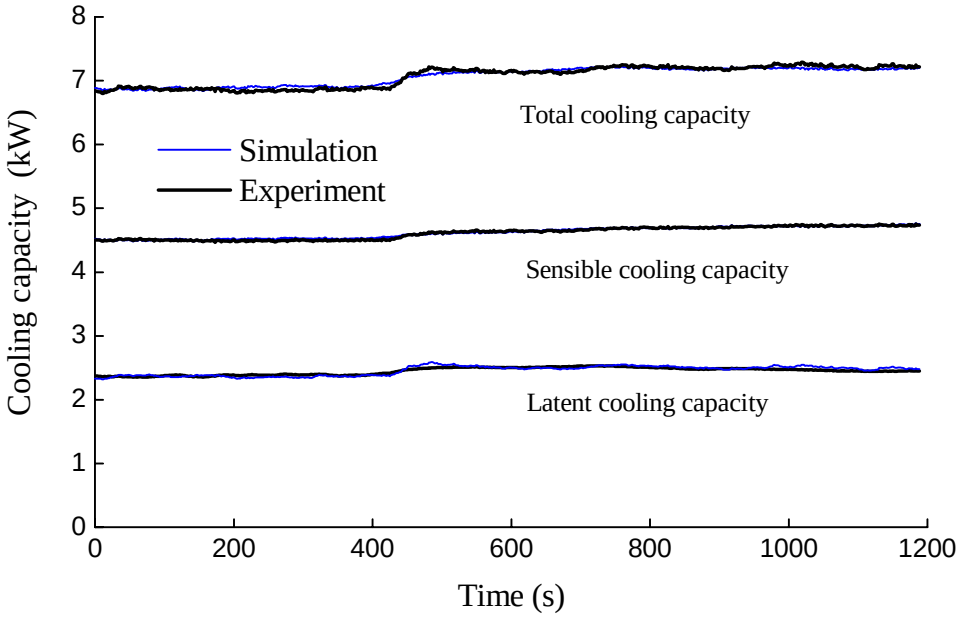

Fig. 5.8 Simulated and measured output cooling capacities in response to a step change in compressor speed

On the other hand, the comparisons between the simulation results and experimental data, in response to a step change in supply fan speed from 2448 rpm to 2160 rpm (from 41 Hz to 36 Hz), introduced at 290 s, are illustrated in Figs. 5.9 to 5.14. When the supply fan speed was reduced, the temperature and moisture content of the air leaving the DX evaporator decreased, as shown in Fig. 5.9 and Fig. 5.10, respectively. Again, in both Figures, a good agreement between the simulated results and measured experimental data can be observed. Similar observations of agreement can also be found for other system parameters as shown in Figures 5.11 to 5.14.

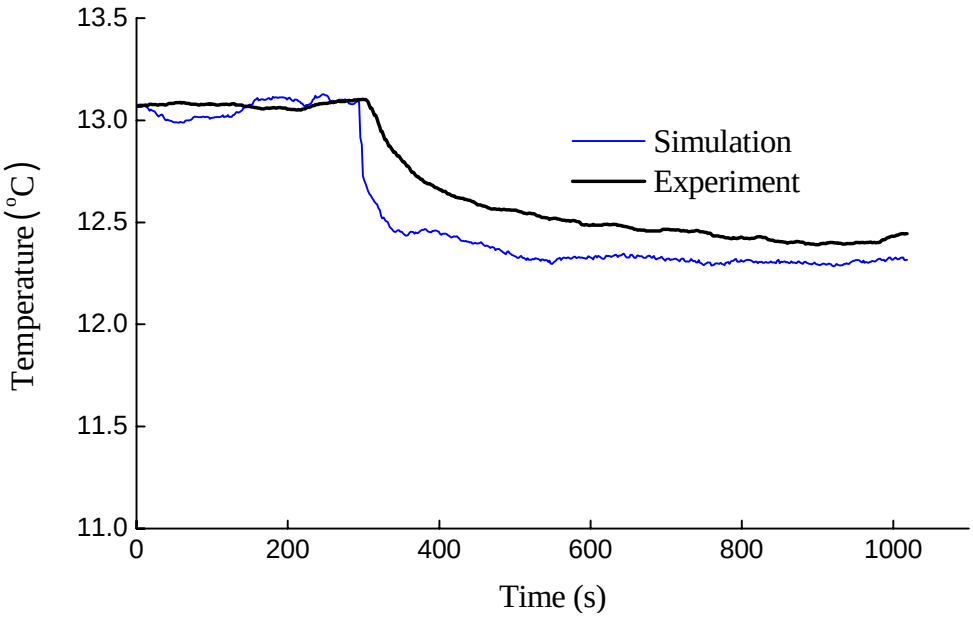

Fig. 5.9 Simulated and measured temperature of the air leaving evaporator in response to a step change in supply fan speed

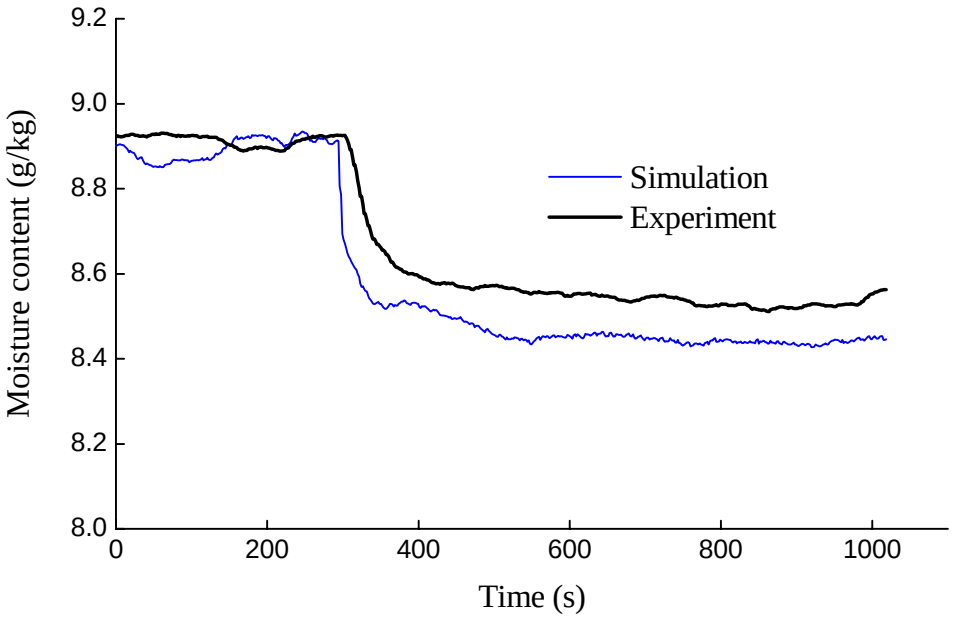

Fig. 5.10 Simulated and measured moisture content of the air leaving evaporator in response to a step change in supply fan speed

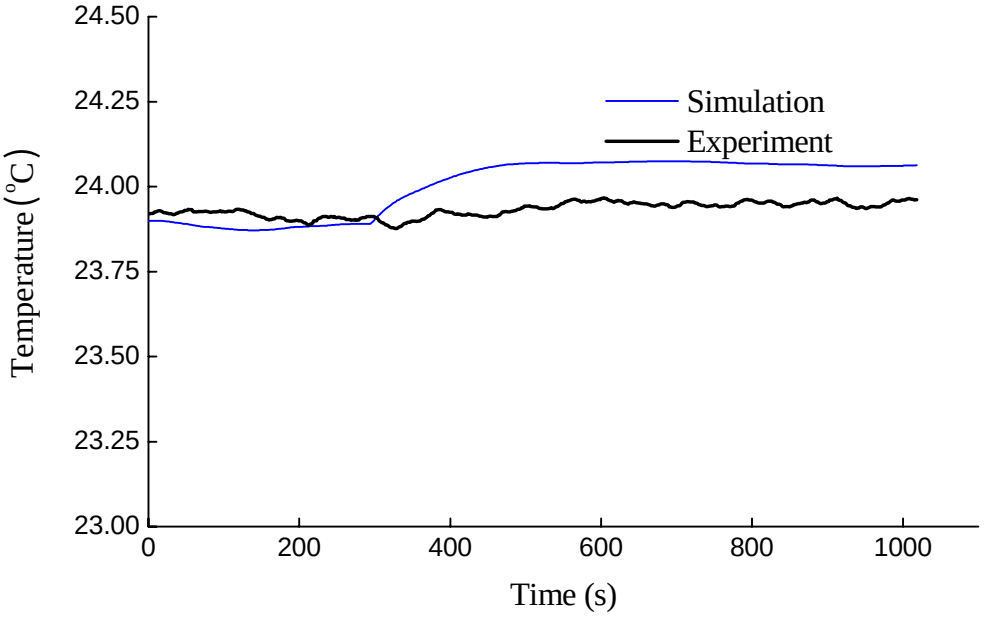

Fig. 5.11 Simulated and measured air temperature in the conditioned space in response to a step change in supply fan speed

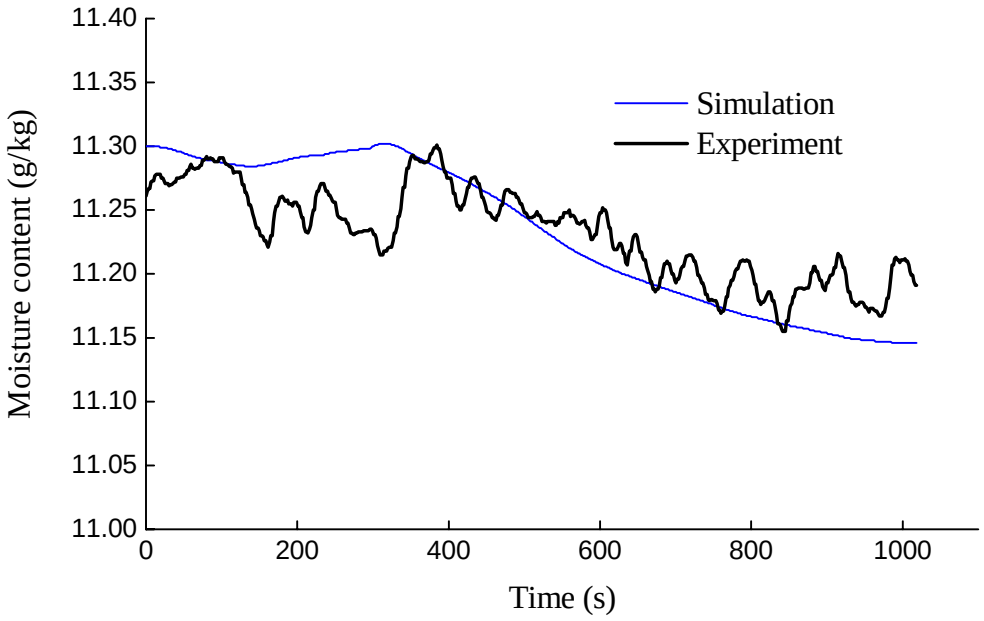

Fig. 5.12 Simulated and measured air moisture content in the conditioned space in response to a step change in supply fan speed

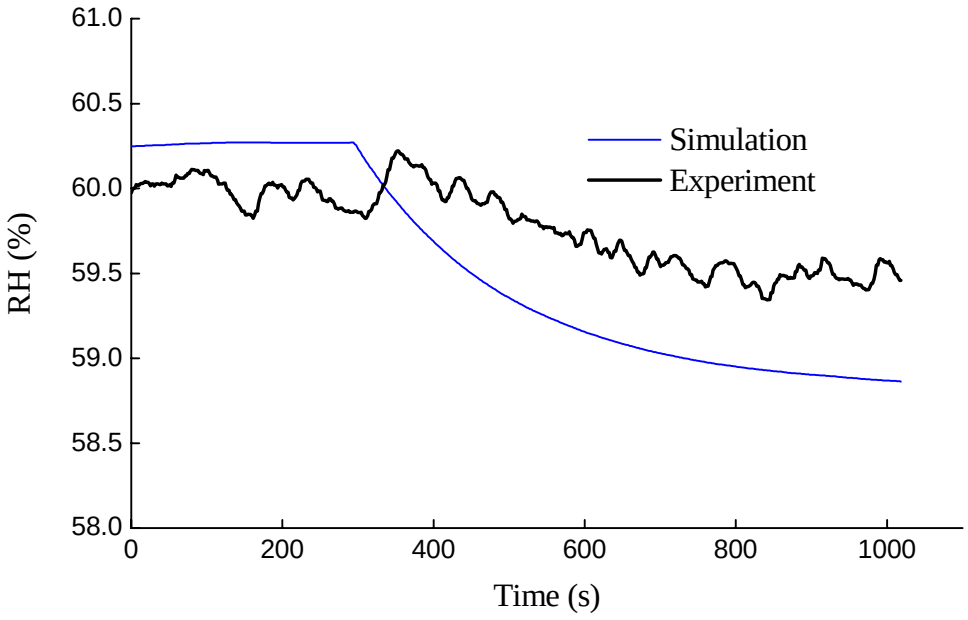

Fig. 5.13 Simulated and measured relative humidity in the conditioned space in response to a step change in supply fan speed

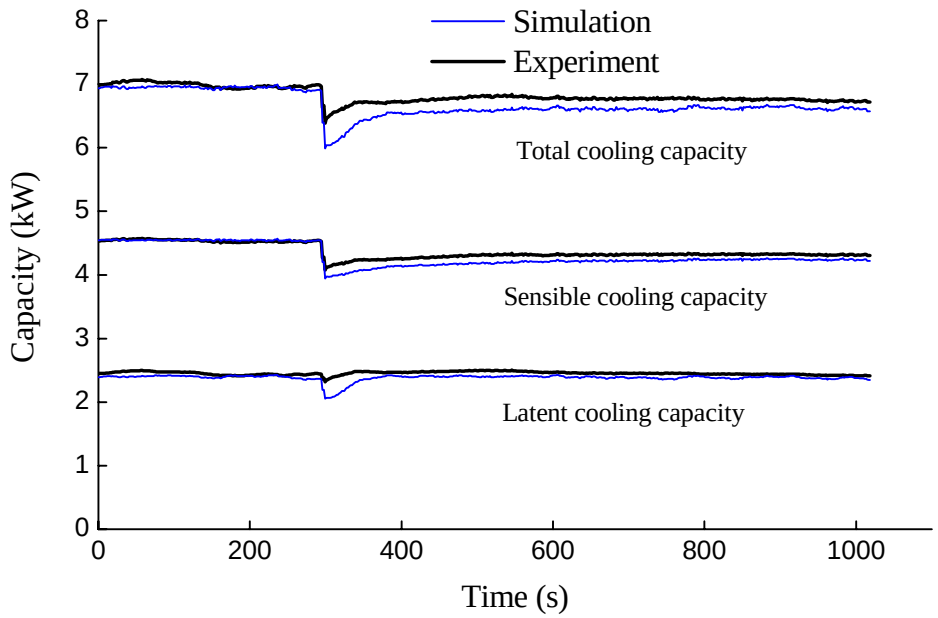

Fig. 5.14 Simulated and measured output cooling capacities in response to a step change in supply fan speed

The comparisons shown in Figures 5.3 to 5.14 confirmed that the developed model after linearization was experimentally validated, being able to both capture the transient change of system parameters in a timely manner, and to represent the steady-state operation with an acceptable accuracy. Although there were a number of points where there existed noticeable differences between the measured and simulated responses possibly due to the fact that the model developed was a simplified one, the general trends for both were consistent. Hence, this model was a good representation of the DX A/C system during both the steady state and transient operating conditions. More importantly, the dynamic model was written in state-space representation, which was high suitable for multivariable controller design and hence is expected to be very useful

in designing an MIMO controller for simultaneously controlling indoor air temperature and humidity.

5.5 Summary

A multivariable control-oriented dynamic model of the experimental DX A/C system has been developed based on the principles of energy and mass conservation. In developing the model, the DX evaporator in the DX A/C system was divided into two regions on its air side, e.g., a dry-cooling region and a wet-cooling region, corresponding to the two regions on its refrigerant side, e.g., a two-phase region and a superheated region. The air dry-cooling and wet-cooling conditions were separately considered when modeling the air handling process taking place in the DX evaporator.

The multivariable control-oriented dynamic model of the experimental DX A/C system was nonlinear in nature, thus it was linearized at its operating point and was written in state-space representation. The linearized dynamic model of the experimental DX A/C system was highly suitable for designing a multivariable control algorithm for the DX A/C system. The multivariable control-oriented dynamic model was experimentally validated by comparing the measured with the simulated open-loop responses for all major operational parameters of the DX A/C system.

The validated multivariable control-oriented dynamic model for the experimental DX A/C system is expected to be very useful in designing an MIMO controller for simultaneously controlling indoor air temperature and humidity in a space served by a DX A/C system, which is reported in Chapter 6.

Chapter 6

The Design of an MIMO Controller for Simultaneous Air Temperature and Humidity Control and its Controllability Tests

6.1 Introduction

As mentioned in Chapter 2, various control strategies have been employed in A/C systems, such as PI, PID, fuzzy and adaptive control strategies, etc. An advantage for using PI or PID control strategy is that there is no need to develop a mathematical model for the A/C system under control. Hence, it is relatively easy to design PI or PID controllers for air conditioning systems. However, most of these control strategies are of SISO nature. For example, the experimental investigation by Krakow et al. [1995] suggested that indoor air temperature and relative humidity may be controlled by a PID controller through separately varying compressor speed and supply fan speed. The two control loops, i.e., the control loop for air temperature by varying compressor speed and that for relative humidity by varying supply fan speed, have been treated as two independent SISO control loops. The transient control performance of the two decoupled feedback loops was inherently poor due to the strong cross-coupling between them. Both indoor air temperature and humidity in a space were affected by the variations in compressor speed and supply fan speed of a DX A/C system serving the space. It can therefore be seen that artificially decoupling the control of two strongly coupled indoor air parameters, i.e., air temperature and humidity, would only yield a

poor control performance. Such a control strategy in which the cross-coupling effects between the two control loops were ignored was fundamentally inadequate.

On the other hand, MIMO control strategies are able to take into account the coupling effects among multiple variables. They are therefore more effective in simultaneously controlling multiple objectives, such as temperature, humidity, capacity and efficiency, etc. The performance of MIMO control strategies is therefore inherently better than that of conventional SISO control strategies.

With the development of variable speed drive technology, the output cooling capacity of DX A/C systems can be adjusted by varying compressor speed, and the supply fan speed can also be modulated to affect the dehumidification in DX evaporator. Therefore for a DX A/C system having a variable speed compressor and variable speed supply fan, it is possible to simultaneously control the two coupled control objectives, e.g., indoor air temperature and humidity through simultaneously varying compressor speed and supply fan speed by an MIMO controller. The MIMO controller would consider the coupling effect between indoor air temperature and humidity when simultaneously varying compressor speed and supply fan speed. This would help eliminate the artificial decoupling of the two coupled control variables, so that the control accuracy and sensitivity can be improved.

This Chapter presents the design of an MIMO controller based on the multivariable control-oriented dynamic model developed and reported in Chapter 5. The control

objective of the MIMO controller for the experimental DX A/C system was to simultaneously control indoor air temperature and humidity to their respective setpoints by simultaneously varying compressor speed and supply fan speed. The MIMO controller was digitally implemented in the experimental DX A/C system. Controllability tests for the MIMO controller were carried out using the experimental DX A/C system. The experimental results of both the disturbance rejection controllability test and the command following controllability test are presented and discussed.

6.2 Design of the MIMO controller

The MIMO-based controller was designed based on the multivariable control-oriented dynamic model of the experimental DX A/C system, i.e. Equation (5.31). A schematic diagram of the MIMO control system is shown in Figure 6.1. The main difference between an MIMO control system and a SISO control system is that the decoupled SISO control system only used one feedback signal to generate a single control input to a controlled object. For example, indoor air temperature is used to generate a signal to control compressor speed. However, the MIMO control system uses two feedback signals, i.e., indoor air temperature and moisture content, to generate two signals to control both compressor speed and supply fan speed simultaneously.

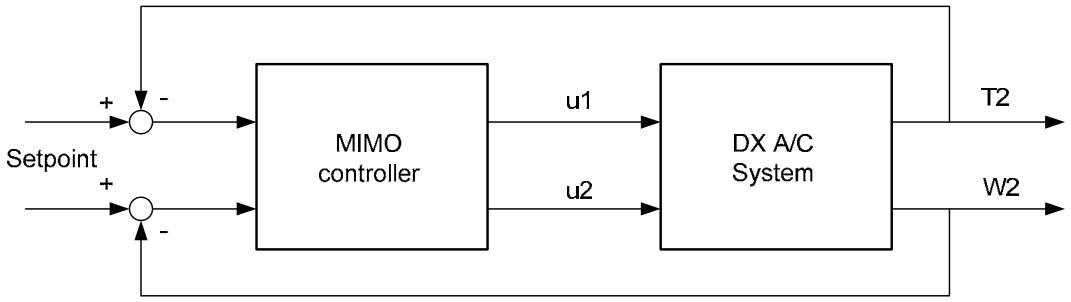

Figure 6.1 Schematic diagram of the MIMO control system

For designing an MIMO controller, several methods can be used, such as Linear Quadratic Regulator (LQR), Linear Quadratic Gaussian (LQG) and H_∞ control, etc [Skogestad and Postlethwaite 1996]. In this study, the MIMO controller was designed using the technique of LQG. The block diagram of the MIMO feedback control system is shown in Figure 6.2.

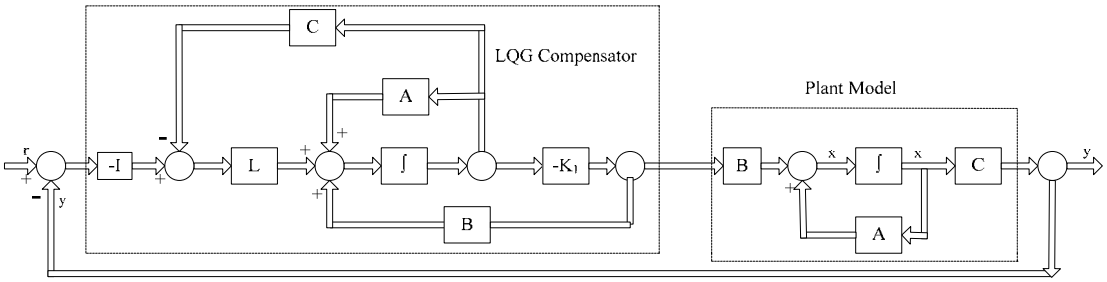

Figure 6.2 Block diagram of the LQG-based MIMO feedback control system

An LQG-based multivariable controller is an observer-based compensator that uses the Kalman filter to optimally estimate unmeasured state variables based on measurements and then uses the optimal full state feedback to generate a control law. The optimal gain

matrix, K_1 , and Kalman filter matrix, L , are determined based on the system matrices A , B , C and D in the system model, the weighting matrices for linear quadratic regulator and the weighting matrices for linear quadratic estimator. An LQG-based multivariable controller can optimize a cost function that compromises output errors and control efforts. Weighting matrices are to be determined to guarantee stability robustness and ensure good control performance [Stefani et al. 2002].

The linearized dynamic model of the experimental DX A/C system around an operating point is previously presented in Chapter 5 in a state-space representation by Equation (5.31) and is repeated here as follows:

$$\begin{cases} \dot{x} = A \cdot x + B \cdot u \\ y = C \cdot x \end{cases} \tag{6.1}$$

The optimal feedback gain matrix, K_1, was calculated such that the feedback law, $u = -K_1 \cdot x$, minimized the cost function:

$$J = \int (y'Qy + u'Ru)dt \tag{6.2}$$

where Q and R were the weighting matrices which can be suitably selected to obtain the desired operating performance of the DX A/C system.

In this study, the same weight for the weighting matrices was assigned, thus Q and R were selected as follows:

$$Q = \begin{bmatrix} 1 & 0 \\ 0 & 1 \end{bmatrix}, \qquad R = \begin{bmatrix} 1 & 0 \\ 0 & 1 \end{bmatrix} \tag{6.3}$$

To obtain Kalman filter gain matrix, L , the linear quadratic estimator design was considered. For the system with process noise and measurement noise [Stefani et al. 2002]:

$$\begin{cases} \dot{x} = A \cdot x + B \cdot u + w \\ y = C \cdot x + v \end{cases} \tag{6.4}$$

where w represented random noise disturbance input (process noise) and v random measurement (sensor) noise. For A/C systems, they could be subject to random heat load disturbances (i.e., process noise). On the other hand, the measuring instruments are not always accurate (i.e., sensor noise). In general, most A/C systems can be subject to both kinds of noise.

The optimal observer for the MIMO control system was given by [Stefani et al. 2002]:

$$\dot{\hat{x}} = (A - LC) \cdot \hat{x} + B \cdot u + Ly \tag{6.5}$$

where $\hat{x}$ was an estimate of the state variables, x, and the observer gain, L, was computed from:

$$L = \sum C' R^{-1} \tag{6.6}$$

where $\sum$ was the solution of an Algebraic Riccati Equation [Stefani et al. 2002], which was expressed as follows:

$$A\sum + \sum A' + Q_0 - \sum C' R_0^{-1} C \sum = 0 \tag{6.7}$$

where the matrices Q_0 and R_0 represented the intensity of the process and sensor noise inputs.

Since the matrices Q_0 and R_0 could be viewed as design parameters and may be suitably selected to obtain the desired performance of the controlled system [Stefani et al. 2002], the matrices were given as follows:

$$Q_0 = \begin{bmatrix} 1 & 0 \\ 0 & 1 \end{bmatrix}, \qquad R_0 = \begin{bmatrix} 1 & 0 \\ 0 & 1 \end{bmatrix} \tag{6.8}$$

After the gain matrices K_1 and L were obtained, the transfer function of the observer-based compensator LQG can be expressed as follows:

$$K(s) = K_1(sI - A + BK_1 + LC)^{-1}L \tag{6.9}$$

Generally, an MIMO controller would have steady state error if a plant itself did not have an integrator, as shown in Fig. 6.2. Therefore, for the experimental DX A/C system which had no integrator in its dynamic model, it was necessary to include an integrator in the controller to eliminate steady state errors. The block diagram of an MIMO feedback control system with an integrator is shown in Fig. 6.3.

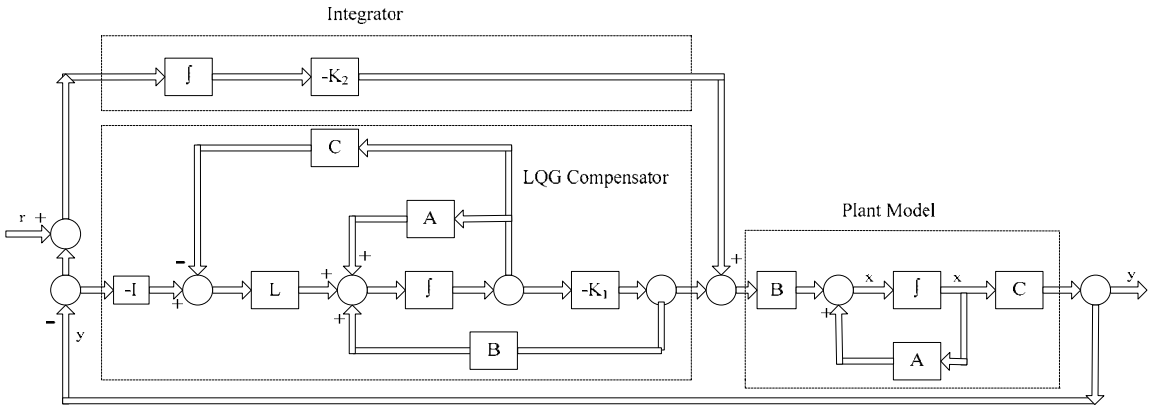

Figure 6.3 Block diagram of an MIMO feedback control system with an integrator

In order to track the reference, the integrator variable, η, was written as follows:

$$\dot{\eta} = r - y \tag{6.10}$$

Thus the augmented state was as follows:

$$x_a = \begin{bmatrix} x \\ \eta \end{bmatrix} \tag{6.11}$$

Therefore the augmented state equations were written as follows:

$$\dot{x}_a = \begin{bmatrix} \dot{x} \\ \dot{\eta} \end{bmatrix} = \begin{bmatrix} A & 0 \\ -C & 0 \end{bmatrix} \begin{bmatrix} x \\ \eta \end{bmatrix} + \begin{bmatrix} B & 0 \\ 0 & I \end{bmatrix} \begin{bmatrix} u \\ r \end{bmatrix} = A_a x_a + B_a u_a \tag{6.12}$$

$$y = [C \quad 0] \begin{bmatrix} x \\ \eta \end{bmatrix} = C_a x_a \tag{6.13}$$

The optimal feedback gain matrix for the augmented MIMO control system, i.e., with the integrator included, was obtained such that the feedback control law, $u = -K_a \cdot x_a$, minimized the cost function:

$$J = \int (y_a' Q y_a + u' R u) dt \tag{6.14}$$

The gain matrix, K_2, can be selected to obtain the desired performance of the controlled system. In this study, the values of K_1 and K_2 were as follows:

$$K_1 = \begin{bmatrix} \text{-0.027466} & \text{-2.45} & \text{-0.00029066} & \text{-0.011415} & 14.504 & \text{-14.495} \\ \text{-0.030336} & \text{-0.74535} & \text{-0.00079833} & \text{-0.026613} & 38.653 & \text{-38.68} \end{bmatrix} \tag{6.15}$$

$$K_2 = \begin{bmatrix} -0.006875 & 0.00165 \\ -0.000405 & -0.000162 \end{bmatrix} \tag{6.16}$$

After obtaining the gain matrix, K_2, the control law can be expressed as follows:

$$u = -K_1 \cdot \hat{\mathrm{x}} - K_2\eta = -[K_1 \quad K_2]\begin{bmatrix} \hat{\mathrm{x}} \\ \eta \end{bmatrix} = -K_a x_a \tag{6.17}$$

Therefore the transfer function of the LQG compensator with an integrator can be expressed as follows:

$$K(s) = K_a(sI - A + BK_a + LC)^{-1}L \tag{6.18}$$

6.3 Controllability tests

After designing the LQG-based MIMO controller for the experimental DX A/C system, it was necessary to carry out the controllability tests to evaluate the performance of the MIMO controller using the experimental DX A/C system. The MIMO controller was digitally implemented in the experimental DX A/C system. With the computerized instrumentation, all the measured data can be recorded for subsequent analysis, and the control inputs to the DX A/C system can be generated based on the feedback signals of

measured indoor air temperature and humidity. The schematic diagram of the experimental DX A/C system and the MIMO controller is shown in Fig. 6.4.

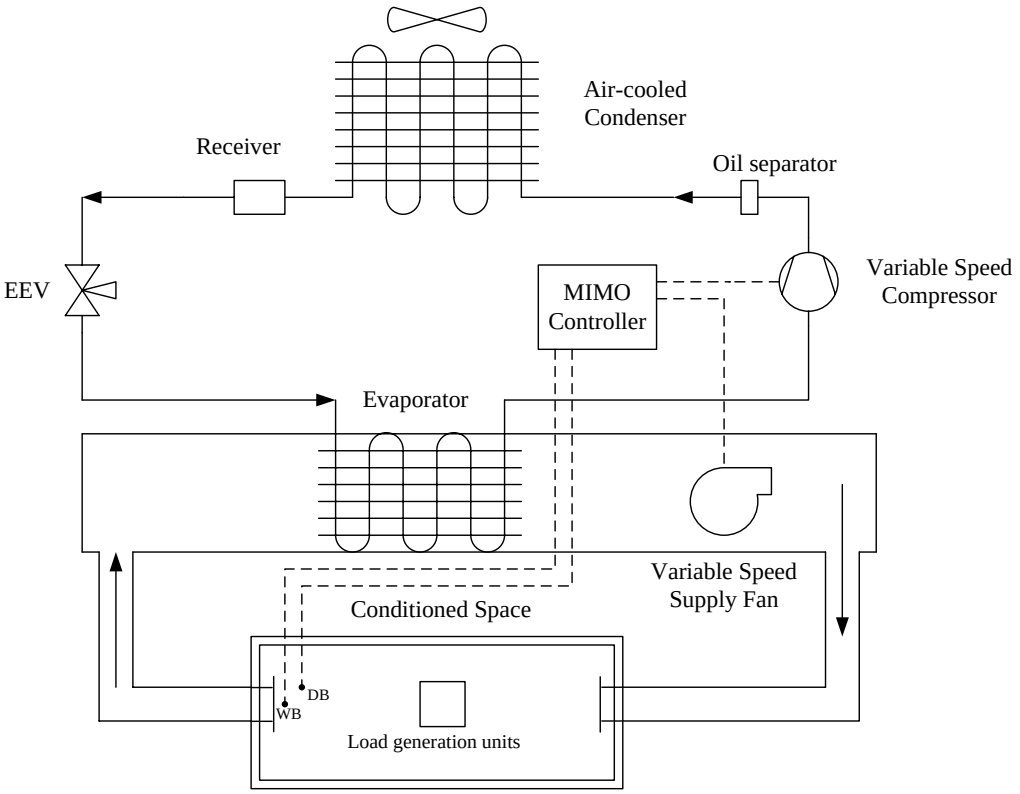

Figure 6.4 Schematic diagram of the DX A/C system and the MIMO controller

For the MIMO controller developed for the experimental DX A/C system, its control performances would be evaluated based on the following criteria:

(1) Disturbance rejection: the output variables, i.e., indoor air temperature and moisture content were to be maintained at their respective set points through simultaneously

varying compressor speed and supply fan speed when the space was subjected to the disturbances of space sensible and latent heat load changes;

(2) Command following: the output variables can track changes of their set points with stability. When the set point of either air temperature or moisture content was changed, the MIMO controller could react so that indoor air temperature or moisture content can be maintained at their respective new setpoints.

For all controllability tests using the experimental DX A/C system, indoor air temperature control was via controlling indoor air dry-bulb temperature, and indoor humidity control was via controlling indoor air wet-bulb temperature. Air moisture content can be evaluated by using the properties of moist air after knowing air dry-bulb and wet-bulb temperatures. Since the MIMO controller was developed based on the linerized dynamic model of the experimental DX A/C system presented in Chapter 6, the MIMO controller was designed around an operating point of an indoor air dry-bulb temperature of 24 ºC and a wet-bulb temperature of 17 ºC (or an equivalent of air moisture content of 0.00934 kg/(kg dry air) or indoor relative humidity of 50%). The compressor speed and supply fan speed were all initially set at 3955 rpm and 2180 rpm, both being 50% of their maximum speeds, respectively. The condenser cooling airflow rate was maintained constant at 3100 m^3/h, with its inlet temperature fixed at 35 ºC. The degree of refrigerant superheat was maintained constant at 6 ºC by using the EEV, which was controlled by a built-in conventional PID controller in the DX A/C system. In order to protect the compressor and supply fan and to avoid the speeds from changing

sharply, each step change of both compressor speed and supply fan speed was set at not more than 5% of their respective maximum speeds when the speeds of compressor and supply fan were varied. The time interval between step changes was 30 seconds in all tests.

6.3.1 Disturbance rejection capability test

For the disturbance rejection capability test, indoor air settings were 24 ºC (dry-bulb temperature) and 17 ºC (wet-bulb temperature), (or an equivalent of indoor air moisture content 0.00934 kg/(kg dry air)). These settings were expected to be maintained after the disturbances of both sensible and latent heat loads were introduced. The MIMO controller would be enabled when either the deviation between the measured indoor air dry-bulb temperature and its setting or the deviation between the measured indoor air wet-bulb temperature and its setting was greater than ±0.5 ºC as a result of the disturbances.

Figures 6.5 and 6.6 present the controllability test results of disturbance rejection capability of the MIMO controller. The variation profile of heat loads imposed over the entire test period is shown in Fig. 6.5(a). At t = 350 s, the disturbances were introduced, with the sensible and latent heat loads increased from 5.0 kW to 5.6 kW, and from 2.0 kW to 2.3 kW, respectively. Fig. 6.5(b) shows the variation profile of indoor air temperatures. During the first 350 s of the test, indoor air temperatures were maintained

at their respective set points, i.e., 24 ºC dry-bulb and 17 ºC wet-bulb before the disturbances were introduced. Afterwards, both air dry-bulb and wet-bulb temperatures increased gradually. At t = 1360 s when indoor air dry-bulb temperature went over 24.5 ºC, the MIMO controller was enabled. Fig. 6.5(c) shows the variation profiles of compressor speed and supply fan speed. Following the action of the MIMO controller, both speeds increased. Towards the end of the test, the speeds of compressor and supply fan stabilized at around 4750 rpm and 2380 rpm, respectively. Fig. 6.5(d) shows the variation profile of the resultant degree of refrigerant superheat. The degree of refrigerant superheat, however, changed significantly when compressor speed and supply fan speed were varied. On the other hand, the variation profiles of indoor air moisture content and relative humidity are presented in Fig. 6.6(a) and Fig. 6.6(b), respectively. As seen from Fig. 6.5(b), the MIMO controller can well control the indoor air dry-bulb and wet-bulb temperatures to their respective set points, achieving a satisfactory performance in terms of disturbance rejection capability. At the end of test, the deviation between indoor air dry-bulb temperature and its setting was less than 0.1 ºC.

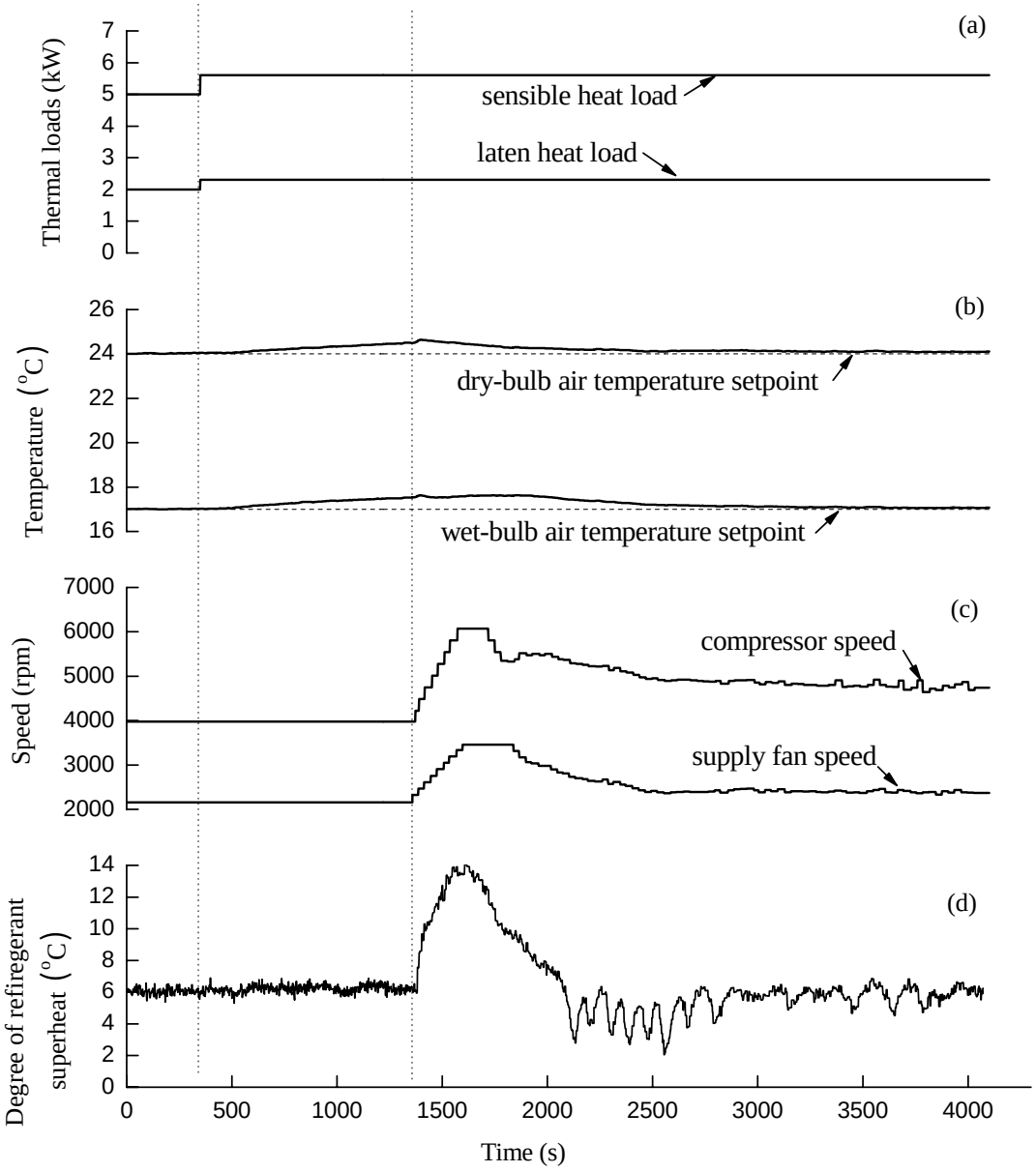

Figure 6.5 The variation profiles of some measured operating parameters in disturbance rejection capability test

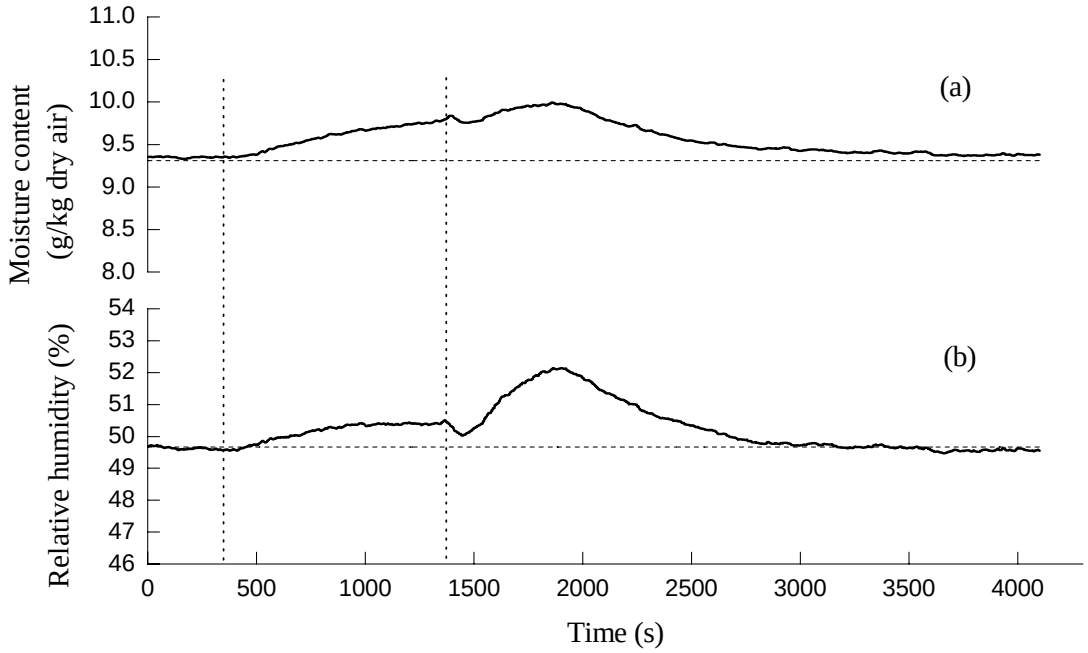

Figure 6.6 The variation profiles of the measured indoor moisture content and relative humidity in disturbance rejection capability test

6.3.2 Command following capability tests

For the command following capability tests, it was expected that when there were changes in settings, the MIMO controller would react so that the new settings can be tracked and maintained. In this investigation, the command following capability tests of the MIMO controller were carried out with respect to the changes of indoor air temperature and humidity settings, respectively.

Figures 6.7 and 6.8 show the controllability test results of the MIMO controller with respect to its command following capability, following a change in the setpoint of

indoor air dry-bulb temperature. When the setpoint was lowered from 24 ºC to 23.5 ºC, with the setting of indoor air moisture content remaining unchanged at 0.00934 kg/(kg dry air), the set point of the indoor air wet-bulb temperature had to be changed correspondingly from 17 ºC to 16.8 ºC. During the first 520 s of the test, the DX A/C system was stable, and both indoor air temperature and moisture content were maintained at their respective setpoints. At t = 520 s, the change of indoor air temperature setting from 24 ºC to 23.5 ºC was introduced, then MIMO controller was immediately enabled, as shown in Fig. 6.7(b). From Fig. 6.7(a), it can be seen that the MIMO controller can well control the indoor air dry-bulb temperature and wet-bulb temperature to their respective setpoints. From Fig. 6.7(c), it can be observed that indoor air moisture content can also be maintained at its set point after the set point of indoor air temperature was altered. Fig. 6.7(d) shows the variation profile of degree of refrigerant superheat, which would however experience a significant variation after the speeds of compressor and supply fan were changed.

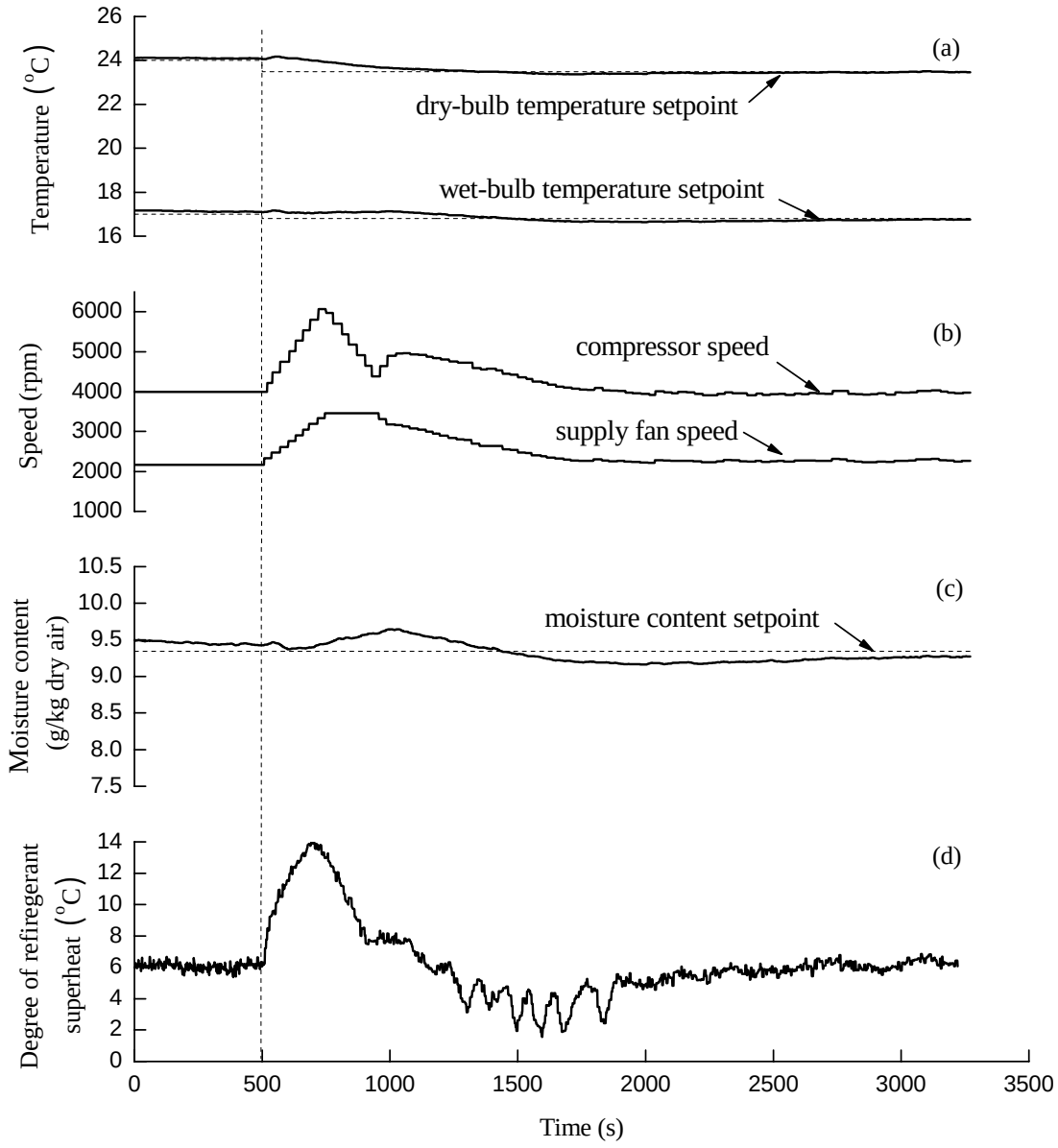

Figure 6.7 The variation profiles of measured operating parameters in command following test with a change in air temperature setting

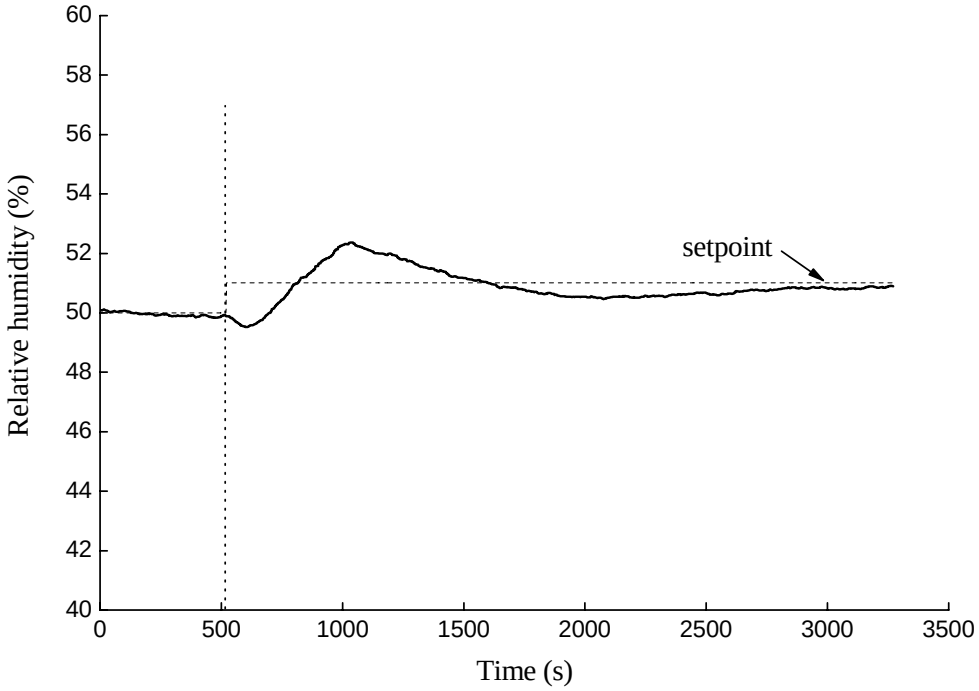

Figure 6.8 The variation profile of the measured indoor air relative humidity in command following test with a change in air temperature setting

Furthermore in this test, since the setting of indoor air dry-bulb temperature was changed from 24 ºC to 23.5 ºC, with the setting of indoor air moisture content remaining unchanged, consequently, the setting of indoor air relative humidity was also changed from 50% to 51.2%. As shown in Fig. 6.8, indoor relative humidity could also reach its new setting after the MIMO controller was enabled.

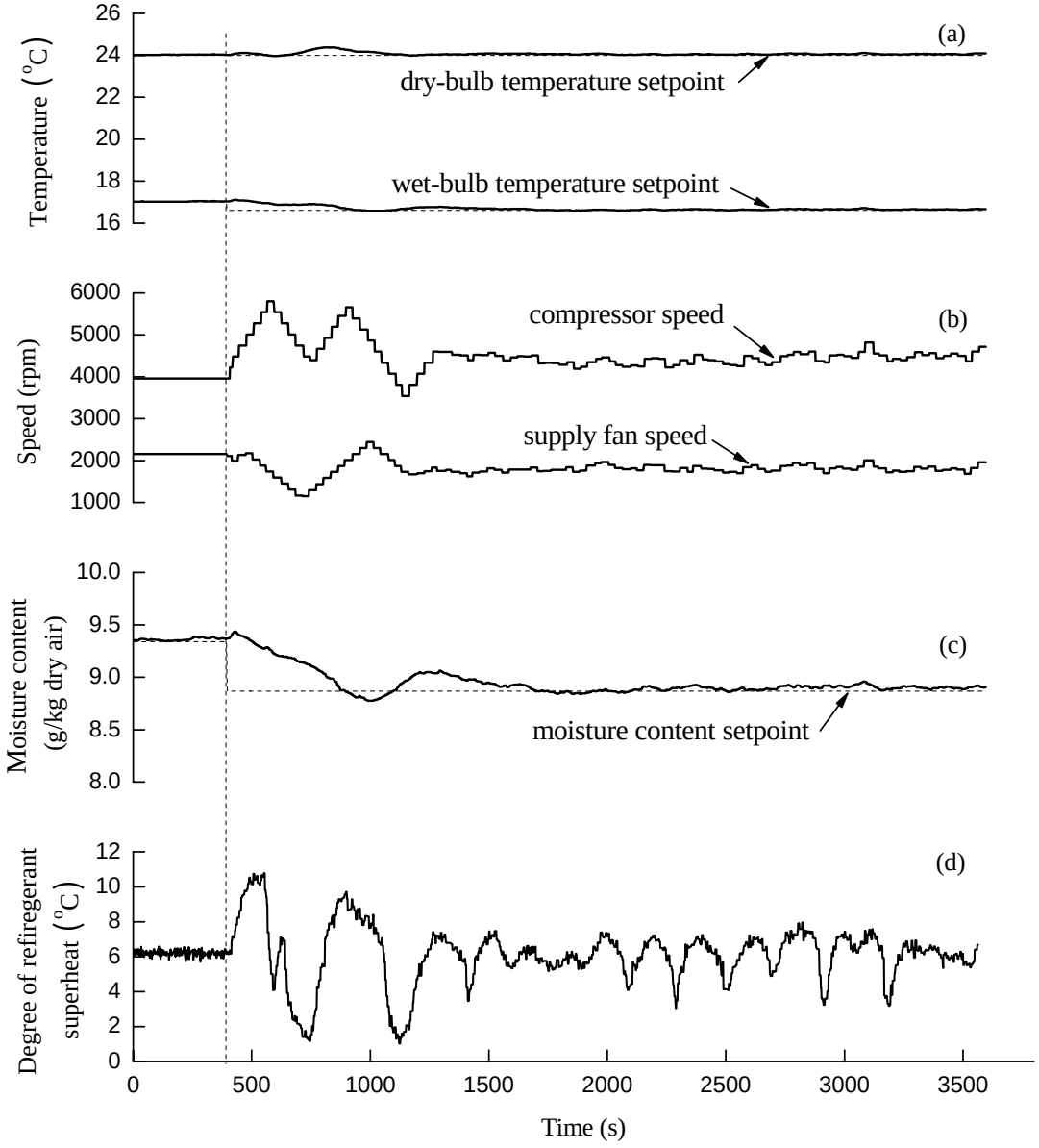

Figure 6.9 The variation profiles of measured operating parameters in command following test with a change in air humidity setting

Figures 6.9 and 6.10 illustrate the controllability test results of the MIMO controller, with respect to its command following capability, following a change in indoor air

moisture content setting which was achieved via a change in indoor air wet-bulb temperature. The setpoint of wet-bulb temperature was changed from 17 ºC to 16.6 ºC, or equivalently moisture content setting from 0.00934 kg/(kg dry air) to 0.00886 kg/(kg dry air), while the indoor air dry-bulb temperature setting was maintained at 24 ºC. The variation profiles of both indoor air dry-bulb and wet-bulb temperatures are shown in Fig. 6.9(a), and that of moisture content in Fig. 6.9(c). As seen from these figures, after the set point was changed, the MIMO controller responded by simultaneously varying speeds of both compressor and supply fan (Fig. 6.9(b)), so that the required new set point was approached in less than 1200s, and well maintained afterwards. The degree of refrigerant superheat fluctuated again significantly as compressor speed and supply fan speed varied, as shown in Fig. 6.9(d).

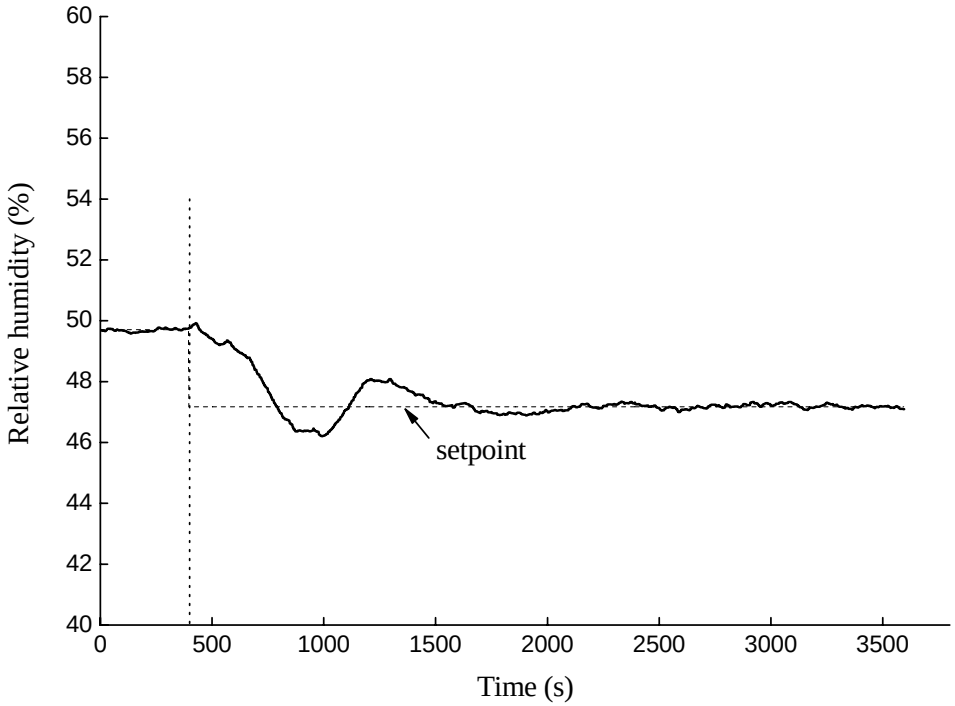

Figure 6.10 The variation profile of measured air relative humidity in conditioned space in command following test with a change in air humidity setting

As the setting of indoor air wet-bulb temperature was changed from 17 ºC to 16.6 ºC with the setting of indoor air dry-bulb temperature remaining unchanged, thus the setting of indoor air relative humidity was also lowered from 50% to 47%. The relative humidity of indoor air, as shown Fig. 6.10, could also reach its new setting after the MIMO controller was enabled. Therefore, the controllability test results shown in Figures 6.7 to 6.10 suggested that the performance of the MIMO controller in terms of its command following capability was also satisfactory.

6.3.3 Discussions

Simultaneous control of indoor air temperature and humidity in a space served by a DX A/C system would require simultaneously varying the speeds of both supply fan and compressor of the DX A/C system. However, the changes in supply fan speed and compressor speed would have difference levels of influence on indoor air temperature and humidity. When space sensible and latent heat loads were increased, the control of air dry-bulb temperature required the speeds of both supply fan and compressor to increase. However, the control of humidity required the speed of supply fan to decrease, but meanwhile required compressor speed to increase to output more cooling capacity for more moisture removal. Thus speed control would be in conflict if the coupling effect was not considered, and the result of control performance would be inherently poor. These can only be resolved by applying multivariable control strategy.

From Figure 6.5 showing the results of disturbance rejection capability test, when the MIMO controller was enabled, both supply fan speed and compressor speed were collaboratively increased to remove more sensible heat load because of a greater output cooling capacity from the DX cooling coil. Afterward, the speed of supply fan was decreased for removing more moisture from return air. Finally the indoor air temperature and humidity stabilized at around their respective settings. On the other hand, in Figure 6.7 showing the results of command following controllability test after a change in indoor air temperature setting, it can be seen that indoor air moisture content rose above its set point before decreasing to under the set point (Figure 6.7(c)). This was because the speed of supply fan was initially increased causing the sensible heat ratio of the DX cooling coil to increase and consequently less moisture was removed even under an increased compressor speed. This also suggested that varying supply fan speed would influence SHR more than varying compressor speed, which agreed well with the results in previous related studies [Li and Deng 2007a, b]. Furthermore, similar phenomena may also be observed in Fig. 6.9.

In the controllability tests, the DX A/C system under MIMO control took around 20 to 30 minutes to achieve their respective new set points, which was much more sensitive than a previous control strategy using SHR as a control variable [Li and Deng 2007b]. The results of controllability tests suggested that simultaneous indoor air temperature and humidity control by using the MIMO controller through simultaneously varying compressor speed and supply fan speed was functional, with satisfactory accuracy. Compared to the previous studies using conventional on-off control method or SISO

control strategy which can only effectively control either air temperature or relative humidity, the MIMO controller can simultaneously control both indoor air temperature and humidity with adequate control sensitivity and accuracy.

From Figures 6.5(d), 6.7(d) and 6.9(d), however, it was noticed that when the compressor speed and supply fan speed were regulated by the MIMO controller for simultaneously controlling indoor air temperature and humidity, it would result in a significant change of operating DS. In the controllability tests, the highest DS reached was 14 ºC when the speeds of compressor and supply fan were changed, as shown in Fig. 6.5(d), much higher than its setpoint of 6 ºC. Therefore the energy efficiency of the DX A/C system would be decreased due to the high DS when the compressor speed and supply fan speed were varied for capacity control. In the experimental DX A/C system, the EEV was controlled by a built-in conventional PID controller. Therefore it became necessary to further develop a new DS controller to replace the built-in conventional PID DS controller in the experimental DX A/C system, thus improving the operating performance in terms of stability and energy efficiency of the DX A/C system.

6.4 Summary

In this Chapter, a multivariable feedback control strategy for simultaneously controlling indoor air temperature and humidity in a space served by a DX A/C system has been developed, and an MIMO controller using Linear Quadratic Gaussian technique

designed based on the multivariable control-oriented dynamic model of the experimental DX A/C system.

Controllability tests with respect to disturbance rejection capability and command following capability were carried out to evaluate the performance of the MIMO controller. In disturbance rejection capability test, the test results showed that MIMO control strategy can effectively control the indoor air temperature and humidity to their respective settings when there were heat load disturbances imposed. The results of command following capability tests showed that the indoor air temperature or humidity can be controlled to their respective new settings, without affecting the other controlled variable, i.e., humidity or temperature. Therefore the results of both the disturbance rejection capability test and the command following capability test showed that the MIMO controller developed can simultaneously control indoor air temperature and humidity by varying compressor speed and supply fan speed of the DX A/C system with adequate control accuracy, sensitivity and stability.

It was however noted that when the compressor speed and supply fan speed were regulated by the MIMO controller, a significant change in operating DS can be resulted in. Therefore the energy efficiency of the DX A/C system would be decreased. Since the EEV in the experimental DX A/C system was controlled by a built-in conventional PID controller, it would be therefore necessary to further develop a new DS controller to replace the built-in conventional PID DS controller in the experimental DX A/C system,

so as to improve the operating performance in terms of stability and energy efficiency of the DX A/C system. This is reported in the Chapter 7.

Chapter 7

Development of a New DS Controller for a DX A/C System under Variable Speed Operation and its Controllability Tests

7.1 Introduction

As reported in Chapter 6, indoor air temperature and humidity may be simultaneously controlled to their respective setpoints by the MIMO controller developed through simultaneously varying compressor speed and supply fan speed in the experimental DX A/C system. However, varying the speeds of both compressor and supply fan can significantly impact on the resultant operating DS, which was regulated by a built-in conventional PID DS controller in the experimental DX A/C system, as observed in Figs. 6.5(d), 6.7(d) and 6.9(d) in Chapter 6. The resultant operating DS could reach a high level compared to its setting, after the speeds of both compressor and supply fan were varied by the MIMO controller for simultaneous indoor air temperature and humidity control.

The above observations were further confirmed by one more test using the experimental DX A/C system under both the MIMO controller for indoor air temperature and humidity control and the conventional PID DS controller for DS control. The measured variation profiles of the operating parameters in the test are shown in Fig. 7.1. After the settings of indoor air dry-bulb and wet-bulb temperatures were both reduced by 0.5 ^{o}C at

t = 510 s, the MIMO controller responded by increasing the speeds of compressor and supply fan to provide a greater output cooling capacity, as shown in Fig. 7.1(d). Although indoor air dry-bulb and wet-bulb temperatures were finally controlled to their

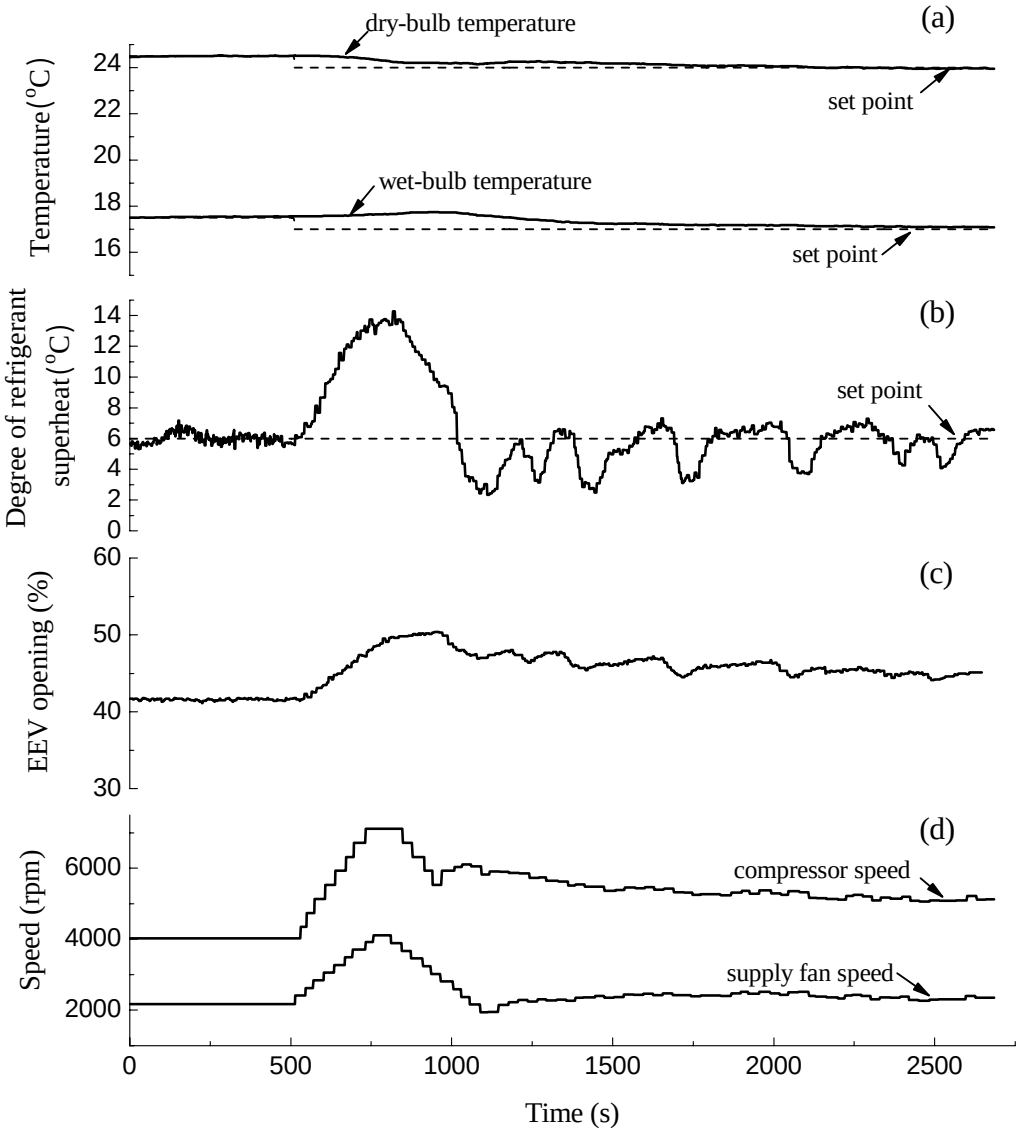

Figure 7.1 Measured variation profiles of operating parameters under the joint control of the MIMO controller and the conventional PID DS controller
(1st test set)

respective setpoints (Fig. 7.1(a)), the resultant operating DS under the conventional PID DS controller experienced significant fluctuation which lasted for many minutes after the speed changes were introduced. The highest DS experienced was 14 ºC (Fig. 7.1(c)). Such a fluctuation in the operating DS would impact the performance of a refrigeration system, in terms of its operating stability and efficiency.

The built-in conventional PID DS controller in the experimental DX A/C system would not respond to take control action until it received the feedback information of the change in DS, so that the opening of an expansion valve can be correspondingly adjusted. However, such a feedback process would take some time before the opening of the expansion valve can be gradually regulated in order to return the DS to its setpoint. This can be seen from Fig. 7.1, between 510 and 750 seconds, when compressor speed and supply fan speed were increased as regulated by the MIMO controller (Fig. 7.1(d)), the rate of increase in DS was at around 130% (Fig. 7.1(b)), much faster than that for the EEV at around 30% (Fig. 7.1(c)). Although in a DX A/C system, its operating DS may be influenced by changes of other operating parameters, changes in both compressor and supply fan speeds can be a major factor causing significant fluctuation of its operating DS, as illustrated in Fig. 7.1(c). The above experimental results demonstrated the drawbacks of DS control using conventional PID DS controller when compressor and supply fan speeds were varied for capacity control in a DX A/C system. On the other hand, although the numerical values of PID parameters in a conventional controller may be adjusted to change the response rate for the opening of the EEV, this would also lead to the instability of DS when there were

other reasons causing the changes in DS. Therefore, developing a new control DS algorithm, which can replace a conventional PID DS controller for better control performance in a DX A/C system when DS fluctuation was caused by changes in its compressor and supply fan speeds, has become necessary.

Over the years, various DS control methods have been developed and applied in refrigeration and air conditioning systems, such as PI, PID and fuzzy control. For example, feedback PI control for DS was adopted in a solar assisted heat pump water heating system [Li et al. 2007], and experimental results showed that the DS in the heat pump system could be controlled stably. Chia et al. [1997] applied a fuzzy logic to DS control in a container refrigeration system using an EEV for better operating performance. The energy efficiency of the container refrigeration system using the EEV was improved by about 15% compared to that of the same system but using a thermal expansion valve (TEV). Fuzzy logic control was also applied to controlling the DS in a commercial refrigeration system using an EEV, and an adaptive DS control algorithm was devised to enhance its evaporator performance [Jolly et al. 2000]. A genetic algorithm was adopted to optimize the membership functions of fuzzy control for DS by Chen et al. [2001]. When compared to PI control, fuzzy control was more stable and accurate in regulating DS although control sensitivity was slightly low. Rasmussen [2008] proposed a method for DS and capacity control in refrigeration systems, and the method was experimentally validated. However, in all these reported studies, the control algorithms developed were of feedback type, so that applying these control algorithms

in a DX A/C system was not considered useful in mitigating the fluctuation of DS when speeds of both compressor and supply fan were varied for capacity control.

He et al. [1997, 1998] developed a two-input two-output control algorithm for DS and the evaporating temperature in a refrigeration system by varying compressor speed and EEV opening. It was shown that for the refrigeration system, establishing a multivariable control-oriented mathematical model for the intended controlled variables, i.e., DS and the evaporating temperature, was very complicated, as there were too many operating parameters to be considered in the multivariable control-oriented mathematical model, as demonstrated in Chapters 6 and 7. Thus it would be even more difficult to develop a multivariable control-oriented mathematical model, which is intended to assist developing algorithms of simultaneously controlling three objectives, e.g., indoor air temperature, humidity and DS through varying compressor speed, supply fan speed and EEV opening using a three-input three-output controller in the DX A/C system. Given the complexity of the three-input three-output controller, it is also very costly to put it into practical use. Therefore it will be more feasible to develop a new DS controller to be used for achieving better DS control performance, in conjunction with the MIMO controller in a DX A/C system when its compressor and supply fan speeds are varied for capacity control.

With the fast development of DDC technique, information on the changes of compressor speed and supply fan speed can be easily obtained and used for control purpose. Therefore the development of this new DS controller can be based on that the

information of the changes of both compressor speed and supply fan speed may be used for predicting the change of DS, thus appropriate control action by an EEV may be timely taken.

This Chapter reports the development of a new DS controller to be used for better DS control performance when compressor speed and supply fan speed are varied for capacity control in a DX A/C system having a variable speed compressor and supply fan. The previously developed MIMO controller and the new DS controller to be developed would be jointly used to control the experimental DX A/C system. Controllability tests of the new DS controller, working together with the MIMO controller to control indoor air temperature, humidity and DS, were carried out in the experimental DX A/C system. The operating performances of the experimental DX A/C system under both the new DS controller and conventional PID DS controller, both working together with the MIMO controller, were compared and are reported.

7.2 Development of a new DS controller

In this section, a new DS controller which was to replace the conventional PID DS controller for better DS control performance when speeds of compressor and supply fan were varied, was developed. The previously developed MIMO controller and this new DS controller would work together to control three objectives, e.g. indoor air temperature, humidity and the DS in the experimental DX A/C system. The schematic

diagram of the complete control for the experimental DX A/C system is shown in Figure 7.2.

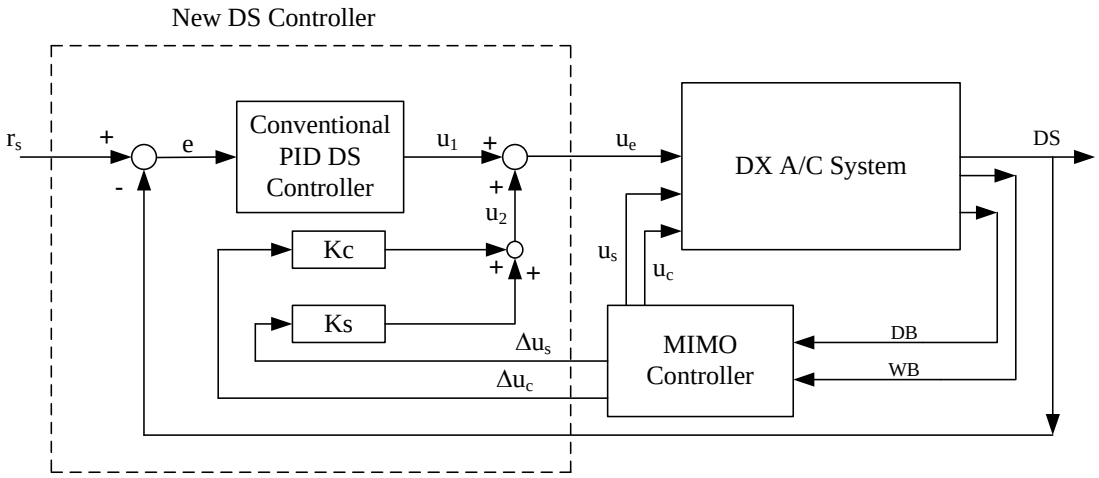

Figure 7.2 The schematic diagram of the complete control for the experimental DX A/C system

As seen from Fig.7.2, the new DS controller in the DX A/C system was developed from a conventional PID DS controller by integrating two feed-forward channels through which the information of changes of both compressor speed, Δu_c, and supply fan speed, Δu_s, was passed to the new DS controller. Since the changes in both compressor speed and supply fan speed would impact on the operating DS in the experimental DX A/C system. For example, increasing compressor speed would lead to an increase in DS. Therefore, when the speeds of compressor and supply fan were changed, the information of speed changes can be timely passed to the new DS controller, and the opening of EEV can be timely adjusted to vary the refrigerant flow into the evaporator, rather than waiting for the DS signal to be fed back such as in a conventional PID DS

controller, the magnitudes of fluctuation in DS due to changes in speed may be significantly mitigated.

The control signal for operating the EEV in the experimental DX A/C system was obtained as follows:

PID feedback loop:

$$u_1(k) = u_1(k-1) + K_P(e(k) - e(k-1)) + K_I e(k) + K_D(e(k) - 2e(k-1) + e(k-2)) \quad (7.1)$$

Feed-forward channels:

$$u_2(k) = K_c \Delta u_c + K_s \Delta u_s \quad (7.2)$$

$$u_e(k) = u_1(k) + u_2(k) \quad (7.3)$$

where k was the discrete time, K_P, K_I, K_D the proportional, integral and derivative coefficients, respectively, and $K_I = TK_P / T_I$, $K_D = T_D K_P / T$. T was the sampling period, T_I the integral time and T_D the derivative time. Δu_c was the change in compressor speed and Δu_s the change in supply fan speed, both being a variable from the MIMO controller. K_s and K_c were coefficients.

The new DS controller was digitally implemented together with the MIMO controller in the experimental DX A/C system. The new DS controller and the previously developed MIMO controller would work together to control three objectives, e.g., indoor air temperature, humidity and the DS in the experimental DX A/C system by varying compressor speed, supply fan speed and EEV opening. The schematic diagram of the experimental DX A/C system and its controllers including the MIMO controller and the new DS controller is shown in Figure 7.3.

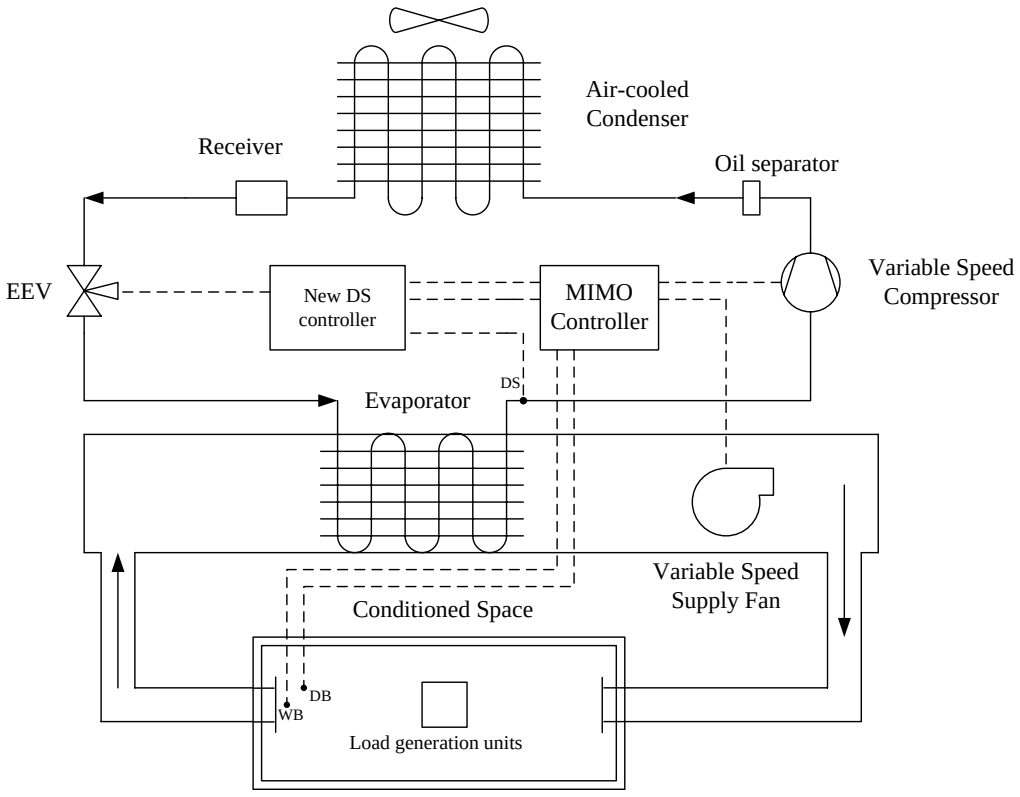

Fig. 7.3 Schematic diagram of the experimental DX A/C system and its controllers

7.3 Controllability tests

Two sets of controllability test for the new DS controller were carried out to evaluate the performance of the new DS controller in the experimental DX A/C system. The first set was to repeat the same experimental operation whose results are shown in Fig. 7.1, by replacing its conventional PID DS controller with the new DS controller. These experimental results are shown in Figures 7.4 to 7.7. The second set was for testing the controllability of the experimental DX A/C system under both the conventional PID DS controller and the new DS controller, both together with MIMO controller, when indoor air temperature settings were increased. The results of the second test set are shown in Figures 7.8 to 7.12.

For the first set of test, indoor air dry-bulb and wet-bulb temperature were set at 24.5 ºC and 17.5 ºC, respectively. The setpoint of DS was 6 ºC. When the above settings were maintained at a steady-state, the compressor speed and the supply fan speed were 4013 rpm and 2168 rpm, respectively. At t =510 s, the settings of both indoor dry-bulb and wet-bulb temperature were reduced by 0.5 ºC.

Fig. 7.4 shows the measured variation profiles of operating parameters under both MIMO controller and new DS controller to simultaneously control the three objectives, e.g., indoor air dry-bulb, wet-bulb temperature, and DS in the DX A/C system. As seen from Fig. 7.4(a), indoor air dry-bulb and wet-bulb temperature were also controlled to their respective setpoints by the MIMO controller after the indoor air settings were

reduced. However, the highest DS experienced was around 10 ºC under the new DS controller (Fig. 7.4(b)) compared to over 14 ºC under the conventional PID DS controller (Fig. 7.1(b)).

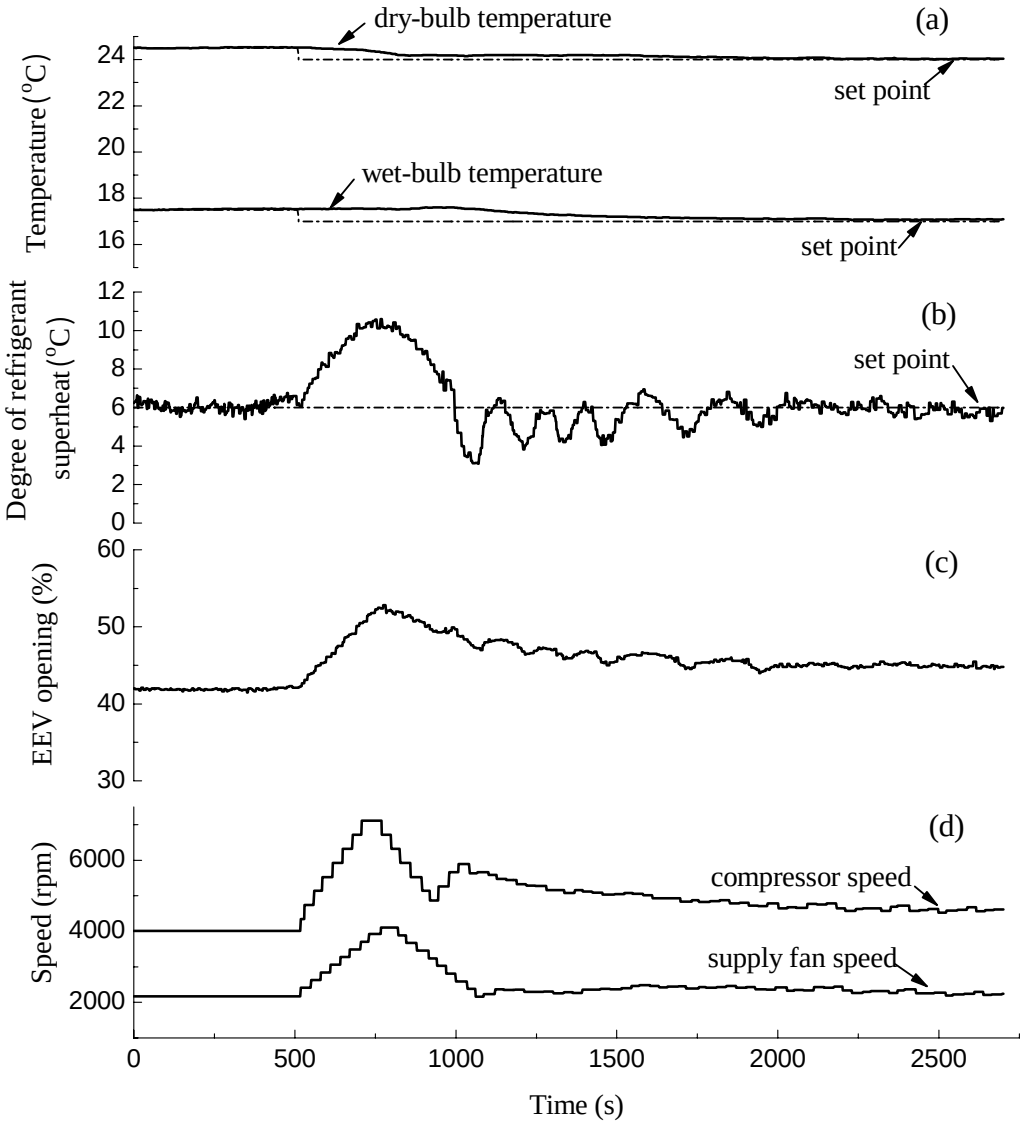

Fig. 7.4 Measured variation profiles of operating parameters under the joint control of the MIMO controller and the new DS controller(1st test set)

Fig. 7.5 shows the comparison of DS under both the new DS controller and the conventional PID DS controller. It demonstrates that the new DS controller can result in a better controlled DS compared to the conventional PID DS controller when the speeds of compressor and supply fan varied as required by the MIMO controller. Better control performance of DS was reflected in two aspects: (1) reduced magnitude of DS fluctuation; (2) fast returning to the DS setting.

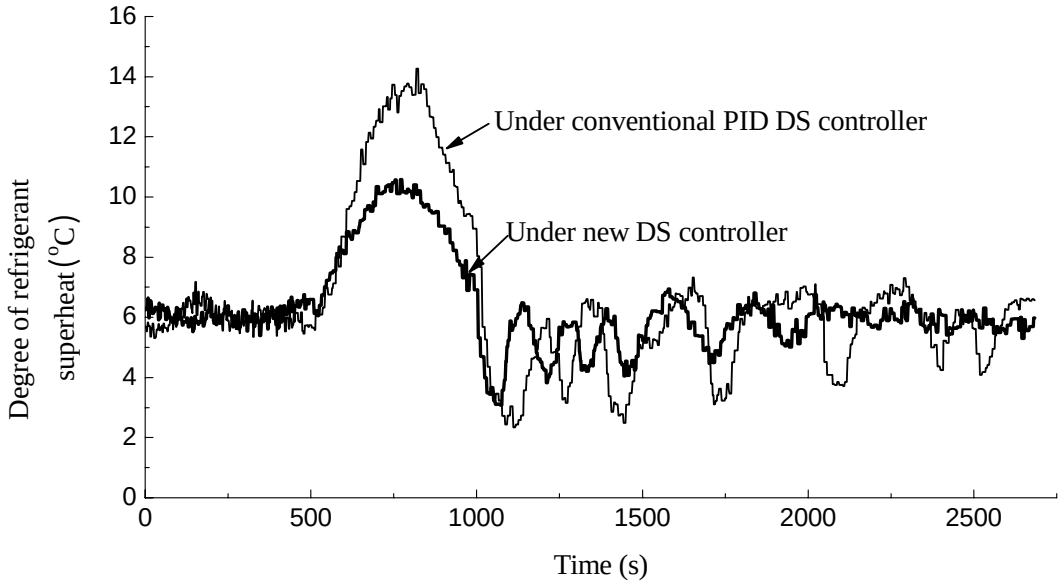

Fig. 7.5 Comparison of DS under the new DS controller and the conventional PID DS controller (1st test set)

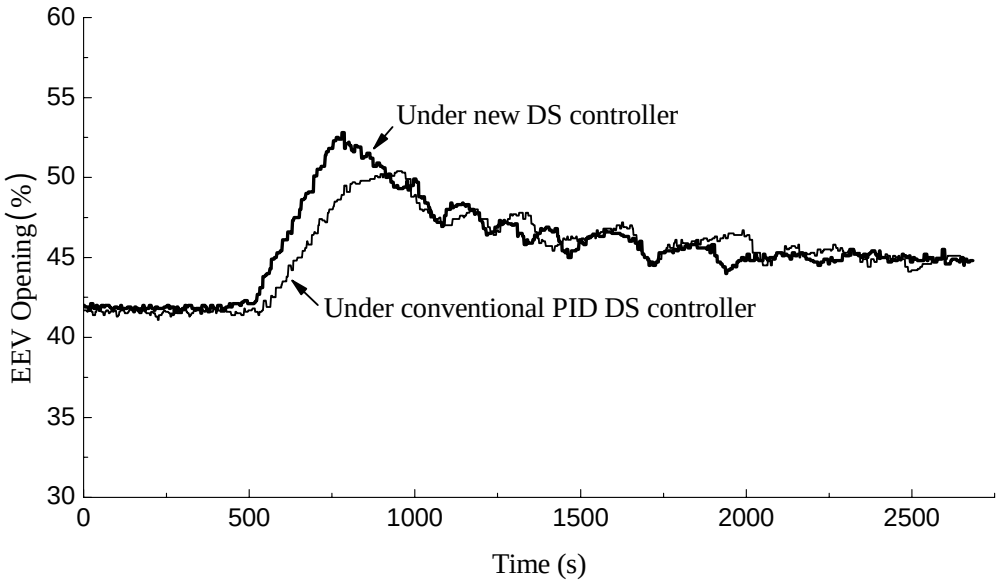

Fig. 7.6 Comparison of EEV openings under the new DS controller and the conventional PID DS controller (1st test set)

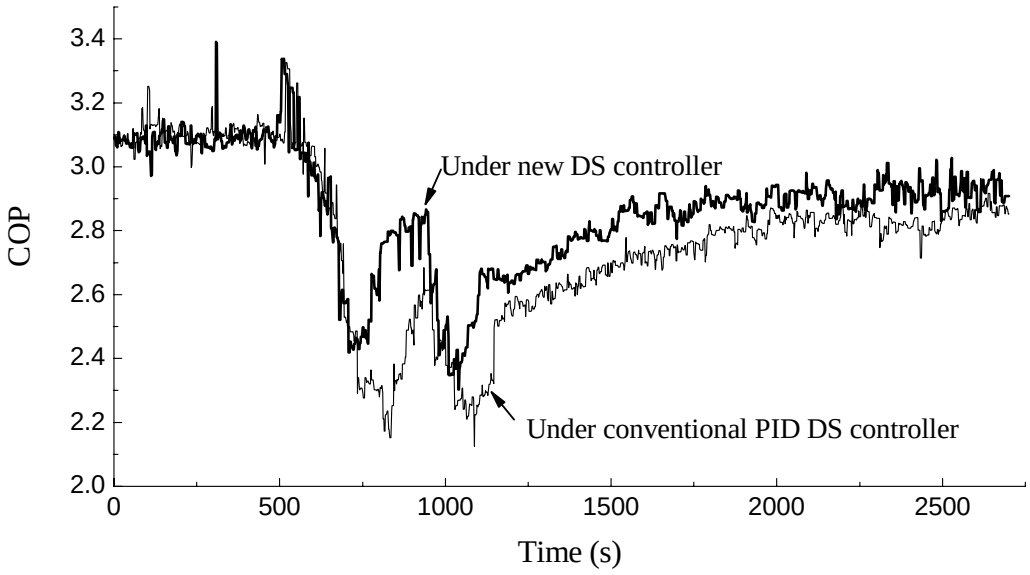

Fig. 7.7 Comparison of COPs under the new DS controller and the conventional PID controller (1st test set)

Fig. 7.6 shows the comparison of EEV openings under the new DS controller and the conventional PID DS controller. Using the new DS controller, the opening of EEV was at about 52.8% of the full opening at t = 780s, larger than which was at 50% under the conventional PID DS controller. This showed that the increasing rate of EEV opening was fast under the new DS controller than that under the conventional PID DS controller.

Fig. 7.7 shows the comparison of the operating efficiency in terms of COP of the DX A/C system under both the new DS controller and the conventional PID DS controller. As seen from the figure, after the changes in speed taking place at t = 510s, the COP of DX A/C system was always better under the new DS controller than that under the conventional PID DS controller. On average, the COP of the DX A/C system under the new DS controller was improved by about 6.4% compared to that under the conventional PID DS controller during the transient period starting from t = 510s. The improvement of the operating efficiency of the DX A/C system was considered to be due to the more effective use of the heat exchange surface area in the DX cooling coil with a smaller operating DS.

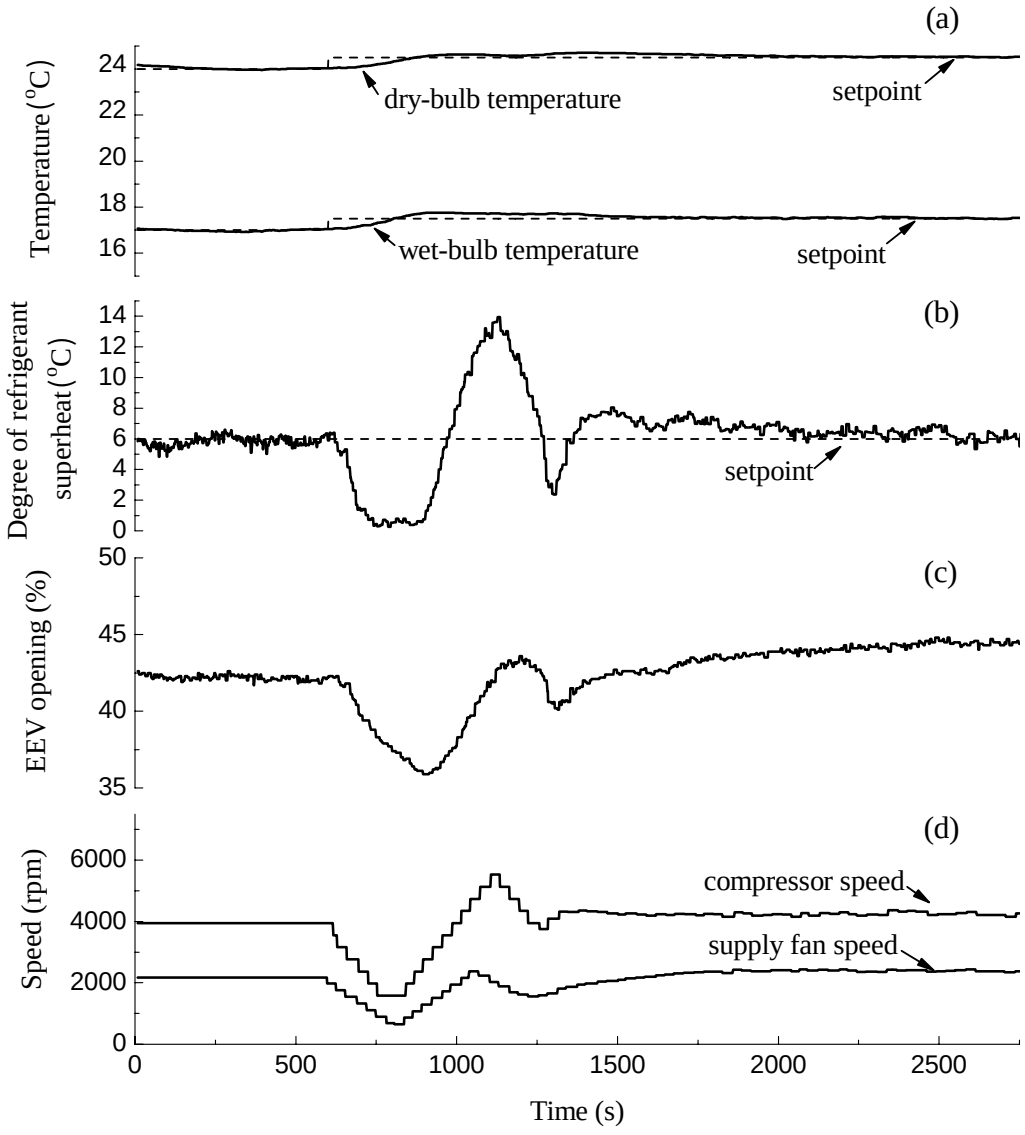

Fig. 7.8 Measured variation profiles of operating parameters under the joint control of the MIMO controller and the conventional PID DS controller (2nd test set)

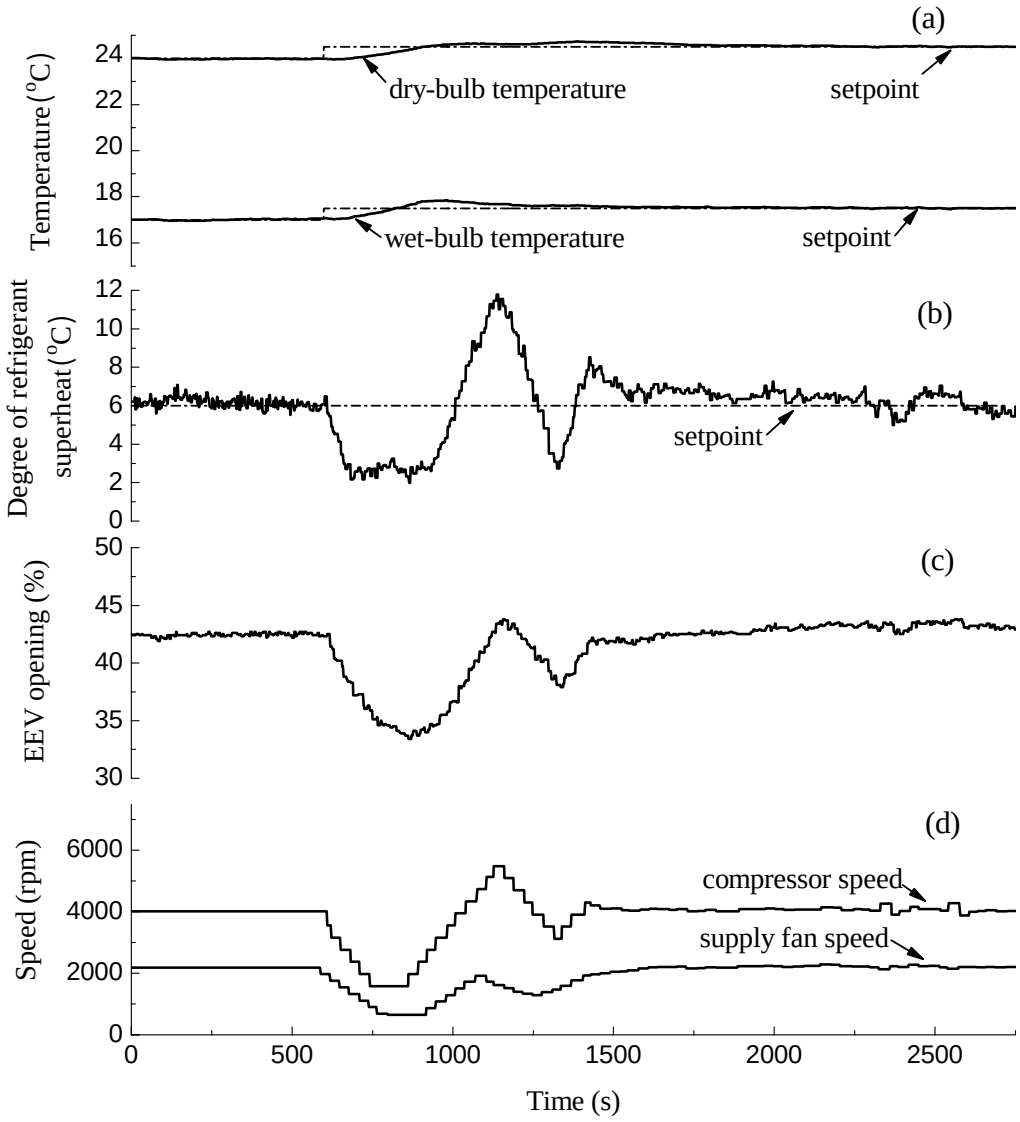

Fig. 7.9 Measured variation profiles of operating parameters under the joint control of the MIMO controller and the new DS controller (2nd test set)

For the second set of test, the indoor air dry-bulb and wet-bulb temperature were initially set at 24 ºC and 17 ºC, respectively. The setpoint of DS was also 6 ºC. When the above settings were maintained at a steady-state, the compressor speed and the supply

fan speed were at 4013 rpm and 2168 rpm, respectively. At t = 600s, the indoor air dry-bulb and wet-bulb temperature settings were increased from 24 ºC to 24.5 ºC and from 17 ºC to 17.5 ºC, respectively. Fig. 7.8 and Fig. 7.9 show the measured variation profiles of the operating parameters in the experimental DX A/C system under the conventional PID DS controller and the new DS controller, both operating together with the MIMO controller for capacity control, respectively. From both diagrams, it can be seen that after the changes in temperature settings were introduced at t = 600 s, as regulated by the MIMO controller, the speeds of compressor and supply fan were decreased to reduce the output cooling capacity from the DX A/C system. Finally the indoor air dry-bulb and wet-bulb temperature were controlled to their respective settings under both the new DS control and conventional PID DS control, as shown in Fig. 7.8(a) and Fig. 7.9(a), respectively. However, a better DS control was achieved using the new DS controller than that using the conventional PID DS controller, as shown in Fig. 7.10. When the compressor speed and supply fan speed were decreased to reduce cooling capacity of the DX A/C system in order to track new indoor air settings, the lowest DS under the conventional PID DS controller was around 0.4 ºC, and that under the new DS controller was around 2.3 ºC. This could effectively prevent the DX A/C system from being operated with a danger of sucking in liquid refrigerant.

Fig. 7.11 shows comparison of the EEV opening under the new DS controller and the conventional PID DS controller. It demonstrates that the closing rate of EEV was fast under the new DS controller than that under the conventional PID DS controller when

the speeds of compressor and supply fan were reduced, leading to a better control performance of DS.

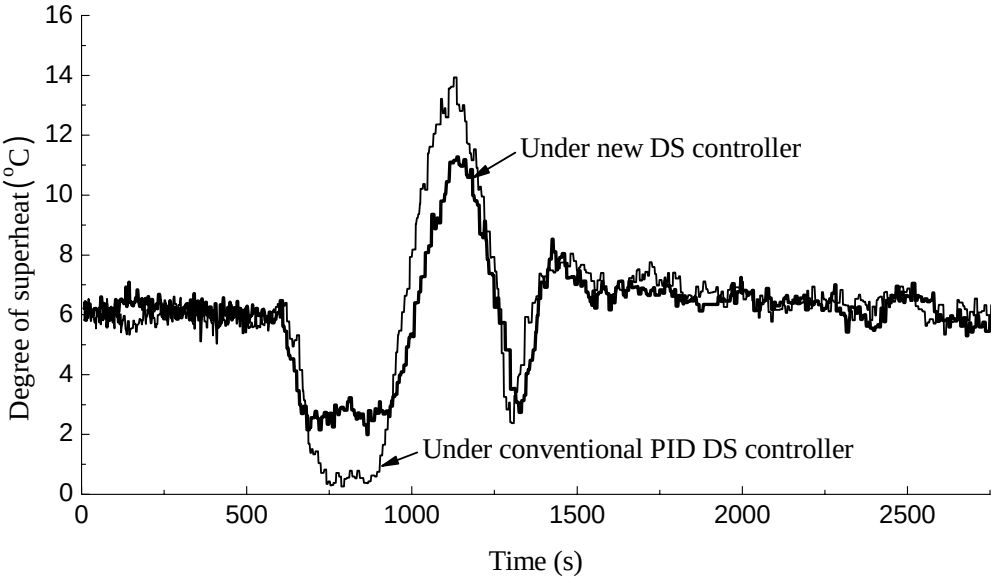

Fig. 7.10 Comparison of DS under the new DS controller and the conventional PID DS controller (2nd test set)

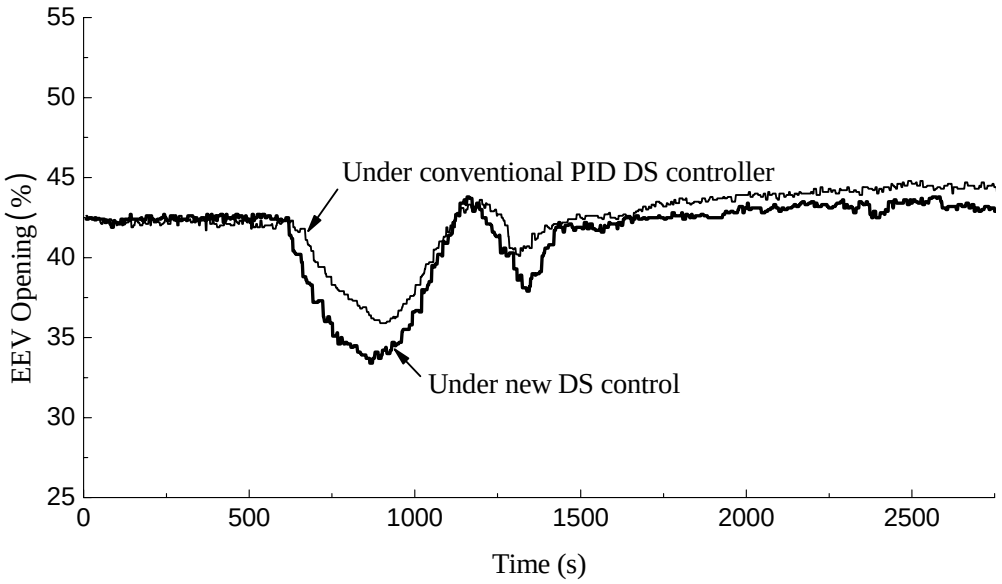

Fig. 7.11 Comparison of EEV openings under the new DS controller and the conventional PID DS controller (2nd test set)

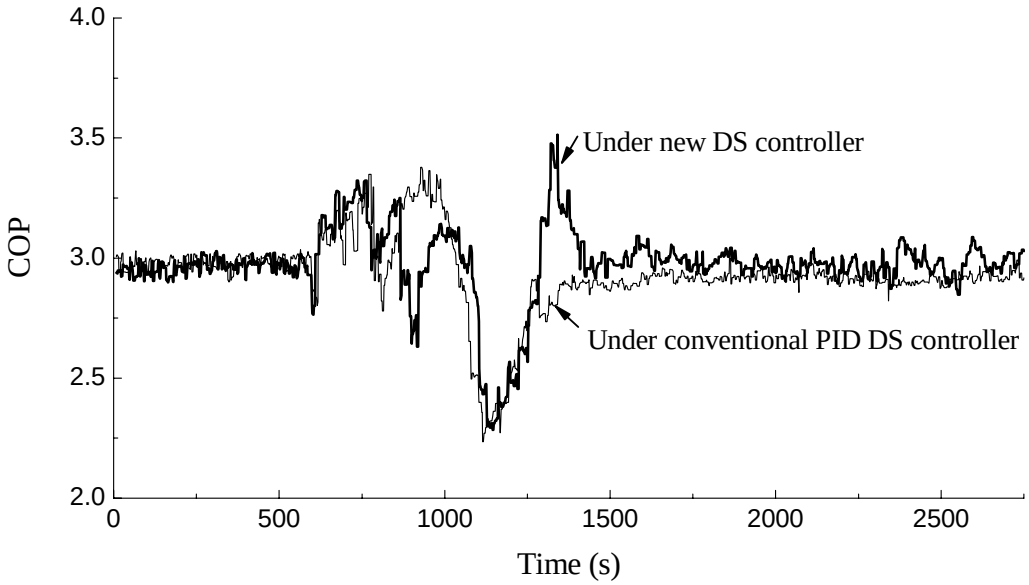

Fig. 7.12 Comparison of COPs under the new DS controller and the conventional PID DS controller (2nd test set)

The comparison of COP under the new DS controller and the conventional PID DS controller is shown in Fig. 7.12. On average, the COP under the new DS controller was 2.98, higher than that of 2.92 under the conventional PID DS controller.

From the experimental results shown above, it can be seen that the new DS controller can lead to a better control over DS when it worked together with the MIMO controller to vary the speeds of both compressor and supply fan to simultaneously control indoor air temperature and humidity using the DX A/C system. Therefore, a better operating performance in terms of operating efficiency and stability of the DX A/C system was resulted in. On the other hand, although the new DS controller was developed in conjunction with the MIMO controller in the DX A/C system, its practical application was not limited to being used together with the MIMO controller. Its application can be in fact extended to any other control algorithm involving varying compressor and supply fan speeds of capacity control, such as the control algorithms developed by Li and Deng [2007a, b], provided that the information of speed changes can be input to the new DS controller.

7.4 Summary

A new DS controller, for improving the control performance of DS in a DX A/C system when the fluctuation of operating DS was resulted from varying speeds of its compressor and supply fan, has been developed and experimentally tested and is reported in this Chapter. The new DS controller was developed from a conventional PID

DS controller by adding two feed-forward channels so that information of speed changes of compressor and supply fan can be timely passed to the new DS controller. Controllability test results showed that an improved DS control performance can be achieved when using the new DS controller over the conventional PID DS controller, and consequently a better operating performance of the DX A/C system in terms of operating efficiency and stability has been achieved. Furthermore, the new DS controller can be used with all other types of capacity control for a DX A/C system provided that the information of speed changes can be made available to the new DS controller.

Chapter 8

Conclusions and Future Work

8.1 Conclusions

In this Thesis, a programmed research work on investigating the multivariable control of indoor air temperature and humidity in a space served by a DX A/C system having a variable speed compressor and a variable speed supply fan has been successfully carried out and is reported. The conclusions of the Thesis are as follows:

(1) A multivariable control-oriented dynamic model of an experimental DX A/C system has been developed based on the principles of energy and mass conservation. The coupling effect of indoor air temperature and humidity was considered in developing the multivariable control-oriented dynamic model. The dynamic model written in state-space representation was linearized at an operating point, making it highly suitable for designing an MIMO controller. The multivariable control-oriented dynamic model has been experimentally validated by comparing the measured open-loop responses for all major operational parameters of the experimental DX A/C system with the simulated open-loop responses using the multivariable control-oriented dynamic model.

(2) A multivariable feedback control strategy for simultaneously controlling indoor air temperature and humidity in a DX A/C system was developed, and an MIMO

controller using Linear Quadratic Gaussian technique was designed based on the multivariable control-oriented dynamic model for the experimental DX A/C system. Controllability tests for both disturbance rejection capability and command following capability were carried out to evaluate the performance of the MIMO controller. In disturbance rejection capability test, the test results showed that MIMO control strategy can effectively control the indoor air temperature and humidity to their respective settings when there were heat load disturbances imposed. Furthermore, the results of command following capability tests showed that the indoor air temperature or humidity can be controlled to their respective new settings, without affecting the other controlled variable, i.e., humidity or temperature. The test results indicated that the MIMO controller developed can simultaneously control indoor air temperature and humidity with adequate control accuracy, sensitivity and stability.

(3) A new DS controller, for improving the control performance of DS in a DX A/C system when the fluctuation of operating DS was resulted mainly from varying speeds of its compressor and supply fan, was developed and experimentally tested. The new DS controller was developed from a conventional PID DS controller by adding two feed-forward channels so that information of speed changes of compressor and supply fan can be timely passed to the new DS controller. Controllability test results showed that an improved DS control performance can be achieved when using the new DS controller over the conventional PID DS controller, and consequently a better operating performance of the DX A/C system

in terms of operating efficiency and stability has been achieved. Furthermore, the new DS controller can be used with all other types of capacity controllers for DX A/C systems provided that the information of speed changes can be made available to the new DS controller.

The research work reported in this Thesis has made important contributions to the dynamic modeling and the development of multivariable feedback control strategies for DX A/C systems to simultaneously control indoor air temperature and humidity. Better indoor thermal comfort and improved IAQ for occupants, and reduced energy use can be realized when using DX A/C systems with variable speed compressor and variable speed supply fan. The MIMO controller developed and reported in this Thesis for a DX A/C system for simultaneous indoor air temperature and humidity control is the first of its kind. On the other hand, the new DS controller can effectively alleviate the fluctuation of operating DS resulted mainly from speed variations for capacity control, so as to help the DX A/C system run more steadily and efficiently. The use of the new DS controller can be extended to any other control algorithms involving varying compressor and supply fan speeds for capacity control in a DX A/C system provided that the information of speed changes can be supplied to the new DS controller, to achieve a better operating performance of the DX A/C system in terms of operating efficiency and stability.

With the development of low-cost variable speed drive technology, a number of DX A/C systems would equip variable speed compressors and variable speed supply fans. It

is expected that the MIMO controller and new DS controller would be applied into these systems to improve indoor thermal comfort and performance of the systems. The MIMO controller developed in this Thesis was based on the linearized multivariable control-oriented dynamic model of the DX A/C system around a specific operating point. Thus it is necessary to make the MIMO controller work over a wider operating range. Compared to conventional PID controller, the MIMO controller is complex since some parameters need to be measured in the dynamic model of the DX A/C system, thus the cost of the MIMO controller is higher than that of the conventional PID controller. Therefore it is necessary to develop a training method to estimate the parameters in the dynamic model and reduce the cost of MIMO controller. The long-term significance of the research work is that it will encourage a wider use of multivariable control strategies in DX air conditioning technology to better control indoor thermal environment, leading to a better thermal comfort and energy saving.

8.2 Proposed future work

A number of future studies following on the successful completion of the research work reported in this thesis are proposed as follows:

(1) An MIMO controller has been developed for simultaneously controlling indoor air temperature and humidity in a space served by a DX A/C system. However, the MIMO controller developed was based on the linearized multivariable control-

oriented dynamic model of the DX A/C system around a specific operating point. Future work should be directed to make the MIMO controller operational over a wider working range using the Gain Schedule Technique [He et al. 1998].

(2) The MIMO controller for the experimental DX A/C system was of two-input two-output nature to simultaneously control indoor air temperature and humidity. An MIMO controller of three-input three-output nature may be further developed for simultaneously controlling indoor air temperature, humidity and the degree of refrigerant superheat by simultaneously varying compressor speed, supply fan speed and the opening of EEV in a DX A/C system. It is however expected that a multivariable control-oriented dynamic model that can be used to facilitate the development of the three-input three-output controller will be much more complicated than the dynamic model reported in Chapter 5.

(3) The MIMO controller developed in this thesis was based on the Linear Quadratic Gaussian technique in modern multivariable control theory. Other control strategies such as adaptive control strategy and fuzzy control strategy may be also used to develop MIMO controllers for DX A/C systems to simultaneously control several variables, such as indoor air temperature, indoor air humidity and degree of refrigerant superheat in DX A/C systems. Therefore future developments of MIMO controllers for DX A/C systems using these control strategies should also be explored.

(4) The multivariable control strategy may be extended to chilled water systems or fan coil systems. Indoor air temperature and humidity may be simultaneously controlled by the multivariable control strategy through simultaneously varying the opening of chilled water valve and the speed of coil fan.

References

1. Ahemd et al. 1998a
Ahmed O., Mitchell J. W. and Klein S.A.
Feedforward-feedback controller using general regression neural network (GRNN) for laboratory HVAC system, Part I - pressure control. *ASHRAE Transactions*, Vol. 104, part 2, pp. 613-625 (1998)

2. Ahemd et al. 1998b
Ahmed O., Mitchell J. W. and Klein S. A.
Feedforward-feedback controller using general regression neural network (GRNN) for laboratory HVAC system, part II: cooling control. *ASHRAE Transactions*, Vol. 104, part 2, pp. 626-633 (1998)

3. Ahemd et al. 1998c
Ahmed O., Mitchell J. W. and Klein S. A.
Feedforward-feedback controller using general regression neural network (GRNN) for laboratory HVAC system, part III: heating control. *ASHRAE Transactions*, Vol. 104, part 2, pp. 634-642 (1998)

4. Amrane et al. 2003
Amrane K., Hourahan G.C. and Potts G.
Latent performance of unitary equipment. *ASHRAE Journal*, 2003, Vol. 45, No. 1, pp. 28-31 (2003)

5. Alcala et al. 2005
Alcala R. , Casillas J., Cordon O., Gonzalez A. and Herrera F.
A genetic rule weighting and selection process for fuzzy control of heating, ventilating and air conditioning systems. *Engineering Applications of Artificial Intelligence*, Vol. 18, pp. 279-296 (2005)

6. Alpuche et al. 2005
Alpuche M.G., Heard C., Best R. and Rojas J.
Energy analysis of air cooling systems in buildings in hot humid climates. *Applied Thermal Engineering*, Vol. 25, No. 4, pp. 507-517 (2005)

7. Anderson et al. 2002
Anderson M., Young P., Hittle D., Anderson C., Tu J. L. and Hodgson D.
MIMO robust control for heating, ventilation and air conditioning systems.
Proceedings of the 41st IEEE conference on decision and control. Las Vegas, Nevada, USA, December 2002

8. Andrade and Bullard 2002
Andrade M. A., Bullard C. W.
Modulating blower and compressor capacities for efficient comfort control. *ASHRAE Transaction*, Vol. 108, Part 1, pp. 63-67 (2002)

9. Angelov 2003
Angelov P. P.
An evolutionary approach to fuzzy rule-based model synthesis using indices for rules. *Fuzzy Sets and Systems*, Vol. 137, No. 3, pp. 325-338 (2003)

10. Aprea et al. 2004
Aprea C., Mastrullo R. and Renno C.
Fuzzy control of the compressor speed in a refrigeration plant. *International Journal of Refrigeration*, Vol. 27, pp. 639-648 (2004)

11. Arens and Baughman 1996
Arens E.A. and Baughman A.V.
Indoor humidity and human health: part II-buildings and their systems. *ASHRAE Transactions*, Vol. 102, No. 1, pp. 212-221 (1996)

12. Arguello-Serrano and Velez-Reyes 1999
Arguello-Serrano B. and Velez-Reyes M.
Nonlinear Control of a Heating, Ventilating, and Air Conditioning System with Thermal Load Estimation. *IEEE Transactions on Control Systems Technology*, Vol. 7, No. 1, pp. 56-63 (1999)

13. Armstrong and Liaw 2002
Armstrong S. and Liaw J.
The fundamentals of fungi. *ASHRAE Journal*, Vol. 44, No. 11, pp. 18-24 (2002)

14. ASHRAE 2000
ASHRAE
Handbook-HVAC Systems and Equipment (2000)

15. ASHRAE 2005
ASHRAE
ASHRAE Standard 62-2005, Ventilation for Acceptable Indoor Air Quality. (2005)

16. Bensafi et al.1997
Bensafi A., Borg S. and Parent D. C.
A computational model for the detailed design of plate-fin-and-tube heat exchangers using pure and mixed refrigerant. *International Journal of Refrigeration*, Vol. 20, No. 3, pp. 218-228 (1997)

17. Berglund 1998
Berglund L.G.
Comfort and humidity. *ASHRAE Journal*, Vol. 40, No. 8, pp. 35-41 (1998)

18. Bordick and Gilbride 2002
Bordick J. and Gilbride T.L.
Focusing on buyer's needs: DOE's engineering technology programme. *Energy Engineering*, Vol. 99, No. 6, pp. 18-38 (2002)

19. Brandemuehl and Katejanekarn 2004
Brandemuehl M.J. and Katejanekarn T.
Dehumidification characteristics of commercial building applications. *ASHRAE Transactions*, Vol. 114, Part. 2, pp. 65-76 (2004)

20. Budaiwi et al. 1999
Budaiwi I., Diasty R. E and Abdou A.
Modelling of moisture and thermal transient behaviour of multi-layer non cavity walls. *Building and Environment*, Vol. 34, pp. 537-551 (1999)

21. Capehart 2003
Capehart B.
Air conditioning solutions for hot, humid climates. *Energy Engineering: Journal of the Association of Energy Engineering*, Vol. 100, No. 3, pp. 5-8 (2003)

22. Capuano et al. 1999
Capuano A., Dell'Isola M. , Massarotti N. and Vanoli L..
A metrological analysis of a Direct Digital Control DDC-based air conditioning system. *Energy and Buildings*, Vol. 19, pp. 155-166 (1999)

23. Cavallini et al. 2001
Cavallini A., Censi G., Delcol D., et al.
Experimental investigation on condensation heat transfer and pressure drop of new HFC refrigerants (R134a, R125, R32, R410A, R236ea) in a horizontal smooth tube. *International Journal of Refrigeration*, Vol. 24, No. 1, pp. 73-87 (2001)

24 Chen 2005
Chen W.
Modeling and control of a direct expansion (DX) variable-air-volume (VAV) air conditioning (A/C) system, *PhD thesis, Hong Kong Polytechnic University*. (2005)

25. Chen et al. 2001
Chen W.Y., Chen Z.J., Zhu R.Q. and Wu Y.Z.
Control algorithm of electronic expansion valve in evaporator superheat

regulation. *Journal of Shanghai Jiaotong University*, Vol. 35, No. 8, pp. 1228-1232 (2001)

26. Chen et al. 2002a
Chen Y., Halm N.P., Groll E.A. and Braun J.E.
Mathematical modeling of scroll compressors. Part I: compression process modeling. *International Journal of Refrigeration*, Vol. 25, pp.731-750(2002).

27. Chen et al. 2002b
Chen Y., Halm N.P., Groll E.A. and Braun J.E.
Mathematical modeling of scroll compressors. Part II: overall scroll compressor modeling, International Journal of Refrigeration, Vol. 25, pp. 751-764 (2002).

28. Chi and Didion 1982
Chi J. and Didion D.
A simulation model of the transient performance of a heat pump. *International Journal of Refrigeration*, Vol. 5, No. 3, pp. 176-184 (1982)

29. Chia et al. 1997
Chia P.K., Tso C.P., Jolly P.G., Wong Y.W. and Jia X.
Fuzzy control of superheat in container refrigeration using an electronic expansion valve. *HVAC and R Research*, Vol. 3, No. 1, pp. 91-98 (1997)

30. Chua et al. 2007
Chua K.J., Ho J.C., Chou S.K.
A comparative study of different control strategies for indoor air humidity. *Energy and Buildings*, Vol. 39, pp. 537-545 (2007)

31. Cleland 1986
Cleland A.C.
Computer sub-routines for rapid evaluation of refrigerant thermodynamic properties. *International Journal of Refrigeration*, Vol. 9, pp. 346-351(1986).

32. Cohen et al. 1974
Cohen R., Hamilton J. F. and Pearson J. T.
Possible energy conservation through the use of variable-capacity compressor. *Proceeding of Purdue Compressor Technology Conference, Purdue, USA*, pp. 50-54(1974)

33. Corberan and Melon 1998
Corberan J. M., Melon M. C.
Modeling of plate finned tube evaporators and condensers working with R134a. *International Journal of Refrigeration*, Vol. 21, No. 4, pp. 273-284 (1998)

34. Damasceno and Rooke 1990
Damasceno G. S. and Rooke S. P.
Comparison of three steady-state heat pump computer models. *ASHRAE Transaction.*, Vol. 96, part 2, pp. 191-204 (1990)

35. Dai et al. 2001
Dai Y.J., Wang R.Z., Zhang H.F. and Yu J.D.
Use of liquid desiccant cooling to improve the performance of vapor compression air conditioning. *Applied Thermal Engineering*, Vol. 21, No. 12, pp. 1185-1202 (2001)

36. de Dear et al. 1989
de Dear R.J., Knudsen H.N. and Fanger P.O.
Impact of air humidity on thermal comfort during step-changes. *ASHRAE Transactions*, Vol. 95, No. 2, pp. 336-350 (1989)

37. Deng 2000
Deng S. M.
A dynamic mathematical model of a direct expansion (DX) water-cooled air conditioning plant. *Building and Environment*, Vol. 35, No. 7, pp. 603-613 (2000)

38. Desta et al. 2005
Desta T.Z., Brecht A.V., et al.
Modelling and control of heat transfer phenomena inside a ventilated air space. *Energy and Buildings*, Vol. 37, No. 7, pp. 777-786 (2005)

39. Dieckmann et al. 2001
Dieckmann J., Roth K.W. and Brodrick, J.
Liquid desiccant air conditioners. *ASHRAE Journal*, Vol. 46, No. 4, pp. 58-59 (2001)

40. Domanski 1991
Domanski P. A.
Simulation of an evaporator with nonuniform one-dimensional air distribution. *ASHRAE Transactions*, Vol. 97, part 1, pp. 793-802 (1991)

41. Domanski and Mclinden 1992
Domanski P. and Mclinden M.
A simplified cycle simulation model for the performance rating of refrigerants and refrigerant mixtures. *International Journal of Refrigeration*, Vol. 15, No. 2, pp.81-88 (1992)

42. Duprez et al. 2007
Duprez M.E., Dumont E. and Frere M.
Modelling of reciprocating and scroll compressors. *International Journal of*

Refrigeration, Vol. 30, pp. 873-886 (2007)

43. Elsarrag et al. 2005
Elsarrag E., Ali E.E.M. and Jain S.
Design guidelines and performance study on a structured packed liquid desiccant air-conditioning system. *HVAC and Research*, Vol. 11, No. 2, pp. 319-337 (2005)

44. Fairey and Kerestecioglu 1985
Fairey P.W. and Kerestecioglu A.A.
Dynamic modeling of combined thermal and moisture transport in buildings: effects on cooling loads and space conditions. *ASHRAE Transactions*, Vol. 91, Part. 2a, pp. 461-473 (1985)

45. Fanger 2001
Fanger P.O.
Human requirements in future air-conditioned environments. *International Journal of Refrigeration*, Vol. 24, pp. 148-153 (2001)

46. Galbraith and Lean 1993
Galbraith G.H. and Lean R. M.
The determination of vapor and liquid transport coefficients as input to combined heat and mass transfer models. *IBPSA International Conference*, Australia, August (1993)

47. Galbraith et al. 1997
Galbraith G. H., Lean R. M. and Song G. J.
The selection of appropriate flow potentials for moisture transport models. *IBPSA International Conference*, Volume II. Prague, September (1997)

48. Gray and Webb 1986
Gray D.L. and Webb R.L.
Heat transfer and friction correlations fro plate finned-tube heat exchangers having plain fins. *Proceeding of The Eighth International Heat Transfer Conference,* San Francisco: American Society of Mechanical Engineers (1986)

49. Green 1982
Green G.H.
The positive and negative effects of building humidification. *ASHRAE Transactions*, Vol. 88, Part. 1, pp. 1049-1061 (1982)

50. Harriman III et al. 1999
Harriman III L.G., Czachorski M., Witte M.J. and Kosar D.R.
Evaluating active desiccant systems for ventilating commercial buildings. *ASHRAE Journal*, Vol. 40, No. 10, pp. 28-37 (1999)

51. Harriman III et al. 2001
Harriman III L.G., Brundrett G.W. and Kittler R.
Humidity control design guide for commercial and institutional buildings. *ASHRAE Engineers, Inc*. (2001)

52. He et al. 1997
He X.D., Liu S. and Asada H.H.
Modeling of vapor compression cycles for multivariable feedback control of HVAC systems. *Transaction of the ASME: Journal of Dynamic Systems, Measurement, and Control*, Vol. 119, pp. 183-191 (1997)

53. He et al. 1998
He X.D., Liu S., Asada H.H. and Itoh H.
Multivariable control of vapor compression systems. *HVAC&R Research*, Vol. 4, No. 3, pp. 205-230 (1998)

54. Henderson et al. 1992
Henderson H.I.Jr., Rengarjan K. and Shirey D.B.
The impact of comfort control on air conditioner energy use in humid climates. *ASHRAE Transactions*, 1992, Vol. 98, No. Part. 2, pp. 104-112 (1992)

55. Hong and Jiang 1997
Hong T. Z. and Jiang Y.
A new multizone model for the simulation of building thermal performance. *Building and Environment*, Vol. 32, No. 2, pp. 123-128 (1997)

56. Howell et al. 1987
Howell R.H., Sauer H.J. and Ganesh R.
Comparison of two control strategies to simulate part-load performance of a simple air-condition system. *ASHRAE Transactions*, Vol. 93, Part.2, pp. 1768-1780 (1987)

57. Hourahan 2004
Hourahan G.C.
How to properly size unitary equipment. *ASHRAE Journal*, 2004, Vol. 46, No. 2, pp. 15-18 (2004)

58. Huang and Franconi 1999
Huang Y.J. and Franconi E.
Commercial heating and cooling loads component analysis. *LBNL Report 37208, Lawrence Berkeley National Laboratory*, Berkeley, Calif (1999)

59. Jahnig et al. 2000
Jahnig D.I., Reindl D.T. and Klein S.A.,
A semi-empirical method for representing domestic refrigerator/freezer

compressor calorimeter test data, *ASHRAE Transactions*, Vol. 106, pp.122-130 (2000).

60. Jia et al. 1995
Jia X., Tso C. P., Chia P. K. and Jolly P.
A distributed model for prediction of the transient response of an evaporator. *International Journal of Refrigeration*, Vol. 18, No. 5. pp. 336-342(1995)

61. Jia et al. 1999
Jia X., Tso C. P., Jolly P. and Wong Y.W.
Distributed steady and dynamic modeling of dry-expansion evaporators. *International Journal of Refrigeration*, Vol. 22, pp.126-136 (1999)

62. Jin et al. 2005
Jin X.Q., Ren H.G. and Xiao X.K
Prediction-based online optimal control of outdoor air of multi-zone VAV air conditioning systems. *Energy and Buildings*, Vol. 37, pp. 939-944 (2005)

63. Jolly et al. 2000
Jolly P.G., Tso C.P., Chia P.K. and Wong Y.W.
Intelligent control to reduce superheat hunting and optimize evaporator performance in container refrigeration. *HVAC& R Research*, Vol. 6, No. 3, pp. 243-255 (2000)

64. Kalman 1995
Kalman I. K., Sui L., et al.
Temperature and humidity control during cooling and dehumidifying by compressor and evaporator fan speed variation. *ASHRAE Transaction*, Vol. 101, part 1, pp. 292-304 (1995)

65. Kam and Tade 2000
Kam K. M. and Tade M. O.
Simulated nonlinear control studies of five-effect evaporator models. *Computers and Chemical Engineering*, Vol. 23, pp.1795-1810 (2000)

66. Keresteciogl u and Gu 1990
Keresteciogl u A. and Gu L.
Theoretical and computational investigation of simultaneous heat and moisture transfer in buildings: Evaporation and condensation theory. *ASHRAE Transactions*, Vol. 96, pp. 455-464 (1990)

67. Kittler 1996
Kittler R.
Mechanical Dehumidification Control Strategies and Psychromatrics. *ASHRAE Transactions*, Vol. 102, No. 2, pp. 613-617 (1996)

68. Kosar et al. 1998
Kosar D.R., Witte M.J., Shirey D.B.III and Hedrick R.L.
Dehumidification issues of standard 62-1989. *ASHRAE Journal*, Vol. 40, No. 3, pp. 71-75 (1998)

69. Kosar 2006
Kosar D.
Dehumidification system enhancements. *ASHRAE Journal*, February, pp. 48-58 (2006)

70. Koury et al. 2001
Koury R.N.N., Machado L. and Ismail K.A.R.
Numerical simulation of a variable speed refrigeration system. *International Journal of Refrigeration*, Vol. 24, pp. 192-200 (2001)

71. Krakow et al. 1995
Krakow K.I., Lin S. and Zeng Z.S.
Temperature and humidity control during cooling and dehumidifying by compressor and evaporator fan speed variation. *ASHRAE Transactions*, Vol. 101, No.1, pp. 292-304 (1995)

72. Lam 1996
Lam J.C.
An analysis of residential sector energy use in Hong Kong. *Energy*, Vol. 21, pp.1-8 (1996)

73. Lam 2000
Lam J.C.
Energy analysis of commercial buildings in subtropical climates. *Building and Environment*, Vol. 35, pp. 19-26 (2000)

74. Leducq et al. 2006
Leducq D., Guilpart J. and Trystram G.
Non-linear predictive control of a vapour compression cycle. *International Journal of Refrigeration*, Vol. 29, pp. 761-772 (2006)

75. Lenarduzzi and Yap 1998
Lenarduzzi F. J. and Yap S. S.
Measuring the performance of a variable-speed drive retrofit on a fixed-speed centrifugal chiller. *ASHRAE Transaction*, Vol. 104, part 2, pp. 658-667 (1998)

76. Li et al. 2004
Li X.Q., Chen J.P., Chen Z.J., Liu W.H., Hu W. and Liu X.B.,
A new method for controlling refrigerant flow in automobile air conditioning. *Applied Thermal Engineering*, Vol. 24, pp. 1073-1085 (2004)

77. Li et al. 2007
Li Y.W., Wang R.Z., Wang T.H., Wu J.Y. and Xu Y.X.
Implementation of PI control for superheat degree of direct expansion solar assisted heat pump water heater. *Journal of Engineering Thermophysics*. Vol. 28, No. 1, pp. 49-52 Language: Chinese

78. Li and Deng 2007a
Li Z. and Deng S.M.
A DDC-based capacity controller of a direct expansion (DX) air conditioning (A/C) unit for simultaneous indoor air temperature and humidity control Part I: Control algorithms and preliminary controllability tests. *International Journal of Refrigeration*, Vol. 30, pp. 113-123 (2007)

79. Li and Deng 2007b
Li Z. and Deng S.M.
A DDC-based capacity controller of a direct expansion (DX) air conditioning (A/C) unit for simultaneous indoor air temperature and humidity control Part II: Further development of the controller to improve control sensitivity. *International Journal of Refrigeration*, Vol. 30, pp. 124-133 (2007)

80. Liang et al. 1999
Liang S.Y., Liu M., Wong T.N., and Nathan G.K.
Analytical study of evaporator coil in humid environment, *Applied Thermal Engineering*, Vol. 19, pp.1129-1145(1999)

81. Lida et al. 1982
Lida K., Yamamoto T., et al.
Development of an energy-saving-oriented variable capacity system heat pump. *ASHRAE Transaction*, Vol. 88, part 1, pp. 441-450 (1982)

82. Lin and Yeh 2007a
Lin J.L. and Yeh T.J.
Modeling, identification and control of air-conditioning systems.
International Journal of Refrigeration, Vol. 30, pp. 209-220 (2007)

83. Lin and Yeh 2007b
Lin J.L. and Yeh T.J.
Identification and control of multi-evaporator air-conditioning systems. *International Journal of Refrigeration*, Vol. 30, pp. 1374-1385 (2007)

84. Lstiburek 2002
Lstiburek J.
Residential ventilation and latent loads. *ASHRAE Journal*, Vol. 44, No. 4, pp. 18-22 (2002)

85. Lucas and Miranville 2004
Lucas F. and Miranville F.
Indoor humidity modeling and evaluation of condensation on interior surfaces. *ASHRAE Transactions*, Vol. 110, Part. 2, pp. 300-308 (2004)

86. MacArthur 1984
MacArthur J. W.
Transient heat pump behavior: a theoretical investigation. *International Journal of Refrigeration*, Vol. 7, No. 2. pp. 123-127 (1984)

87. Mahmoud and Ben-Nakhi 2003
Mahmoud M. A. and Ben-Nakhi A. E.
Architecture and performance of neural networks for efficient A/C control in buildings. *Energy Conversion and Management*, Vol. 44, No. 20, pp. 3207-3226 (2003)

88. Masato et al. 2000
Masato K., Yoshiaki K., et al.
Physical model of an air-conditioned space for control analysis. *ASHRAE Transaction*, Vol. 106, pp. 304-317 (2000)

89. Matthew and Banasal 1998
Matthew W. B., Banasal P. K.
Challenges in modeling vapor-compression liquid chillers. *ASHRAE Transaction*, Vol. 104, Part 1b, pp. 474-486 (1998)

90. Mazzei et al. 2005
Mazzei P., Minichiello F. and Palma D.
HVAC dehumidification systems for thermal comfort: a critical review. *Applied Thermal Engineering*, 2005, Vol. 25, pp. 677-707

91. Miro 2005
Miro C.
ASHRAE issues guidance on minimizing mold, mildew. *ASHRAE Journal*, Vol. 47, No. 3, pp. 86 (2005)

92. Nagaya et al. 2006
Nagaya K., Senbongi T., Li Y., Zheng J. and Murakami I.
High energy efficiency desiccant assisted automobile air-conditioner and its temperature and humidity control system. *Applied Thermal Engineering* , Vol. 26, pp. 1545-1551(2006)

93. Navarro-Esbrı et al. 2007
Navarro-Esbrı J., Berbegall V., Verdu G., Cabello R., Llopis R.
A low data requirement model of a variable-speed vapor compression refrigeration system based on neural networks. *International Journal of*

Refrigeration, pp. 1-8 (2007)

94. Niu et al. 2002
Niu J.L., Zhang L.Z. and Zuo H.G.,
Energy savings potential of chilled-ceiling combined with desiccant cooling in hot and humid climates. *Energy and Buildings*, Vol. 34, pp. 487-495(2002)

95. Nyers and Stoyan 1994
Nyers J. and Stoyan G.
Dynamical model adequate for controlling the evaporator of a heat pump. *International Journal of Refrigeration*, Vol. 17, pp. 101-108(1994)

96. Park et al. 2007
Park C., Cho H., Lee Y. and Kim Y.
Mass flow characteristics and empirical modeling of R22 and R410A flowing through electronic expansion valves. *International Journal of Refrigeration*, Vol. 30, pp.1401-1407(2007)

97. Peng and Howell 1981
Peng C. S. and Howell J. R.
Analysis and design of efficient absorbers for low-temperature desiccant air conditioners. *Journal of Solar Energy*, Vol.103, pp. 67-74 (1981)

98. Perez-Segarra et al. 2003
Perez-Segarra C.D., Rigola J. and Oliva A.,
Modeling and numerical simulation of the thermal and fluid dynamic behavior of hermetic reciprocating compressors. Part 1: theoretical basis, *HVAC & R Research*, Vol. 9, No. 2, pp. 215-235(2003)

99. Popovic and Shapiro 1995
Popovic P. and Shapiro H.N.
A semi-empirical method for modeling a reciprocating compressor in refrigeration systems, *ASHRAE Transactions*, Vol. 101, pp. 367-382 (1995)

100. Porkhial et al. 2004
Porkhial S., Khastoo B. , Saffar-Avval M.
Transient response of dry expansion evaporator in household refrigerators. *Applied Thermal Engineering*, Vol. 24, pp. 1465-1480 (2004)

101. Qureshi and Tassou 1996
Qureshi T. Q. and Tassou S. A.
Variable-speed capacity control in refrigeration systems. *Applied Thermal Engineering*, Vol. 16, No. 2, pp. 103-113(1996)

102. Rasmussen 2008
Rasmussen H.
Nonlinear Superheat and Capacity Control of a Refrigeration Plant. *17th IEEE International Conference on Control Applications, Part of 2008 IEEE Multi-conference on Systems and Control*, San Antonio, Texas, USA, 97-101

103. Rigola et al. 2003
Rigola J., Perez-Segarra C.D. and Oliva A.,
Modeling and numerical simulation of the thermal and fluid dynamic behavior of hermetic reciprocating compressors. Part 2: experimental investigation, *HVAC & R Research*, Vol. 9, No. 2, pp. 237-249(2003)

104. Rowland et al. 2005
Rowland C.A., Wendel J. and Martin J.
Dehumidification technologies. *HPAC Heating, Piping, Air Conditioning Engineering*, Vol. 77, No. 3, pp. 48 (2005)

105. Saman and Alizadeh 2002
Saman W. Y. and Alizadeh S.
An experimental study of a cross-flow type plate heat exchanger for dehumidification/cooling. *Solar Energy*, Vol. 73, No. 1, pp. 59-71(2002)

106. Scalabrin and Bianco 1994
Scalabrin G. and Bianco G.
Experimental and thermodynamic analysis of a variable-speed open reciprocating refrigeration compressor. *International Journal of Refrigeration*, Vol. 17, No. 1, pp. 68-75 (1994)

107. Shah et al. 2004
Shah R., Rasmussen B.P., and Alleyne A. G.
Application of a multivariable adaptive control strategy to automotive air conditioning systems. *International Journal of Adaptive Control and Signal Processing*, Vol. 18, pp. 199-221 (2004)

108. Sherman 1999
Sherman M.
Indoor air quality for residential buildings. *ASHRAE Journal*, Vol. 41, No. 5, pp. 26-30 (1999)

109. Shirey 1993
Shirey D.B
Demonstration of efficient humidity control techniques at an art museum. *ASHRAE Transactions*, Vol. 99, No. Pt. 1, pp. 694-703 (1993)

110. Shirey and Henderson 2004
Shirey D.B. and Henderson H.I.

Dehumidification at part load. *ASHRAE Journal*, Vol. 46, No. 3, pp. 42-47 (2004)

111. Silver et al.1990
Silver S. C., Fine P. J., et al.
Performance monitoring of DX rooftop cooling equipment. Energy Engineering: *Journal of the Association of Energy*, Vol. 87, No. 5, pp. 32-41 (1990)

112. Skogestad and Postlethwaite 1996
Skogestad S. and Postlethwaite I.
Multivariable feedback control analysis and design. *John Wiley &Sons Ltd*. (1996)

113. So et al. 1997
So A. T. P., Chan W. L., et al.
Self-learning fuzzy air handling system controller. *Building Services Engineering Research & Technology*, Vol. 18, No. 2, pp. 99-108 (1997)

114. Stefani et al. 2002
Stefani R. T., Shahian B., Savant C. J. and Hostetter G. H.
Design of feedback control systems. *Oxford University Press*. 2002

115. Stephenson and Mitalas 1967
Stephenson D. G. and Mitalas G. P.
Room thermal response factors. *ASHRAE Transaction*, Vol. 73, Part 2. pp. 31-38 (1967)

116. Stephenson and Mitalas 1971
Stephenson D. G., Mitalas G. P.
Calculation of heat conduction of transfer functions for multiplayer slabs. *ASHRAE Transaction*, Vol. 77, part 2, pp. 117-123 (1971)

117. Straube 2002
Straube J. F.
Moisture in buildings. *ASHRAE Journal*, Vol. 44, No. 1, pp. 15-19 (2002)

118. Subramanyam et al. 2004
Subramanyam N., Maiya M.P. and Murthy S.S.
Application of desiccant wheel to control humidity in air-conditioning systems. *Applied Thermal Engineering*, Vol. 24, No.17-18, pp. 2777-2788 (2004)

119. Tanabe and Kimura 1994
Tanabe, S. and Kimura, K.
Effects of air temperature, humidity, and air movement on thermal comfort in hot and humid conditions. *ASHRAE Transactions*, Vol. 100, No. 2, pp. 953-969

(1994)

120. Tewari 2002
Tewari A.
Modern Control Design with Matlab and Simulink. *John Wiley &Sons Ltd*. 2002

121. Thomas and Burch 1990
ThomasW.C. and Burch D.M.
Experimental validation of a mathematical model for predicting water sorption at interior building surfaces. *ASHRAE Transactions*, Vol. 96, pp. 487-496 (1990)

122. Thompson and Dexter 2005
Thompson R. and Dexter A.
A fuzzy decision-making approach to temperature control in air-conditioning systems. *Control Engineering Practice*, Vol.13, pp. 689-698 (2005)

123. Tiwari et al. 2004
Tiwari M.K., Mukhopadhyay A. and Sanyal D.
Numerical simulation of optimal multiple-input, multiple-output control of jet impingement cooling of a glass plate. *Numerical Heat Transfer*, Part A, Vol.46, pp.401-424(2004)

124. Todescat and Fagotti 1992
Todescat M.L. and Fagotti F.
Thermal energy analysis in reciprocating hermetic compressors, in:
Proceedings of the International Compressor Engineering Conference at Purdue University, USA, pp. 1419-1428 (1992)

125.. Turaga et al. 1988
Turaga M., Lin S. and Fazio P. F.
Correlations for heat transfer and pressure drop factors for direct expansion air cooling and dehumidifying coils. *ASHRAE Transaction*, Vol. 94, part 2, pp. 616-629 (1988)

126. Vargas and Parise 1995
Vargas J. V. C. and Paris J. A. R.
Simulation in transient regime of a heat pump with closed-looped and on-off control. *International Journal of Refrigeration*, Vol. 18, No. 4, pp. 25-243 (1995)

127. Wang et al. 1999
Wang C. C., Lee C. J., Chang C. T., et al.
Heat transfer and friction correlation for compact louvered fin-and-tube heat exchangers. *International Journal of Heat and Mass Transfer*, Vol. 42, No. 11,

pp. 1945-1956 (1999)

128. Wang et al. 2000
Wang C. C., Lin Y. T. and Lee C. J.
Heat and momentum transfer for compact louvered fin-and-tube heat exchangers in wet conditions. *International Journal of Heat and Mass Transfer*, Vol. 43, No. 18, pp. 3443-3452 (2000)

129. Wang and Touber 1991
Wang H. and Touber S.
Distributed and non-steady-state modeling of an air cooler. *International Journal of Refrigeration*, Vol.14, pp. 98-111(1991)

130. Webb 1990
Webb R. L.
Air-side heat transfer correlations for flat and wavy plate fin-and tube geometries. *ASHRAE Transaction*, Vol. 96, pp. 445-449 (1990)

131. Winandy et al. 2002a
Winandy E., Saavedra O.C. and Lebrun J.
Simplified modeling of an open-type reciprocating compressor, *International Journal of Thermal Science*, Vol. 41, pp.183-192(2002).

132. Winandy et al. 2002b
Winandy E., Saavedra O.C. and Lebrun J.,
Experimental analysis and simplified modelling of a hermetic scroll refrigeration compressor. *Applied Thermal Engineering*, Vol. 22, pp. 107-120 (2002).

133. Xiao et al. 1997
Xiao P.W., Johnson P. and Akbarzadeh A.
Application of heat pipe heat exchangers to humidity control in air-conditioning systems. *Applied Thermal Engineering*, Vol. 17, No. 6, pp. 561-568 (1997)

134. Xu et al.1996
Xu Z.G., Gotham D.H.T., Collins M.W., Coney J.E.R., Sheppard C.G.W. and Merdjani S.
A numerical and experimental study of turbulent flow through the evaporator coil in an air conditioning unit, *International Journal of Refrigeration*, Vol. 19, No. 6, pp. 369-381(1996)

135. Yang and Lee 1991
Yang K. H and Lee M. L.
Analysis of an inverter-driven air-conditioning system and its application in a hot and humid area. *International Journal of Energy Research*, Vol. 15, No. 5,

pp. 357-365 (1991)

136. Yaqub and Zubair 2001
Yaqub M. and Zubair S.M.
Capacity Control for Refrigeration and Air-Conditioning Systems: A Comparative Study. *Transactions of the ASME*, Vol. 123, pp. 92-99 (2001)

137. Yasuda et al. 1983
Yasuda H., Touber S. and Machielsen C.H.M.
Simulation model of a vapor compression refrigeration system. *ASHRAE Transactions*, Vol. 98, pp. 408-25(1983)

138. Yau 2007
Yau Y.H.
Application of a heat pipe heat exchanger to dehumidification enhancement in a HVAC system for tropical climates--a baseline performance characteristics study. *International Journal of Thermal Sciences*, Vol. 46, pp. 164-171(2007)

139. Youn et al. 2002
Youn C. P., Kim Y., et al.
Thermodynamic analysis on the performance of a variable speed scroll compressor with refrigerant injection. *International Journal of Refrigeration*, Vol. 25, No. 8, pp.1072-1082 (2002)

140. Yuan and Perez 2006
Yuan S. and Perez R.
Multiple-zone ventilation and temperature control of a single-duct VAV system using model predictive strategy. *Energy and Buildings*, Vol. 38, pp. 1248-1261 (2006)

141. Zhang 2002
Zhang G.Q.
China HVACR Annual Business Volume Ⅱ. *Chinese Construction Industry Press*, pp. 44-45

142. Zhang and Zhang 2006
Zhang W.J. and Zhang C.L.
A generalized moving-boundary model for transient simulation of dry-expansion evaporators under larger disturbances. *International Journal of Refrigeration*, Vol. 29, pp. 1119-1127(2006)

Appendix A

Program listing

% The following program written in *Matlab 6.5* was used for simulating the open-loop response of major parameters when the step change of compressor speed or supply fan speed was introduced in the experimental DX A/C system--------

```
clear all


Cp=1.005;      % kJ/kg.k; specific heat of air
p=1.2;         % kg/m^3;  density of air,;
V=77;          % m^3; the volume of conditioned space room;
hfg=2450;      %kJ/kg; latent heat of vaporization of water
Cpmwall=29;  % kJ/k; specific heat *density*volume of evaporator wall

At=22.07;      % m^2; heat transfer area of DX evaporator, calculated according to size
                of DX evaporator

Aratio=0.2;            % dry-cooling region area/total area
A1=Aratio*At;      % m^2; dry region area
A2=(1-Aratio)*At;  % m^2; wet region area

Vh=0.2;              % m^3, volume of DX evaporator on air side, calculated according to
size of DX evaporator
V1=Aratio*Vh;        % m^3, the volume of DX evaporator on air side in dry-cooling
region
V2=(1-Aratio)*Vh; % m^3, the volume of DX evaporator on air side in dry-cooling
region



% ----------------------operating point parameters----------------
 fs=0.347;           %m^3/s, =1250m^3/h, airflow rate at operating point;
 T1s=13.25;          %degree, supply air temperature at operating point;
 W1s=9.03/1000;   % kg/kg,  moisture content of supply air

 T2s=24;              %degree,   air temperature of air leaving conditioned space;
 W2s=11.35/1000;   % kg/kg, moisture content of  air leaving conditioned space;

 T3s=15.7;           % degree , the dewpoint temperature;
 W3s=11.3/1000;    % kg/kg,  moisture of air leaving dry-cooling region;
 Tws=13;             % degree, temperature of evaporator's wall
```

```
% ----------------------operating point parameters----------------


alldata=compressor_stepchange_data;  % data from experiment

% -----get some parameters needed for simulation------
all_parameters=[alldata(:,22) alldata(:,4) alldata(:,5) alldata(:,10) alldata(:,11)
alldata(:,12) alldata(:,13) alldata(:,14) alldata(:,6) alldata(:,7)];
% -----get some parameters needed for simulation------

num=size(all_parameters);
n=num(1);

for i=1:1:n

AHUairflowrate(i)=all_parameters(i,1);
Ref_flow(i)=all_parameters(i,4);

T2_exp(i)=all_parameters(i,2);
W2_exp(i)=t_ts_Mc(all_parameters(i,2),all_parameters(i,3));
T1_exp(i)=all_parameters(i,9);
W1_exp(i)=t_ts_Mc(all_parameters(i,9),all_parameters(i,10));
H1_exp(i)=t_ts_H(all_parameters(i,9),all_parameters(i,10));
H2_exp(i)=t_ts_H(all_parameters(i,2),all_parameters(i,3));

RH2_exp(i)=t_ts_RH(all_parameters(i,2),all_parameters(i,3));
H_out(i)=P_T_H(all_parameters(i,6),all_parameters(i,5))/1000; %kj/kg
H_in(i)=P_T_H(all_parameters(i,8),all_parameters(i,7))/1000;%kj/kg

end


n=700;
T1=zeros(1,n);
T2=zeros(1,n);
T3=zeros(1,n);
Tw=zeros(1,n);

W1=zeros(1,n);
W2=zeros(1,n);
W3=zeros(1,n);


%---------------initial values (increase)---------------------
T1(1)=0.0;
W1(1)=0.00/1000;
```

```
T2(1)=0;
W2(1)=0.00/1000;

T3(1)=0;
W3(1)=0;

Tw(1)=0;
%---------------initial values (increase)---------------------


%----------system inputs --------------

for i=1:1:n
  mr(i)=(Ref_flow(i)-2.52)/60;  % change of refrigerant mass flow
  Refcapacity(i)=alldata(i,24);

end

for i=1:1:n
  hr1(i)=H_in(i);   % enthalpy of refrigerant at inlet of evaporator
end

for i=1:1:n
  hr2(i)=hr1(i)+171;   %  enthalpy of refrigerant at outlet of evaporator
end

for i=1:1:n
  f(i)=(AHUairflowrate(i)-1250)/3600;  % change of air flow rate
end
%----------system inputs--------------



Q1=Cp*p*fs*(T2s-T3s);    % heat load in dry region at steady state
a1=Q1/(A1*((T2s+T3s)/2-Tws)); % heat tranfer coefficiency in dry region at steady state

Q2=Cp*p*fs*(T3s-T1s);    % heat load in dry region at steady state
a2=Q2/(A2*((T3s+T1s)/2-Tws)); % heat tranfer coefficiency in dry region at steady state



n_htr=1/3;
%-------heat transfer coefficent in operation point(stable state)-------------
```

```
eva_a1s=a1*(fs/fs).^(n_htr);  %dry region
eva_a2s=a2*(fs/fs).^(n_htr);  %wet region
%-------heat transfer coefficent in operation point(stable state)----------



tt=1.7; % interval time, s


T2_a(1)=T2(1)+T2s;
W2_a(1)=W2(1)+W2s;
RH2(1)=aT_MC_RH(T2_a(1),W2_a(1)*1000)*100;

T1_a(1)=T1(1)+T1s;
W1_a(1)=W1(1)+W1s;


  AHUsenTotal=9.0;
  AHUlatentTotal=4.74;
  AHUcapacityTotal=13.7;
  AHUsenTotal_exp=0;
  AHUlatentTotal_exp=0;
  AHUcapacityTotal_exp=0;

 SpacesenTotal=9.0;



for k=1:1:n-1

%------heat transfer coefficent changing with airflow rate-----
eva_a1=a1*((fs+f(k+1))/fs).^(n_htr);
eva_a2=a2*((fs+f(k+1))/fs).^(n_htr);
%------heat transfer coefficent changing with airflow rate-----


%---------------evaporator wall----------------------
right_side(k+1)=Cpmwall/tt*Tw(k)-0.8*mr(k+1)*(hr2(k+1)-
hr1(k+1))+eva_a2*A2*T1(k)/2+eva_a1*A1*T2(k)/2+(eva_a1*A1+eva_a2*A2)*T3(k)/
2;
Tw(k+1)=right_side(k+1)/(Cpmwall/tt+eva_a1*A1+eva_a2*A2);
Tw_a(k+1)=Tws+Tw(k+1);
%---------------evaporator wall----------------------

Qplus(k+1)=Refcapacity(k+1);
```

```
 %------------the air temperature at the end of dry-cooling region-------------------

T3(k+1)=((Cp*p*fs*eva_a1*A1/2)*tt*T2(k)+Cp*p*V1*T3(k)+eva_a1*A1*tt*Tw(k+1)
+Cp*p*(T2s-T3s)*tt*f(k+1))/(Cp*p*V1+Cp*p*fs*tt+eva_a1*A1*tt/2);
W3(k+1)=W2(k);
  %------------the air temperature at the end of dry-cooling region-------------------
T3_a(k+1)=T3s+T3(k+1);   % absolute value
 W3_a(k+1)=W3s+W3(k+1);   % absolute value

  LL1(k+1)=p*(fs+f(k+1))*(Cp*(T2_a(k)-T3_a(k+1)));
  LL2(k+1)=-eva_a1*A1*((T3_a(k+1)+T2_a(k))/2-Tw_a(k+1));




%----------temperature and moisture at the end of wet-cooling region-----------------
a1=Cp*p*V2+hfg*(2*0.0198/1000*T1s+0.085/1000)*p*V2;
b1=Cp*p*fs-eva_a2*A2/2;
b2=-Cp*p*fs-eva_a2*A2/2-hfg*p*fs*(2*0.0198/1000*T1s+0.085/1000);
b3=eva_a2*A2;
b4=hfg*p*fs;
b5=Cp*p*(T3s-T1s)+hfg*p*(W3s-W1s);

T1(k+1)=(b1*T3(k+1)+a1*T1(k)/tt+b3*Tw(k+1)+b4*W3(k+1)+b5*f(k+1))/(a1/tt-b2);
W1(k+1)=(2*0.0198/1000*T1s+0.085/1000)*T1(k+1);
%----------temperature and moisture at the end of wet-cooling region-----------------

  T1_a(k+1)=T1s+T1(k+1);   % absolute value
  W1_a(k+1)=W1s+W1(k+1);   % absolute value




  LL3(k+1)=p*(fs+f(k+1))*(Cp*(T3_a(k+1)-T1_a(k+1))+hfg*(W3_a(k+1)-
W1_a(k+1)));
  LL4(k+1)=-eva_a2*A2*((T3_a(k+1)+T1_a(k+1))/2-Tw_a(k+1));


 %-----------------supply fan--------------
   Q_supplyfan(k+1)=1*f(k+1)*0.17/(0.347-0.304)*1;
   Qload=0.9*(0-T2(k));
 %-----------------supply fan--------------
```

```
 %---------------------------------conditioned space energy balance -------------------------

 T2(k+1)=(Cp*p*V*T2(k)/tt+Cp*p*fs*T1(k+1)+Cp*p*(T1s-
T2s)*f(k+1)+Q_supplyfan(k+1)+Qload)/(Cp*p*V/tt+Cp*p*fs);

T2_a(k+1)=T2(k+1)+T2s; % absolute value

W2(k+1)=(W2(k)+tt*fs*W1(k+1)/V+tt*(W1s-W2s)*f(k+1)/V)/(1+fs*tt/V);  %
W2_a(k+1)=W2(k+1)+W2s;

 RH2(k+1)=aT_MC_RH(T2_a(k+1),W2_a(k+1)*1000)*100;  % relative humidity


Spacesen(k+1)=Cp*p*(fs+f(k+1))*(T2_a(k+1)-T1_a(k+1));
SpacesenTotal=SpacesenTotal+Spacesen(k+1);
SpacesenTotalplus=SpacesenTotal-4.51;

 %---------------------------------conditioned space energy balance----------------------------


  hra2(k+1)=aT_MC_H(T2_a(k+1),W2_a(k+1));
  hra1(k+1)=aT_MC_H(T1_a(k+1),W1_a(k+1));
  Q(k+1)=(fs+f(k+1))*(hra2(k+1)-hra1(k+1))*p;

 AHUsen(k+1)=Cp*p*(fs+f(k+1))*(T2_a(k)-T1_a(k+1));   % sensbile cooling capacity
 AHUlatent(k+1)=hfg*p*(W2_a(k)-W1_a(k+1))*(fs+f(k+1));  % latent cooling capacity
 AHUcapacity(k+1)=Cp*p*(fs+f(k+1))*(T2_a(k)-T1_a(k+1))+hfg*p*(W2_a(k)-
W1_a(k+1))*(fs+f(k+1)); % total cooling capacity


  AHUsenTotal=AHUsenTotal+AHUsen(k+1);
  AHUlatentTotal=AHUlatentTotal+AHUlatent(k+1);
  AHUcapacityTotal=AHUcapacityTotal+AHUcapacity(k+1);


   AHUsen_exp(k+1)=Cp*p*(fs+f(k+1))*(T2_exp(k+1)-T1_exp(k+1));
  AHUsen_differece(k+1)=AHUsen(k+1)-AHUsen_exp(k+1);% the difference


end   % for


T2_a(1)=T2(1)+T2s;  % absolute value
```

```
W2_a(1)=W2(1)+W2s;  % absolute value
RH2(1)=aT_MC_RH(T2_a(1),W2_a(1)*1000)*100;  % reltaive humidity

T1_a(1)=T1(1)+T1s; % absolute value
W1_a(1)=W1(1)+W1s; % absolute value



hra2(1)=aT_MC_H(T2_a(1),W2_a(1));  % Enthalpy of moisture
hra1(1)=aT_MC_H(T1_a(1),W1_a(1));  % Enthalpy of moisture
Qq=(fs)*(hra2(1)-hra1(1))*p;

  AHUsen(1)=AHUsen(2);
  AHUlatent(1)=AHUlatent(2);
  AHUcapacity(1)=AHUcapacity(2);

for k=0:1:n-1

  AHUsen_exp(k+1)=Cp*p*(fs+f(k+1))*(T2_exp(k+1)-T1_exp(k+1));
% sensible cooling capapcity in experiment

  AHUlatent_exp(k+1)=hfg*p*(W2_exp(k+1)-W1_exp(k+1))*(fs+f(k+1))/1000;
% latent cooling capapcity in experiment

 AHUcapacity_exp(k+1)=Cp*p*(fs+f(k+1))*(T2_exp(k+1)-
T1_exp(k+1))+hfg*p*(W2_exp(k+1)-W1_exp(k+1))*(fs+f(k+1))/1000;
 AHUsenTotal_exp=AHUsenTotal_exp+AHUsen_exp(k+1);
 AHUlatentTotal_exp=AHUlatentTotal_exp+AHUlatent_exp(k+1);

  AHUcapacityTotal_exp=AHUcapacityTotal_exp+AHUcapacity_exp(k+1);
% Total cooling capapcity in experiment

end



t=1:1:n;
h1=figure;
plot(t,Tw), grid;
xlabel('Time (s)');
ylabel('Temperature (C)');
title('Evaporator wall temperature');


h2=figure;
plot(t,T3), grid;
```

```
xlabel('Time (s)');
ylabel('T3');


%---------- T2, W2 and the their comparisons between simulated and measured results---
-
h2=figure;
plot(t,T2), grid;
xlabel('Time (s)');
ylabel('T2');

T2_exp=T2_exp(1:n);

h2=figure;
plot(t,T2_exp), grid;
xlabel('Time (s)');
ylabel('T2_exp');

T2_a=T2_a(1:n);

h2=figure;
plot(t,T2_a,t,T2_exp), grid;
xlabel('Time (s)');
ylabel('Temperature (C)');
legend('Simulation','Experiment');
title('Air temperature in space room');

h3=figure;
plot(t,W2), grid;
xlabel('Time (s)');
ylabel('W2');

W2_a=W2_a(1:n);
W2_exp=W2_exp(1:n);
h3=figure;
plot(t,W2_a*1000,t,W2_exp), grid;
xlabel('Time (s)');
ylabel('Moisture (g)');
legend('Simulation','Experiment');
title('Air moisture in space room');



RH2=RH2(1:n);
RH2_exp=RH2_exp(1:n);
h3=figure;
```

```
plot(t,RH2,t,RH2_exp), grid;
xlabel('Time (s)');
ylabel('RH (100%)');
legend('Simulation','Experiment');
title('Relative humidity in space room');
%---------T2, W2 and the their comparisons between simulated and measured results----



%---------T1, W1 and the their comparisons between simulated and measured results-----
h2=figure;
plot(t,T1), grid;
xlabel('Time (s)');
ylabel('T1');

h2=figure;
plot(t,T1_a), grid;
xlabel('Time (s)');
ylabel('T1_a');

T1_a=T1_a(1:n);
T1_exp=T1_exp(1:n);
h2=figure;
plot(t,T1_a,t,T1_exp), grid;
xlabel('Time (s)');
ylabel('Temperature (C)');
legend('Simulation','Experiment');
title('Air temperature after evaporator');


W1_exp=W1_exp(1:n);
W1_a=W1_a(1:n);
h3=figure;
plot(t,W1_a*1000,t,W1_exp), grid;
xlabel('Time (s)');
ylabel('Moisture (g)');
legend('Simulation','Experiment');
title('Air moisture after evaporator');

%------T1, W1 and the their comparisons between simulated and measured results--------


%------cooling capacity and their comparisons between simulated and measured results--

h3=figure;
plot(t,Refcapacity), grid;
```

```
xlabel('Time (s)');
ylabel('Refcapacity');


h3=figure;
plot(t,AHUsen,t,AHUlatent,t,AHUcapacity), grid;
xlabel('Time (s)');
ylabel('AHUcapacity)');
title('AHUcapacity');


h3=figure;
plot(t,AHUsen_exp,t,AHUlatent_exp,t,AHUcapacity_exp), grid;
xlabel('Time (s)');
ylabel('AHUcapacity)');
title('AHUcapacity_exp');

h3=figure;
plot(t,AHUsen,t,AHUlatent,t,AHUcapacity,t,AHUsen_exp,t,AHUlatent_exp,t,AHUcapa
city_exp), grid;
xlabel('Time (s)');
ylabel('AHUcapacity)');
title('AHUcapacity');
%-----cooling capacity and their comparisons between simulated and measured results---


% ----------------------End----------------
```

%----------The main program of MIMO controller was written in *Labview* in this study. The following program was the sub-program written in *Matlab* which was used as a part of the main controller program----------%

% --------operating parameters in different conditions --------

if DBT2>25.5

fs=0.308; % m^3/s, airflow rate at operating point;
T1s=12.43; % degree, supply air temperature at operating point;
W1s=8.54/1000;

T2s=26; %degree, temperature of air leaving conditioned space;
W2s=10.62/1000; % kg/kg, moisture content of air leaving conditioned space;

T3s=15.1; % degree , the dewpoint temperature;
W3s=10.62/1000; % kg/kg, moisture of air leaving dry-cooling region;
Tws=10.5; % degree, temperature of evaporator's wall;

mrs=2.38/60; % L/s, mass flowrate of refrigerant;
vsup=0.0461; % specific volume of superheated refrigerant
efficient_com=0.9; % efficient of compressor

hr2= Enth_out; % kJ/kg, enthalpy of refrigerant at outlet of evaporator
hr1=Enth_in; % kJ/kg, enthalpy of refrigerant at outlet of evaporator

else if DBT2>24.5

fs=0.308; % m^3/s, airflow rate at operating point;
T1s=11.85; % degree, supply air temperature at operating point;
W1s=8.26/1000;

T2s=25; %degree, temperature of air leaving conditioned space;
W2s=10.03/1000; % kg/kg, moisture content of air leaving conditioned space;

T3s=14.7; % degree , the dewpoint temperature;
W3s=10.03/1000; % kg/kg, moisture of air leaving dry-cooling region;
Tws=10; % degree, temperature of evaporator's wall;

```
mrs=2.36/60;      % L/s, mass flowrate of refrigerant;
vsup=0.0461;      % specific volume of superheated refrigerant
efficient_com=0.9;  % efficient of compressor


hr2= Enth_out;      % kJ/kg, enthalpy of refrigerant at outlet of evaporator
hr1=Enth_in;        % kJ/kg, enthalpy of refrigerant at outlet of evaporator


else if DBT2<23.5

fs=0.308;         % m^3/s, airflow rate at operating point;
T1s=10.17;        % degree, supply air temperature at operating point;
W1s=7.4/1000;     % kg/kg, moisture content of supply air at operating point;

T2s=23;           %degree, temperature of air leaving conditioned space;
W2s=8.93/1000;    % kg/kg, moisture content of air leaving conditioned space;

T3s=12.8;          % degree , the dewpoint temperature;
W3s=8.93/1000;     % kg/kg,  moisture of air leaving dry-cooling region;
Tws=9;            % degree, temperature of evaporator's wall;


mrs=2.33/60;      % L/s, mass flowrate of refrigerant;
vsup=0.0461;      % specific volume of superheated refrigerant
efficient_com=0.9;  % efficient of compressor


hr2= Enth_out;      % kJ/kg, enthalpy of refrigerant at outlet of evaporator
hr1=Enth_in;        % kJ/kg, enthalpy of refrigerant at outlet of evaporator

else

fs=0.308;         % m^3/s, airflow rate at operating point;
T1s=11.2;         % degree, supply air temperature at operating point;
W1s=7.5/1000;     % kg/kg, moisture content of supply air at operating point;

T2s=24;          %degree, temperature of air leaving conditioned space;
W2s=9.34/1000;    % kg/kg, moisture content of air leaving conditioned space;

T3s=14;          % degree , the dewpoint temperature;
W3s=9.34/1000;    % kg/kg,  moisture of air leaving dry-cooling region;
Tws=10;          % degree, temperature of evaporator's wall;
```

```
mrs=2.35/60;      % L/s, mass flowrate of refrigerant;
vsup=0.0461;      % specific volume of superheated refrigerant
efficient_com=0.9;  % efficient of compressor

 end   % else if

end   % else if

end  % if



Q1=Cp*p*fs*(T2s-T3s);
a1=Q1/(A1*((T2s+T3s)/2-Tws));
Q2=Cp*p*fs*(T3s-T1s);
a2=Q2/(A2*((T3s+T1s)/2-Tws));

n_htr=1/3;

eva_a1=a1*(fs/fs).^(n_htr);
eva_a2=a2*(fs/fs).^(n_htr);


tt=30;    % second, time interval of each step


d11=0; d12=Cp*p*V/tt+Cp*p*fs+Heat_wall;d13=0;d14=0;d15=0;d16=0;
a11=Cp*p*fs; a12=Cp*p*V/tt;a13=0;a14=0;a15=0;a16=0;
b11=Cp*p*(T1s-T2s)+0.17/(0.347-0.304);b12=0;


d21=0; d22=0;d23=0;d24=0;d25=0;d26=1+fs*tt/V;
a21=0; a22=0;a23=0;a24=0;a25=fs*tt/V;a26=1;
b21=tt*(W1s-W2s)/V;b22=0;

d31=0; d32=0;d33=Cp*p*V1/tt+Cp*p*fs+eva_a1*A1/2;;d34=0;d35=0;d36=0;
a31=0; a32=Cp*p*fs-eva_a1*A1/2;a33=Cp*p*V1/tt;a34=eva_a1*A1;a35=0;a36=0;
b31=Cp*p*(T2s-T3s);b32=0;

d41=Cp*p*V2/tt+Cp*p*fs+eva_a2*A2/2;
d42=0;d43=0;;d44=0;d45=hfg*p*V2/tt+hfg*p*fs;d46=0;
a41=Cp*p*V2/tt; a42=0;a43=Cp*p*fs-
eva_a2*A2/2;a44=eva_a2*A2;a45=hfg*p*V2/tt;a46=hfg*p*fs;
b41=Cp*p*(T3s-T1s)+hfg*(W3s-W1s);b42=0;
```

```
d51=-(2*0.0198/1000*T1s+0.085/1000); d52=0;d53=0;d54=0;d55=1;d56=0;
a51=-(2*0.0198/1000*T1s+0.085/1000); a52=0;a53=0;a54=0;a55=1;a56=0;
b51=0;b52=0;


d61=0;d62=0;d63=0;d64=Cpmwall/tt+eva_a1*A1+eva_a2*A2;d65=0;d66=0;
a61=eva_a2*A2/2;
a62=eva_a1*A1/2;a63=eva_a1*A1/2+eva_a2*A2/2;a64=Cpmwall/tt;a65=0;a66=0;
b61=0;b62=-(hr2-hr1);

D1=[ d11 d12 d13 d14 d15 d16;
   d21 d22 d23 d24 d25 d26;
   d31 d32 d33 d34 d35 d36;
   d41 d42 d43 d44 d45 d46;
   d51 d52 d53 d54 d55 d56;
   d61 d62 d63 d64 d65 d66];     % matrix

Aa1=[a11 a12 a13 a14 a15 a16;
   a21 a22 a23 a24 a25 a26;
   a31 a32 a33 a34 a35 a36;
   a41 a42 a43 a44 a45 a46;
   a51 a52 a53 a54 a55 a56;
   a61 a62 a63 a64 a65 a66];     % matrix



Bb1=[b11 b12;
    b21 b22;
    b31 b32;
    b41 b42;
    b51 b52;
    b61 b62];

 C1=[0 1 0 0 0 0;
   0 0 0 0 0 1];

A=inv(D1)*Aa1;   % matrix in state space equation
B=inv(D1)*Bb1;   % matrix in state space equation
C=C1;          % matrix in state space equation
D=zeros(2,2);


Q0=eye(2);
R0=eye(2);
F=0.01*ones(6,2);
```

```
Q=[1 0;
   0 1];
R= [1 0;
  0 1];

[K1 P E]=dlqry(A,B,C,D,Q,R);  % LQR, using tool box in matlab

[L M P E]=dlqe(A,F,C,Q0,R0);  % using tool box in matlab

t_set_differece=DBT2-T2_set_DB;  % the difference between setting and actual T


K2=0.2*[0.055/15 -0.055/60;
0.0054/20 0.0054/50];        % coefficient


k=lp; % the k time of scan

xe=zeros(6,1000);    % the matrix for storing state variables
u22=zeros(2,1000);
u_last=zeros(2,1000)  % the matrix for storing last output variables
Y=zeros(2,1000);
u=zeros(2,1000);
uk1=zeros(2,1);
uk=zeros(2,1);
uk2=zeros(2,1);
xeout=zeros(6,1);
u_outpercent=zeros(2,1000);

DBT2_set=T2_set_DB;

Y(1,k)=DBT2-DBT2_set;  % difference of dry-bulb temperature
Y(2,k)=(Moisture_exp-Moisture_set)/1000;  % difference of moisture content


xe(2,1)=DBT2-DBT2_set;
xe(6,1)=(Moisture_exp-Moisture_set)/1000;
if k>1
xe(:,k)=xelast;
u_last(:,k)=ulastinput;
else
end


xe(:,k+1)=(A-L*C)*xe(:,k)+L*Y(:,k)+B*u_last(:,k);  % estimation of state variables
```

```
u(:,k+1)=-K1*xe(:,k+1)-1*eintegrate+K2*Y(:,k)*tt;  % inputs according control law

fs_acutal(k+1)=u(1,k+1)+fs;  % actual air flowrate, adding the value of steady state
u_outpercent(1,k+1)=235.89*fs_acutal(k+1)-21.812;  % percent of maximum
f_out=u_outpercent(1,k+1);

mr_acutal(k+1)=u(2,k+1)+mrs;  % actual mass flowrate of refrigerant,
n_rps=mr_acutal(k+1)*vsup/(0.00003041*efficient_com);
n_out=(n_rps*60-1320)/52.8;  % percent of maximum, compressor speed
u_outpercent(2,k+1)=n_out;

xee(:,k+1)=xe(:,k+1);
xeout=xe(:,k+1);

fs_last=u_last(1,k)+fs;
f_outlast=235.89*fs_last-21.812;

mr_last=u_last(2,k)+mrs;
n_rpslast=mr_last*vsup/(0.00003041*efficient_com);
n_outlast=(n_rpslast*60-1320)/52.8;


if f_out-f_outlast>5     % the increase of compressor speed at each step no more
   f_out=f_outlast+5;   % than 5 percent
  else if f_out-f_outlast<-5
   f_out=f_outlast-5;
     else
   end
end

if n_out-n_outlast>5    % the increase of supply fan speed at each step no more
  n_out=n_outlast+5;  % than 5 percent
else if n_out-n_outlast<-5
   n_out=n_outlast-5;
else
end
end

if f_out>95    % the maximum of supply fan speed was constrained at 95 percent
u_out1=95;
u_last(1,k+1)=(u_out1+21.812)/235.89-fs;
else if f_out<15
u_out1=15;     % the minimum of supply fan speed was constrained at 15 percent
u_last(1,k+1)=(u_out1+21.812)/235.89-fs;
else
```

```
u_out1=f_out; u_last(1,k+1)=(u_out1+21.812)/235.89-fs;
end
end

if n_out>90  % the maximum of compressor speed was constrained at 90 percent
u_out2=90;
u_last(2,k+1)=(u_out2*52.8+1320)/60*(0.00003041*efficient_com)/vsup-mrs;
else if n_out<20
u_out2=20;  % the minimum of compressor speed was constrained at 20 percent
u_last(2,k+1)=(u_out2*52.8+1320)/60*(0.00003041*efficient_com)/vsup-mrs;
else
u_out2=n_out;
u_last(2,k+1)=(u_out2*52.8+1320)/60*(0.00003041*efficient_com)/vsup-mrs;
end
end
u22(:,k+1)=u_last(:,k+1);
uout=zeros(2,1);
uout=u_outpercent(:,k+1);
loop=k;

% ----------------------End----------------
```

%------ The following program was the sub-program written in *Matlab* which was used as a part of the main controller program, using for the calculation of refrigerant enthalpy------

```
Pr_com_out=Pr_com_out_r*1000000+101325;
Pr_com_in=Pr_com_in_r*1000000+101325;
Pr_eva_out=Pr_eva_out_r*1000000+101325;

efficient_com=0.98*(1-0.015*((Pr_com_out/Pr_com_in).^(1/1.18)-1));

tsat_eva_out=(-2025.4518/(log(Pr_eva_out)-21.25384))-248.94;
temp2=-11.82344+2390.321/(tsat_eva_out+273.15);

vv=exp(temp2)*(1.01859+0.000509433*tsat_eva_out-0.0000148464*tsat_eva_out.^2-
0.000000249547*tsat_eva_out.^3);

temp=250027+367.265*tsat_eva_out-1.84133*tsat_eva_out.^2-
0.0114556*tsat_eva_out.^3;

tsup=tr_eva_out-tsat_eva_out;

hr2=temp*(1+0.00285446*tsup+0.00000040129*tsup*tsup+0.0000133612*tsup*tsat_e
va_out-
0.0000000811617*tsat_eva_out*tsup*tsup+0.000000141194*tsup*tsat_eva_out*tsat_ev
a_out-0.000000000953294*tsup*tsup*tsat_eva_out*tsat_eva_out);

hr_com_in=(hr2+155482)/1000;

vsup=vv*(1.0+0.00523275*tsup-
0.00000559394*tsup*tsup+0.0000345555*tsup*tsat_eva_out-
0.000000231649*tsup*tsup*tsat_eva_out+0.000000580303*tsup*tsat_eva_out*tsat_eva
_out-0.00000000320189*tsup*tsup*tsat_eva_out*tsat_eva_out);


hr1=200000+1170.36*tr_EEV_in+1.68674*tr_EEV_in.^2+0.0052703*tr_EEV_in.^3;
hr_EEV_in=hr1/1000;

hr_d=hr_com_in-hr_EEV_in;

hr_inout=zeros(1,2);
hr_inout(1,1)=hr_EEV_in;
hr_inout(1,2)=hr_com_in;
```

```
% ----------------------End----------------
```

% -------The following subprograms are used for the calculations of moisture air and refrigerant operating parameters---------

(1) %//Ha is the enthalpy of moisture air

```
 function  t_ts_Ha=t_ts_H(t,ts)

 %LD t_ts_Ha; //Ha is the enthalpy of moisture air

    t_ts_Ha=1.005*t+0.001*t_ts_MC(t,ts)*(2501+1.88*t);

    % return t_ts_Ha;
```

(2) % t_ts_MCa; // MCa is the moisture content of moisture air

```
function t_ts_MCa=t_ts_MC(t,ts)   %// g/kg dry air
% t_ts_MCa; // MCa is the moisture content

    t_ts_MCa=((2500-2.347*ts)*ts_MCb(ts)-1010*(t-ts))/(2500+1.84*t-4.187*ts);

    %return t_ts_MCa;
```

(3) %LD t_ts_RHa; // RHa is the relative humidity of moisture air

```
function t_ts_RHa=t_ts_RH(t,ts)

%LD t_ts_RHa; // RHa is the relative humidity of moisture air

t_ts_RHa=t_ts_Pq(t,ts)/t_Pqb(t)*100;

    % return t_ts_RHa;
```

(4) %/air saturated moisture content as a function of saturated vapor pressure

```
 function ts_MCba=ts_MCb(ts)
%  LD ts_MCba; // MCba is the saturated moisture content

    ts_MCba=(622*ts_Pqbs(ts))/(101325.0-ts_Pqbs(ts));
```

```
    % return ts_MCba;
```

(5)% // Pqbsa is the saturated vapour pressure for wb

```
 function t_Pqbsa=ts_Pqbs(ts)


          c1 = -5674.5359;
          c2 = 6.3925247;
          c3 = -0.9677843*(10.^(-2));
          c4 = 0.62215701*(10.^(-6));
          c5 = 0.20747825*(10.^(-18));
          c6 = -0.9484024*(10.^(-12));
          c7 = 4.1635019;
          c8 = -5800.2206;
          c9 = 1.3914993;
          c10 = -0.04860239;
          c11 = 0.41764768*(10.^(-4));
          c12 = -0.14452093*(10.^(-7));
          c13 = 6.5459673;


          % LD ts_Pqbsa; // Pqbsa is the saturated vapour pressure for wb
     t=ts;

     if(t>=-100&t<0)
       t_Pqbsa=exp(c1/t_T(t)+c2+c3*t_T(t)+c4*(t_T(t).^2)+c5*(t_T(t).^3)
                    +c6*(t_T(t).^4)+c7*log(t_T(t)));
    end

          if(t>=0&t<200)

t_Pqbsa=exp(c8/t_T(t)+c9+c10*t_T(t)+c11*(t_T(t).^2)+c12*(t_T(t).^3)+c13*log(t_T(t)
));
      end

     % return t_Pqbsa;
```

(6) % hs is enthalpy of superheated vapor refrigerant

```
function hs=P_T_H(P,T)   % for superheated vapor refrigerant
```

```
        Tsat3=P_T(P);
        Tsup=T-Tsat3;
        temp=T_Hi1(Tsat3);

hi2=temp*(1+0.00285446*Tsup+0.00000040129*(Tsup.^2.0)+0.0000133612*Tsup*Ts
at3-0.0000000811617*Tsat3*(Tsup.^2.0)+0.000000141194*Tsup*(Tsat3.^2.0)-
0.000000000953294*(Tsup.^2.0)*(Tsat3.^2.0));
        a12=155482.0;

        hs=hi2+a12;
        % return hs;
```

(7) % saturated temperature from saturated pressure

```
function Tsat=P_Tsat(P) %// to get saturated temperature from saturated pressure

Tsat=-2025.4518/(log(P)-21.25384)-248.94; %//unit of P: pa
        %return Tsat;//unit: centri degree
```

(8) % specific volume for superheat vapor refrigerant

```
function Vs=P_T_V(P,T)    % specific volume for superheat vapor refrigerant

        Tsat5=P_T(P);
        Tsup=T-Tsat5;
        temp=P_V(P);

        Vs=temp*(1.0+0.00523275*Tsup-
0.00000559394*(Tsup.^2.0)+0.0000345555*Tsup*Tsat5-
0.000000231649*Tsup*Tsup*Tsat5+0.000000580303*Tsup*Tsat5*Tsat5-
0.00000000320189*(Tsup.^2.0)*(Tsat5.^2.0));

        % return Vs;
```

(9) % heat transfer coefficiency for evaporator dry-cooling region

```
 function Heat_transf_coeffi_dryregion=Heat_transf_coeffi_dryregion(Maef)
```

```
% Mae=0.1; m3/s
Mae=Maef;
S1e=0.025;
S2e=0.02165;
Sfe=0.0018;
Thfe=0.00015;
Dbe=0.00982;
Doe=0.00952;
Die=0.00886;
LH=0.00107;
LP=0.00235;

Lengthe=0.42*1.0;
Heighte=0.45;
Numberoftube1e=18.0;
Numberoftube2e=6.0;
Ze=4.0;


Cpae=1035.0;

Denae=1.205;

HCondae=0.02590;
Visae=0.0000181;
Prae=0.703;

   Wye=Mae/Denae/(Lengthe*Heighte);  %//windward area
        AreaRatio=(S1e-Dbe)*(Sfe-Thfe)/(S1e*Sfe); %//area ratio
        Wmaxe=Wye/AreaRatio;  %//maximum air velocity

        Pre=Visae*Cpae/HCondae;

        Rene=Denae*Wmaxe*Doe/Visae;


        j5=0.0-0.6027+0.02593*(Sfe/Dbe).^0.52*(Numberoftube2e).^(-
0.5)*log(LH/LP);

   j6=-0.4776+0.40774*((Numberoftube2e).^(0.7)/(log(Rene)-4.4));

   j7=-0.58655*(Sfe/Dbe).^2.3*(S2e/S1e).^-1.6*(Numberoftube2e).^-0.65;

   j8=0.0814*(log(Rene)-3);

         %LD j=9.717*pow(Rene,j1)*pow(Sfe/Dbe,j2)
```

```
        %  *pow(S2e/S1e,j3)*log(j4)*pow(Numberoftube2e,-0.543)*10.0;
   %// multiply by 10 for debuging chen wu, original wrong correlation by CCWang

jdr=1.1373*(Rene).^j5*(Sfe/S2e).^j6*(LH/LP).^j7*(S2e/S1e).^j8*(Numberoftube2e).^(
0.3545);
         CHae2=jdr*Denae*Wmaxe*Cpae/(Pre).^(2.0/3.0);


   %return CHae2;  %//unit: w/K.m2


% the fin surface efficiency Pg94

 Afep=2.0*(S1e*S2e-0.25*3.14*Dbe*Dbe)/Sfe;

 Abep=3.14*Dbe*(Sfe-Thfe)/Sfe;

 Atep=Afep+Abep;
 Aiep=3.14*Die;

          HCondf=203.0; %//heat conductivity of aluminium, w/m.k
         Temp=2*CHae2/(HCondf*Thfe);

         me=Temp.^0.5;

         he=0.5*Doe*(S1e/Doe-1.0)*(1.0+0.35*log(1.063*S1e/Doe));
         Temp1=me*he;
   fin_efficiency=tanh(Temp1)/Temp1; % pg82

  fin_surface_efficiency=1.0-Afep/Atep*(1.0-fin_efficiency);


   Heat_transf_coeffi_dryregion=CHae2*fin_surface_efficiency;  % w/m2.k



(10) % heat transfer coefficiency for evaporator wet-cooling region


 function Heat_transf_coeffi_wetregion=Heat_transf_coeffi_wetregion(Mae)

 % Mae=0.1; m3/s
 S1e=0.025;
 S2e=0.02165;
 Sfe=0.0018;
```

```
Thfe=0.00015;
Dbe=0.00982;
Doe=0.00952;
Die=0.00886;
LH=0.00107;
LP=0.00235;

Lengthe=0.42*1.0;
Heighte=0.45;
Numberoftube1e=18.0;
Numberoftube2e=6.0;
Ze=4.0;


Cpae=1035.0;
Denae=1.205;
HCondae=0.02590;
Visae=0.0000181;
Prae=0.703;

  Wye=Mae/Denae/(Lengthe*Heighte);  %//windward area
       AreaRatio=(S1e-Dbe)*(Sfe-Thfe)/(S1e*Sfe); %//area ratio

       Wmaxe=Wye/AreaRatio;  %//maximum air velocity

       Pre=Visae*Cpae/HCondae;
       Rene=Denae*Wmaxe*Doe/Visae;


       j1=0.0-0.023634-1.2475*(Sfe/Dbe).^0.65*(S2e/S1e).^0.2*(Numberoftube2e).^-
0.18;
       j2=0.856*exp(LH/LP);

       j3=0.25*log(Rene);

       cw=log(3.0-LP/Sfe);
       j4=(cw).^0.07162;

        %LD j=9.717*pow(Rene,j1)*pow(Sfe/Dbe,j2)
       %  *pow(S2e/S1e,j3)*log(j4)*pow(Numberoftube2e,-0.543)*10.0;
  %// multiply by 10 for debuging chen wu, original wrong correlation by CCWang
    j=9.717*(Rene).^j1*(Sfe/Dbe).^j2*(S2e/S1e).^j3*j4*(Numberoftube2e).^(-0.543);
        CHae2=j*Denae*Wmaxe*Cpae/(Pre).^(2.0/3.0)


  %return CHae2;  %//unit: w/K.m2
```

```
% the fin surface efficiency

 Afep=2.0*(S1e*S2e-0.25*3.14*Dbe*Dbe)/Sfe;
 Abep=3.14*Dbe*(Sfe-Thfe)/Sfe;
 Atep=Afep+Abep;
 Aiep=3.14*Die;

          HCondf=203.0; %//heat conductivity of aluminium, w/m.k
         Temp=2*CHae2/(HCondf*Thfe);
         me=Temp.^0.5;
         he=0.5*Doe*(S1e/Doe-1.0)*(1.0+0.35*log(1.063*S1e/Doe));
         Temp1=me*he;
  fin_efficiency=tanh(Temp1)/Temp1; % pg82
 fin_surface_efficiency=1.0-Afep/Atep*(1.0-fin_efficiency);

  Af=1.1; % dehumidifying augumentation factor, pg95
  Heat_transf_coeffi_wetregion=Af*CHae2*fin_surface_efficiency; %% w/m2.k
```

Appendix B

Photos of the Experimental DX A/C system

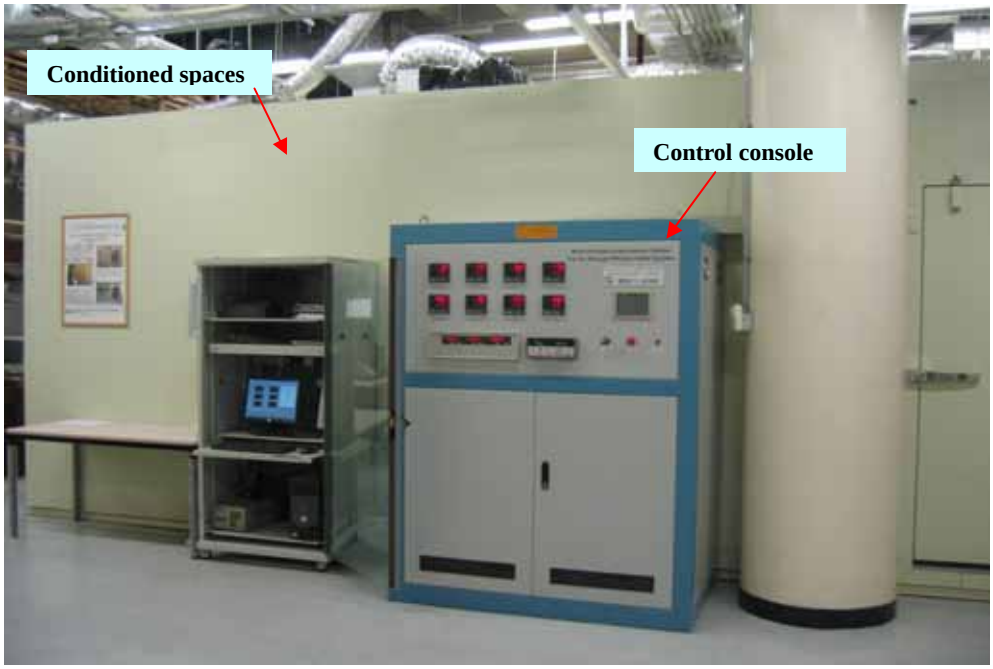

Photo 1 Overview of the experimental rig (1)

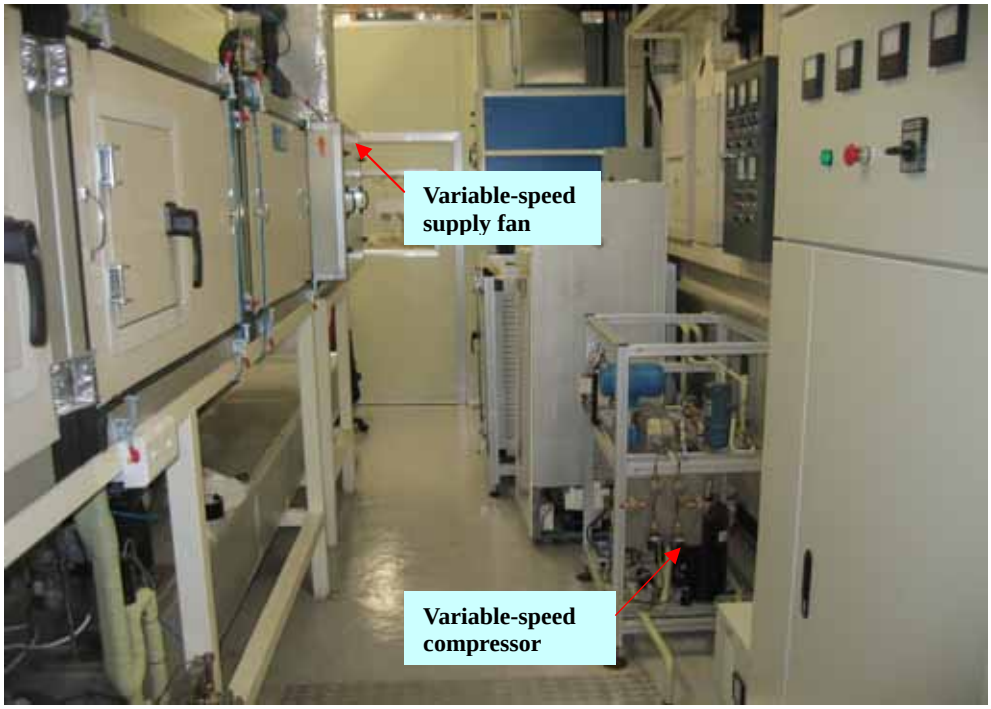

Photo 2 Overview of the experimental rig (2)

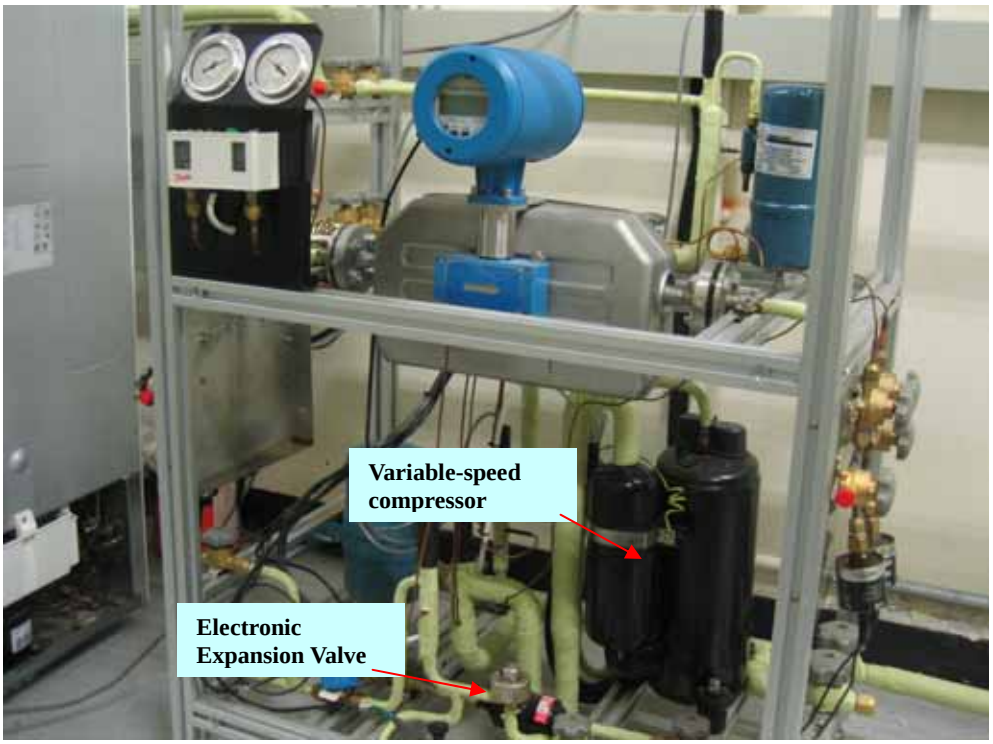

Photo 3 Variable-speed compressor in the DX A/C system

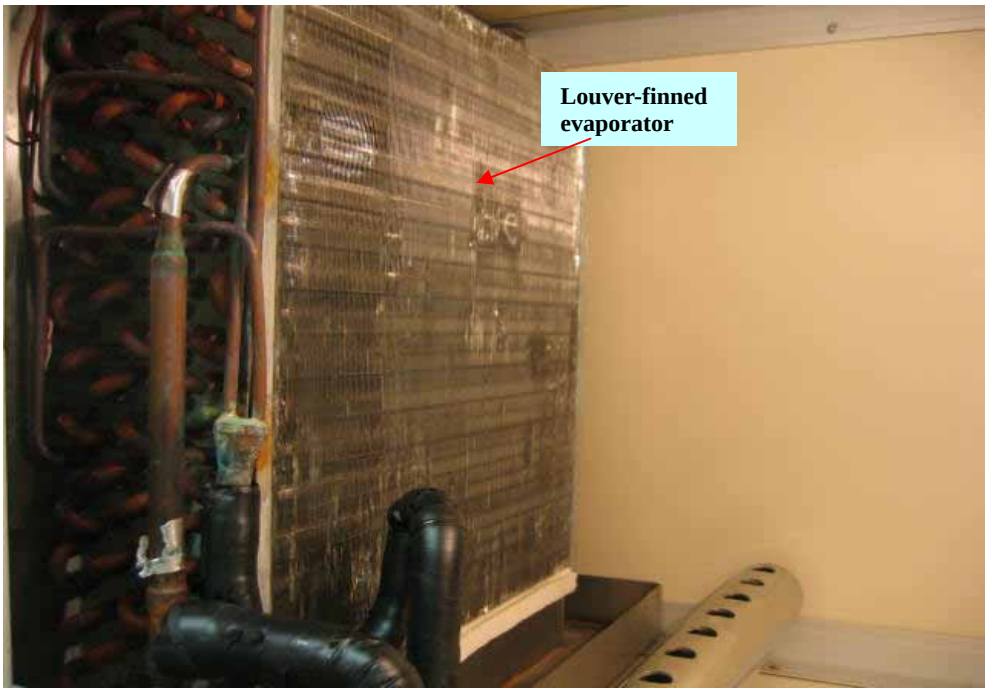

Photo 4 DX cooling coil in the DX A/C system

Photo 5 Load generation units inside conditioned space

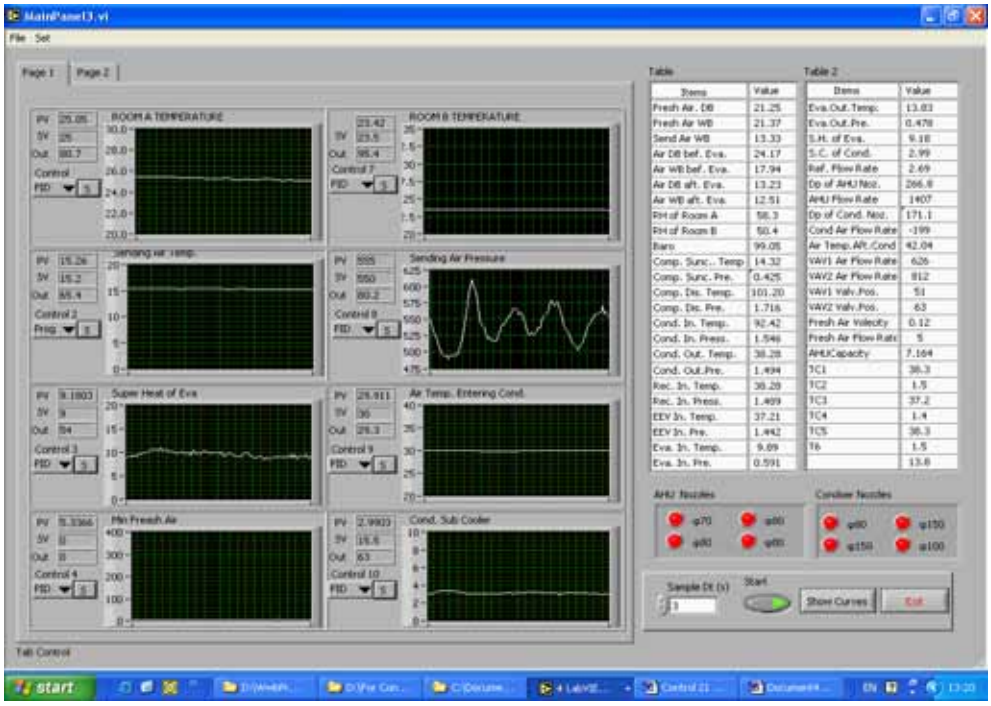

Photo 6 Logging & control supervisory program

Appendix C

Publications Arising from the Thesis

I. Journal papers

- Qi Qi, Shiming Deng. Multivariable control-oriented modeling of a direct expansion (DX) air conditioning (A/C) System. *International Journal of Refrigeration*, 31(5), 841-849 (2008)
- Qi Qi, Shiming Deng. Multivariable control of indoor air temperature in a direct expansion (DX) air conditioning (A/C) System. *Building and Environment*, 44, 1659-1667 (2009)
- Qi Qi, Shiming Deng, Xiangguo Xu, MY Chan. Improving degree of superheat control in a direct expansion air conditioning system. Accepted by *International Journal of Refrigeration*

II. Conference paper

- Qi Qi and Shiming Deng. A new control approach for a direct expansion (DX) air conditioning (A/C) system with variable speed compressor and variable speed supply fan. *12th International Refrigeration and Air Conditioning Conference* at Purdue University, Indiana, US, 2008